Development of a Whole Cell Fermentation Process for Glycosylation of Small Molecule Flavonoids

Dissertation

Zur Erlangung der Würde des Doktors der Naturwissenschaften

des Fachbereichs Biologie, der Fakultät für Mathematik, Informatik und Naturwissenschaften,

der Universität Hamburg

vorgelegt von

Tanja Vanessa Heyer

aus Norderstedt

Hamburg 2019

Vollständiger Abdruck der von der Fakultät für Mathematik, Informatik und Naturwissenschaften der Universität Hamburg zur Erlangung des akademischen Grades eines Doktors der Naturwissenschaften genehmigten Dissertation.

Gutachter:

Prof. Dr. Wolfgang R. Streit

PD Dr. Andreas Pommerening-Röser

Tag der Disputation: 08.11.2019

Eidesstattliche Versicherung

Hiermit erkläre ich an Eides statt, dass ich die vorliegende Dissertationsschrift selbst verfasst und keine anderen als die angegebenen Quellen und Hilfsmittel benutzt habe.

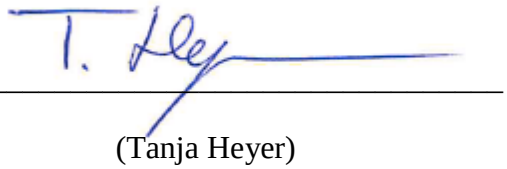

(Tanja Heyer)

Funding

This work was part of the project “GO-Bio 6: GLYCONIC - Selektiv glykosylierte Polyphenole” funded by the GO-Bio initiative from the German Federal Ministry of Education and Research (BMBF, funding number: 031A376).

Abstract

Flavonoids are known to have multiple beneficial effects on human health. These make them desired compounds as bioactives, e.g. in cosmeceutical products. The glycosylation of flavonoids has positive impact on their solubility, bioavailability, and stability and is furthermore able to improve their physiological effects. In this study, flavonoid glycosides were produced in a whole-cell biocatalytic process in *Escherichia coli* by directed transfer of activated sugar residues to hydroxy groups of the polyphenolic scaffold within an enzymatic reaction by use of glycosyltransferases.

The goal of this work was the development and optimization of the production process for glycosylated flavonoids in gram-scale, comprising the upstream (USP) and downstream (DSP) processing. Metagenome-derived glycosyltransferase GtfC and the glycosyltransferase GtfD from *Dyadobacter fermentans* were used for production of two promising flavonoid-rhamnosides as active ingredients in cosmetics: hesperetin-5-O-rhamnoside, a candidate for anti-aging, and naringenin-5-O-rhamnoside, a candidate for hair growth.

First optimizations were achieved by high cell density fermentation in a fed-batch process with addition of glucose feed for cell growth as well as for the glycosylation itself. Further a repeated fed-batch fermentation process with exchange of the culture medium was established to feed the polyphenol step by step in small amounts after complete biotransformation of the first added amount, due to the fact that polyphenols are highly insoluble in water and high amounts could be toxic to the cells. First improvements of the process, e.g., from low to high cell density and repeated feeding of the polyphenol in several batches already increased the production yield by a factor of 5 to 10. The choice of the glycosyltransferase had a great impact on the production. The productivity and the product spectrum varied according to the different glycosyltransferases. Naringenin biotransformation with GtfD showed more than twice as high naringenin-5-O-rhamnoside titer than with GtfC and biotransformation of hesperetin with GtfD resulted in a complete different product spectrum with 30-fold higher hesperetin-5-O-rhamnoside production.

Another goal within this work was to improve the membrane transport of flavonoid-glycosides out of the cell. Accumulation of flavonoid-glycosides in the cells can be a limiting factor in the production. The export from the cells could be increased by overexpressing of the outer membrane protein TolC and an 8-fold higher production titer of naringenin-5-O-rhamnoside could be achieved.

For purification of flavonoid-rhamnosides a DSP consisting of a tangential flow filtration for cell removal, followed by a solid phase extraction with reversed-phase material for further separation of the hydrophobic glycosides from the complex culture supernatant, and a crystallization process was developed. The products could be received as a white amorphous powder.

Zusammenfassung

Flavonoide besitzen eine Vielzahl gesundheitsfördernder Eigenschaften für den Menschen, was sie zu gefragten Inhaltsstoffen für u.a. kosmetische Produkte macht. Die Glykosylierung von Flavonoiden kann dessen Eigenschaften wie die Löslichkeit, Bioverfügbarkeit und Stabilität positiv beeinflussen und sie zusätzlich in ihrer physiologischen Wirkung verbessern.
In dieser Arbeit wurden Flavonoid-Glykoside in einer Ganzzellkatalyse in *Escherichia coli* Zellen mittels Glykosyltransferasen hergestellt, die in einer enzymatischen Reaktion aktivierte Zuckerreste an die freien Hydroxylgruppen der Flavonoide übertragen.
Das Ziel der Arbeit war die Entwicklung und Optimierung eines Produktionsprozesses, bestehend aus Up-Stream-(USP) und Down-Stream-Prozess (DSP), für die Produktion von glykosylierten Flavonoiden im Gramm-Bereich. Dafür wurden eine Metagenom-basierte Glykosyltransferase GtfC und die Glykosyltransferase GtfD aus dem Bakterium *Dyadobacter fermentas* verwendet und zwei vielversprechende Flavonoid-Rhamnoside als potenzielle Kosmetikinhaltsstoffe produziert: das Hesperetin-5-O-rhamnosid im Bereich Anti-Aging und das Naringenin-5-O-rhamnosid als Kandidat für Haarwachstum. Erste Optimierungen wurden mit einer Hochzelldichtefermentation im Fed-Batch Prozess durch Zugabe eines Glucose-Feeds erzielt, der zu einem verbesserten Zellwachstum und höheren Ausbeuten bei der Glykosylierung führte. Weiterhin wurde ein Repeated-Fed-Batch Prozess entwickelt, bei dem nach jedem Batch ein Mediumwechsel durchgeführt wurde und die vorherige Menge des Ausgangsstoffs nach vollständiger Umsetzung erneut zugegeben wurde. Dies ist von Vorteil, da Polyphenole schwer wasserlöslich sind und in hohen Konzentrationen für die Zellen toxisch sein können. Die ersten Verbesserungen am Prozess, die durch hohe Zelldichten und mehrere hintereinander folgende Batches im Repeated-Batch Verfahren erreicht werden konnten, führten bereits zu einer Steigerung der Produktausbeute um den Faktor 5 bis 10. Einen großen Einfluss auf die Produktion hatte die Wahl der Glykosyltransferase, aufgrund

der unterschiedlichen Produktivität und der Produktspektren von GtfC und GtfD bei der Umsetzung von Naringenin und Hesperetin. Mit GtfD konnten doppelt so hohe Konzentrationen an Naringenin-5-O-rhamnosid erreicht werden wie mit GtfC und bei der Umsetzung von Hesperetin zeigte GtfD ein komplett anderes Produktspektrum als GtfC mit einer 30-fach höhere Konzentration des Hesperetin-5-O-rhamnosids.

Ein weiteres Ziel im Rahmen dieser Arbeit war es, den Membrantransport der gebildeten Flavonoid-Glykoside aus der Zelle heraus zu verbessern. Eine Akkumulierung des Produktes in der Zelle wirkt sich inhibierend auf die Glykosylierung aus. Durch die Überexpression des Membrantransporters TolC konnte die Produktausbeute des Naringenin-5-O-rhamnosids um ein 8-Faches gesteigert werden.

Für die Aufarbeitung der produzierten Flavonoid-Rhamnoside wurde ein DSP entwickelt, der aus einer Tangential-Fluss-Filtration zur Zellabtrennung, einer Festphasenextraktion mit Umkehrphase für die weitere Aufreinigung der hydrophoben Glykoside aus dem komplexen Kulturüberstand und einem Ausfällungsprozess besteht. Das Endprodukt ist ein amorphes weißes Pulver.

Table of Contents

Acknowledgements

I would like to offer my special thanks to my supervisor and reviewer Prof. W. R. Streit for the advice he has provided throughout the last years and his useful critiques of my research work.

PD Dr. A. Pommerening-Röser, I would like to thank for being the second reviewer of my thesis.

Ulrich Rabausch, I would like to thank for the opportunity to work on this interesting project, all the support and the experience I have gathered throughout the years in your group.

Henning Rosenfeld, I would like to thank for supervising me through most of the time of my work, for all your advice and support.

I would also like to thank my bachelor and master students, Anton Letzer, Boby Tendi Rik Mandenda, Charles Wiedenhöfer, Nele Bredehöft, and Robert Knoll, for your contribution to this PhD thesis.

Constantin Ruprecht and Friedericke Bönisch, I would like to thank for proofreading my thesis.

Furthermore I want to thank all members of the Glyconic-team for the great time we shared. Constantin Ruprecht and Friedericke Bönisch, I would like to thank for discussions and encourage exchange of ideas. Sarah Strehlow, Kerstin Wolf, and Nele Bredehöft, I would like to thank for the technical support in the lab.

I would also like to thank the whole working group of the last years for the great working atmosphere, for always helping each other and for the great time I had during my PhD.

Finally, I wish to thank my family, especially my parents and my beloved husband for their support, understanding and encouragement in the last years.

Figures

Tables

List of Abbreviations

Å	Ångström, a unit of length (1 Å = 10^{-10} m)
ABC	ATP-binding cassette
Amp	ampicillin
ATP	adenosine triphosphate
°C	degree Celsius
CAZy	Carbohydrate-Active enZYmes (CAZymes)
DNA	deoxyribonucleic acid
dNTP	deoxyribonucleotide triphosphate
DO	dissolved oxygen
DSMZ	German collection of microorganisms and cell cultures
DSP	downstream processing
dTDP	deoxythymidine diphosphate
dTMP	deoxythymidine monophosphate
dTTP	deoxythymidine triphosphate
E. coli	*Escherichia coli*
EDTA	ethylene-diamine-tetraacetic-acid
et al.	et alii (Latin: and others)
FDA	Food and Drug Administration
Fig.	figure
g	gram(s)
G-1-P	glucose-1-phosphate
GT	glycosyltransferase
h	hour(s)
H3'R	hesperetin-3'-O-rhamnoside
H5R	hesperetin-5-O-rhamnoside
Hes	hesperetin
HPLC	high performance liquid chromatography
IPTG	isopropyl β-D-1-thiogalactopyranoside

k_La	volumetric oxygen transfer coefficient, h^{-1}
K_S	saturation constant of the limiting substrate, g L^{-1}
Kan	kanamycin
Kb	kilobases
kDa	kilodaltons
L	litre(s)
LB	Lysogeny broth
µ	micro- (1×10^{-6}) or specific growth rate, h^{-1}
m	milli- (1×10^{-3}) or meter(s)
M	molar
mA	milliampere
max.	maximal
MFS	major facilitator superfamily
min	minute(s)
MS	mass spectrometry
NaCl	sodium chloride
N4'R	naringenin-4'-O-rhamnoside
N5R	naringenin-5-O-rhamnoside
Nar	naringenin
NDK	nucleotide diphosphate kinase
NMR	nuclear magnetic resonance
OD	optical density
OTR	oxygen transfer rate
OUR	oxygen uptake rate
PCR	polymerase chain reaction
pH	negative logarithm of the molar concentration of dissolved hydronium ions
q_P	specific production rate, g g^{-1} h^{-1}
q_S	specific substrate uptake rate, g g^{-1} h^{-1}
RmlA	glucose-1-phosphate thymidylyltransferase
RmlB	dTDP-D-glucose 4,6-dehydratase

RmlC	dTDP-4-dehydrorhamnose 3,5-epimerase
RmlD	dTDP-4-dehydrorhamnose reductase
RND	resistance nodulation division
rpm	rotations per minute
SPE	solid phase extraction
Spec	spectinomycin
Strep	streptomycin
t	time, h
Tab.	table
TB	terrific broth
TCA	tricarboxylic acid cycle
TFA	trifluoroacetic acid
TFF	tangential flow filtration
TK	thymidine kinase
TMK	thymidylate kinase
TMP	transmembrane pressure
tRNA	transfer ribonucleic acid
UDP	uridine diphosphate
UHPLC	ultra-high performance liquid chromatography
USP	upstream processing
UV	ultraviolet radiation

1 Introduction

1.1 Flavonoids

In nature a wide range of polyphenols is present in many different plants. They are highly lipophilic small molecules (< 1 kDa), which are produced in plants as bioactive substances, for example as natural dye, flavors or tanning agents. The health-promoting effects of these secondary plant metabolites on humans like anti-inflammatory, antioxidant, antibiotic, antiviral, vascular protective, and cancer protective effects attracted attention in research, development and industry, mainly in the food and cosmetics industry (Ververidis et al. 2007). Especially their multiple cosmeceutical effects make them attractive as ingredients for skin care products. Polyphenols have an inhibiting effect on collagenase and elastase activity, as well as they protect against UV damages and oxidative stress, the main causes of skin ageing (Zillich et al. 2015).

Polyphenols are classified in five groups: lignans, stilbenes, hydroxybenzoic acids, hydroxycinnamic acids and flavonoids. Flavonoids are divided into six subgroups and the chalcones, which are precursors of the other flavonoid groups due to their open chain with three carbon molecules whose closure results in the typical flavonoid structure. This study is focused on the conversion of the flavanones naringenin and hesperetin (Fig.1.1).

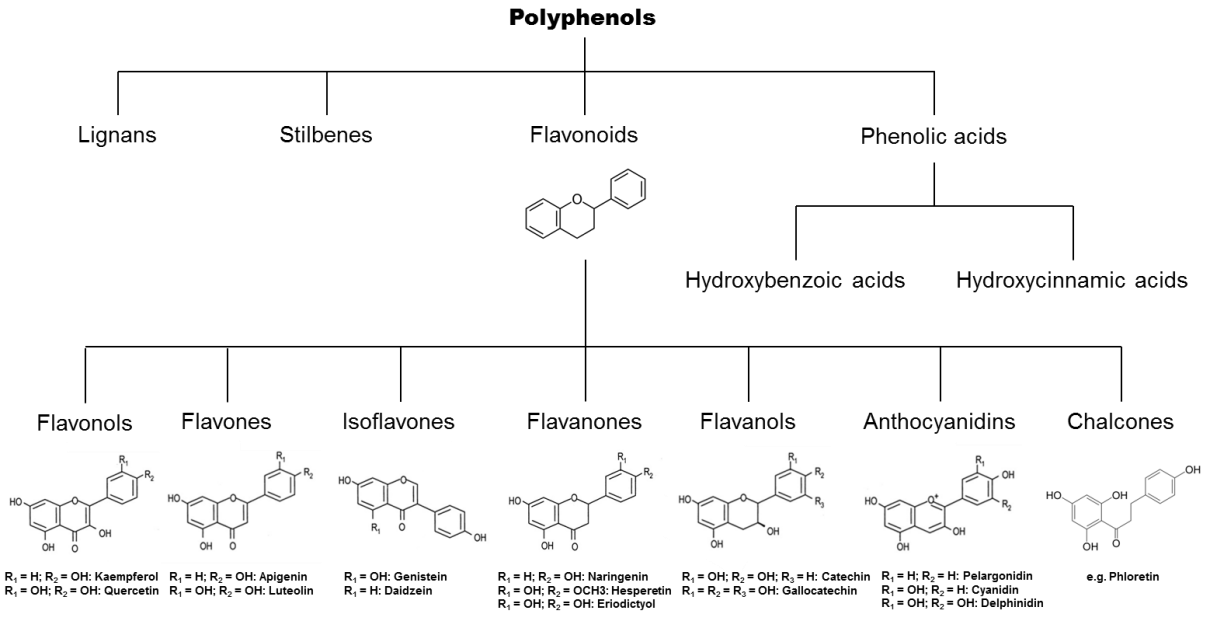

Figure 1.1: Polyphenol classification and the chemical structures of flavonoid groups. (Structures made with ChemSketch).

The basic structure of flavonoids consists of two aromatic rings linked with an oxidized pyran ring (Fig. 1.2). Due to the great variety of different oxidation states of the pyran ring, attached residues to the aromatic rings and glycosylations there is a huge diversity of compounds in nature (Zillich et al. 2015, Manach et al. 2004).

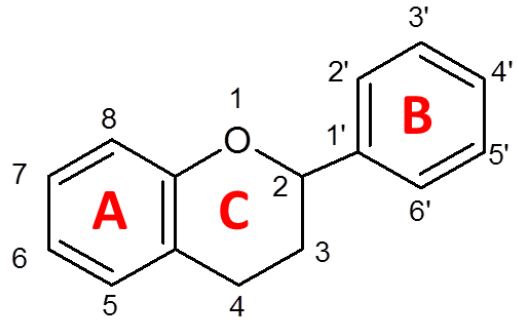

Figure 1.2: Basic structure of flavonoids, the flavan molecule, consisting of two aromatic rings (A, B) and a tetrahydropyran ring (C). (Structure made with ChemSketch).

Glycosylation is one of the predominant mechanism by which the bioactivity of flavonoids is modulated in nature. Most natural bioactives derive their activity from their sugar residue and variations in the structure of glycosides can impact the biological properties of the precursor molecule. For example, attaching rhamnose to the 2-OH or 6-OH of the glucose residue of naringenin-7-O-glucoside affects the bitterness of grapefruit or the tastelessness of mandarin (Simkhada et al. 2010). Glycosylation has positive impact on stabilization, detoxification and the low water solubility of flavonoids.

A major problem is the limited availability, especially of glycosylated polyphenols. They occur in plants at low levels and have to be extracted with large quantities of solvents (Manach et al. 2004, Rabausch et al. 2013).

In a biotechnological process, where flavonoids are glycosylated in a whole cell biotransformation with recombinant glycosyltransferases, sufficient amounts of new active polyphenol-glycosides can be produced (Rabausch et al. 2013, Kim et al. 2007). These compounds have a better solubility, stability and bioavailability than their aglycones (Simkhada et al. 2010, Ahn et al. 2009, Bowles et al. 2005).

1.1.1 Naringenin and naringenin-glycosides

Naringenin is mainly found in citrus fruits (grapefruit and oranges) as aglycon and glycosides. It is a flavanone with three hydroxy groups at the positions C-5, C-7 and C-4' (Fig. 1.1). Most common glycoside of naringenin is naringin, the naringenin-7-O-neohesperidoside. Naringin is the major flavonoid glycoside in grapefruits and gives them its bitter flavor (Simkhada et al. 2010).
Because of its various biological activities naringenin is used in cosmetic and in different pharmaceutical formulations. It is known to have anti-oxidant, anti-inflammatory, cholesterol-lowering, and anti-carcinogenic effects (Barreca et al. 2017, Miler et al. 2016, Krishnakumar et al. 2011, Tripoli et al. 2007, Lee et al. 2001).

Naringenin-5-O-α-L-rhamnoside (N5R) is a glycosylated product of naringenin, which was produced in this work by whole-cell biotransformation as a potential healthcare candidate for hair growth. Activity tests that were implemented externally by Bioalternatives show *in vitro* high stimulation activities of the vascular endothelial growth factor (VEGF), which induces proliferation of human hair follicle dermal papilla cells (data from *in vitro* tests see appendix, A1).

1.1.2 Hesperetin and hesperetin-glycosides

Hesperetin is a flavanone with a methoxy group at the position C-4' and three hydroxy groups at the positions C-5, C-7 and C-3' (Fig. 1.1). Hesperetin and its glycoside hesperidin are most abundant in citrus fruits and have antioxidant, anti-inflammatory and anti-carcinogenic activities (Stanisic et al. 2018, Miler et al. 2016). Hesperetin is also known to improve melanin synthesis, whereas hesperidin inhibits melanin synthesis (Liu-Smith and Meyskens 2016, Usach et al. 2015).

Hesperetin-5-O-α-L-rhamnoside (H5R) was produced in this project as a novel natural substance with potential anti-aging, anti-wrinkle and wound healing activities (data from *in vitro* tests see appendix, A1).

1.2 Glycosyltransferases

Glycosyltransferases (GTs) transfer sugar residues from an activated donor substrate to an acceptor molecule. Based on their sequence similarities, GTs are classified into 106 families (CAZy database – status April 2019, *http://www.cazy.org/GlycosylTransferases.html*). However, with the discovery of new GTs the number of families is constantly increasing. GTs that glycosylate polyphenols are members of the GT family 1, which comprises enzymes that catalyze the glycosylation of small lipophilic molecules (Bowles 2006). The activated sugars for the enzymatic reaction of plant GTs are typically UDP-glucose, UDP-rhamnose, UDP-galactose, UDP-xylose, and UDP-glucuronic acid. The glycosylation takes place at free –OH, –COOH, –NH2, –SH, and C–C groups of the lipophilic molecule.

GT folds primarily consist of alpha-beta-alpha (α/β/α) sandwiches, very similar to the Rossmann fold, a common structural motif in nucleotide-binding proteins, which is composed of six-stranded parallel beta-sheets with 321456 topology, means the strands are arranged in the order of 321456 (1 = N-terminal, 6 = C-terminal). Three structural folds have been described for GTs, named GT-A, GT-B and GT-C (Fig. 1.3). GT family 1 consists of the GT-B fold (Bowles 2006).

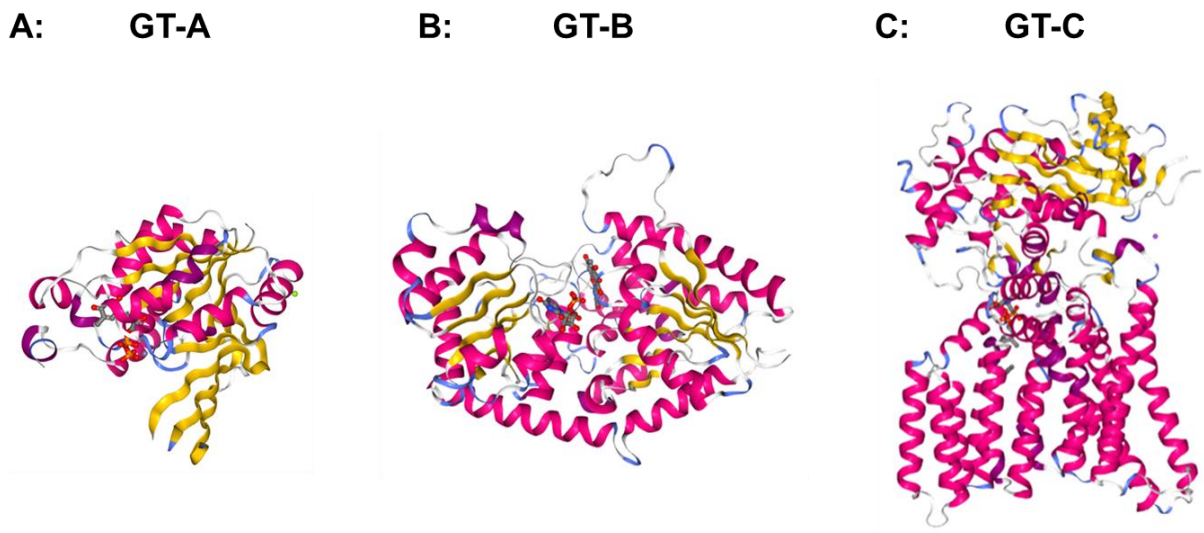

Figure 1.3: Representative structures of GT-A, GT-B and GT-C glycosyltransferase folds. Helices are shown in magenta and beta-strands in yellow. Ligands are shown as ball-and-stick, metal ions as purple or green spheres. A: Glycosyltransferase SpsA from *Bacillus subtilis* in complex with TDP and the ions of magnesium and manganese (PDB ID: 1H7Q, Tarbouriech et al. 2001); B: The red grape flavonoid 3-O-glycosyltransferase (VvGT1) from *Vitis vinifera* in complex with UDP and Quercetin (PDB ID: 2C9X, Offen et al. 2006); C: Oligosaccharyltransferase PglB from *Campylobacter lari* in complex with sodium and manganese ions, as well as an acceptor peptide and lipid-linked oligosaccharide analog (PDB ID: 5OGL, Napiorkowska et al. 2017).

The GT-A structure consists of two tightly packed Rossmann-like folds that form a continuous central beta-sheet. Typical for all GT-A enzymes is the DxD motif within the active side, which interacts with the phosphate groups of nucleotide donor through the coordination of a divalent cation. The GT-B fold comprises two Rossmann-like domains with the active site in the connecting region between these separated domains. GT-B enzymes have been observed to work without the need of a metal ion (Breton et al. 2006, Gloster 2014). GT-C enzymes are hydrophobic integral membrane proteins using lipid phosphate-linked sugar donors (Gloster 2014).

1.3 Metabolism of *Escherichia coli*

Escherichia coli (*E. coli*) K12 strain is the best known model organism in molecular biology with fully sequenced genome (Blattner et al. 1997). Optimal growth conditions are at temperatures around 37°C and pH 6 – 8. *E. coli* cells grow fast at complex peptide-based media with a doubling time of 0.3 – 1 h and use sugars like glucose, fructose, mannose, glycerol or organic acids as carbon and energy source.

The metabolism of *E. coli* is facultative anaerobe. The bacteria can draw their energy from aerobic respiration as well as under anaerobic conditions by mixed acid fermentation in which the organic acids acetate, succinate, ethanol, formate and lactate are synthesized (Clark 1989). Glucose is the preferred carbon source for *E. coli* that is utilized first and represses the uptake of other sugars (Stülke and Hillen 1999, Görke and Stülke 2008). Glucose is primary transported into the cell by the phosphotransferase system and then catabolized to pyruvate during glycolysis. Under aerobe conditions pyruvate is converted into acetyl-CoA, which is further oxidized to water and carbon dioxide in the tricarboxylic acid cycle (TCA cycle). Under anaerobe conditions the TCA cycle is inactive and acetyl-CoA is metabolized to acetate in the mixed acid fermentation (Fig. 1.4).

Acetate formation also occurs under aerobe conditions at high glucose concentrations in an overflow metabolism, where the uptake rate of glucose by the phosphotransferase system is so efficient, the respiration capacity is depleted. Due to the saturation of the TCA cycle the accumulating acetyl-CoA is metabolized to acetate over the two pathways pyruvate oxidase (*poxB*) and acetate kinase/ phosphotransacetylase (*ackA-pta*) (Dittrich et al. 2005).

Acetate accumulation is a major problem in high cell density fed-batch fermentations of *E. coli*. Due to high acetate concentrations in the medium the cell growth and recombinant protein expression are inhibited (De Mey et al. 2007).

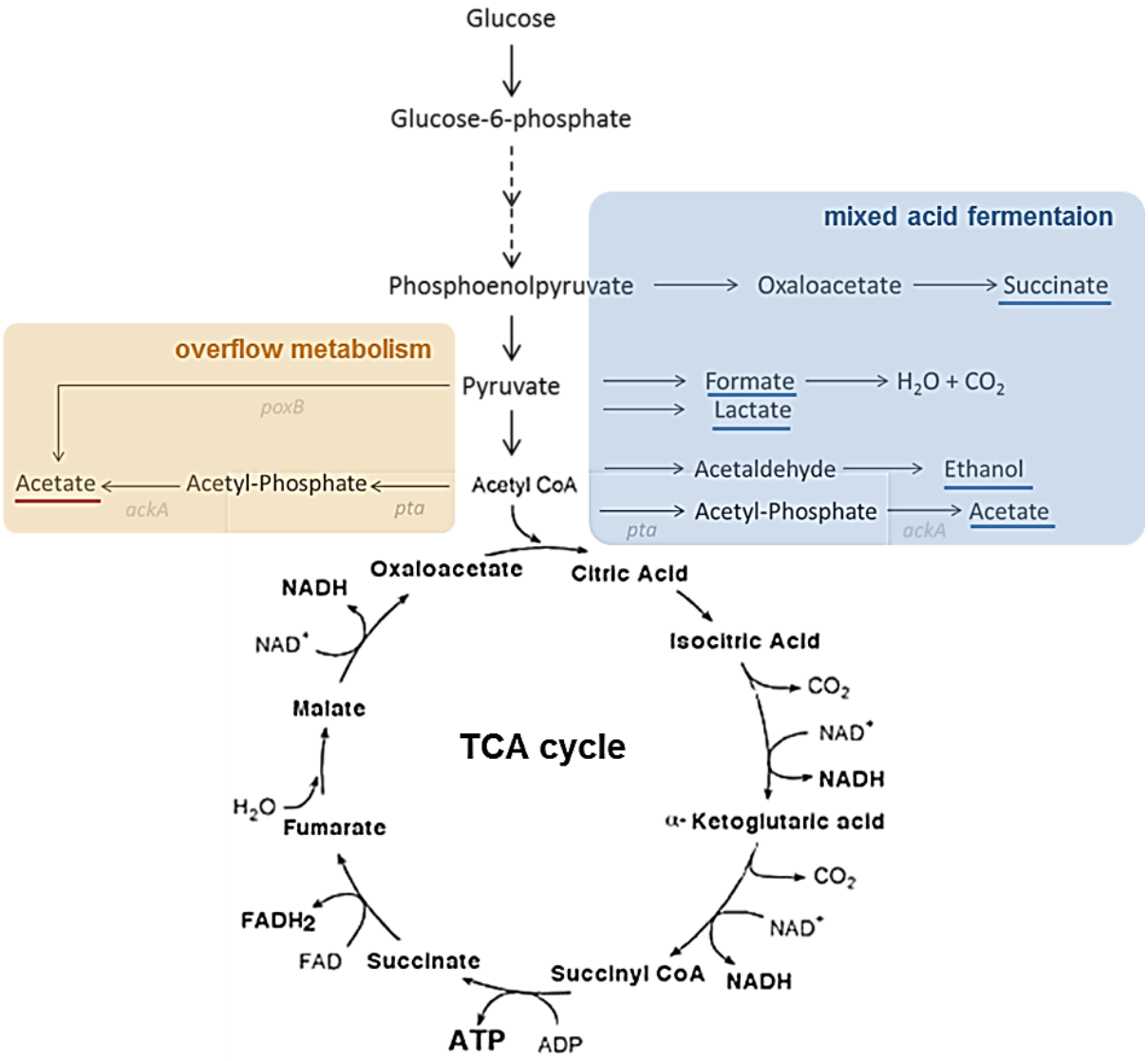

Figure 1.4: Central carbon metabolism of E. coli during growth on glucose. Aerobe and anaerobe metabolic pathways. (Figure from Kiuru 2002, modified).

Feeding of glucose results in an extended growth phase during which high cell densities are reached. Acetate formation highly depends on the growth rate. The critical growth rate depends on the strain and the growth conditions like process parameters and medium. To avoid overflow metabolism during *E. coli* fermentations the growth rate can be limited by glucose-limited fed-batch (De Mey et al. 2007). Under glucose-limited conditions cells start to consume the excreted acetate. The glucose concentration in culture medium has to be constantly close to zero where the cells co-metabolize acetate and glucose (Wolfe 2005).

In large scale fermentations reduced mixing qualities can cause inhomogeneity in high cell density cultures with oxygen-limited areas (anaerobe mixed acid fermentation) or excess of glucose near to the feed inlet (overflow metabolism). In these areas the cells produce larger

amounts of acetate. That's why the reduction of acetate production is more complicated in industrial production scale (Schmidt 2005).

1.4 Recombinant protein expression in *Escherichia coli*

The most popular organism for the production of recombinant proteins is *E. coli*. The use of *E. coli* as an expression system is well-established and many advances have been made over the years in optimization of high-level protein expression.
In most cases *E. coli* is the best choice because of its cost effectiveness and the level of knowledge on its genetic modification and fermentation for recombinant protein production (Joseph et al. 2015). It has a fast growth rate and high cell densities can be achieved, whereas inexpensive media costs (Rosano and Ceccarelli 2014). Transformation with exogenous DNA is fast and easy and the protein expression occurs at high levels. However, if the protein should be available extracellular or if the protein requires post translational modifications, *E. coli* is not the right expression system (Rosano and Ceccarelli 2014, Joseph et al. 2015).

Most common and easy tool for placing a gene encoding for a recombinant protein into a cell are expression vectors. They consist of a replicon, a selection marker, a promoter and terminator, and a multiple cloning site for gene insertion (Rosano and Ceccarelli 2014).
The replicon is important for the copy number of the expression vector. A high copy number of the plasmid causes a high yield of recombinant protein, but can decrease the bacterial growth rate due to metabolic burden or leads to inclusion bodies (aggregates of the recombinant protein). Selection markers, typically antibiotic resistances, ensure cell growth of only the cells carrying the plasmid. Cells without plasmid are not able to grow on medium containing the antibiotic; cells with plasmid are able to grow (Rosano and Ceccarelli 2014).

There are many different *E. coli* strains available as expression hosts. The BL21 and its derivatives are the most preferred, also some K-12 strains like Origami derivatives (Rosano and Ceccarelli 2014, Joseph et al. 2015). The *E. coli* BL21 (DE3) strain, developed by Studier and Moffat in 1986, derived from the B line (Rosano and Ceccarelli 2014). The characteristic lack of *lon* and *ompT* proteases of the B line was the reason for various modifications of those strains for protein expression hosts. The missing genes of these proteases, which degrade many foreign proteins, stabilize the expression of recombinant proteins (Joseph et al. 2015). The Origami strain (Novagen) is a *trxB* (thioredoxin reductase) and *gor* (glutathione reductase) mutant with greatly enhanced disulfide bond formation in the cytoplasm (Rosano

and Ceccarelli 2014). The enhanced formation of disulfide bonds improves protein folding and yields in more active protein (Prinz et al. 1997). In this study the Rosetta-gami 2 (DE3) strain (Novagen) was used for expression of the glycosyltransferases. This strain combines a BL21-derived Rosetta (DE3) strain, providing tRNA genes for codons rarely in *E. coli*, with the benefits of the Origami (DE3) strain.

DE3-strains can be used for high level protein expression by induction of the T7 promotor system. The genome of these strains contains the prophage DE3, derived from a bacteriophage λ, which expresses the T7 RNA polymerase under the control of the *lacUV5* promoter. The gene of interest can be cloned behind the T7 promoter on a plasmid and the expression of the recombinant protein is induced by the T7 polymerase, which is synthesized after induction of the *lacUV5* promoter (Rosano and Ceccarelli 2014). *LacUV5* is a mutant of the *lac* promotor to achieve expression in the presence of glucose. The *lac* operon comprised the genes encoding for lactose-metabolizing enzymes, e.g. β-galactosidase. Presence of lactose induces the expression of these enzymes. If glucose and lactose are both present, *E. coli* prefers the uptake und metabolism of glucose. Until glucose is available as carbon source, the synthesis of β-galactosidase is not needed and the induction of the *lac* promotor is inhibited due to catabolite repression by the glucose (Rosano and Ceccarelli 2014).

The *lac* operon and the T7 promotor system are common tools for expression of recombinant proteins in *E. coli*. For the induction a non-hydrolyzable analog of lactose, isopropyl β-D-1-thiogalactopyranoside (IPTG) can be used (Rosano and Ceccarelli 2014).

1.5 Whole-cell biotransformation

In nature, flavonoids are glycosylated by regio- and stereospecific glycosyltransferases. These enzymes can be used for biotechnologically production of flavonoid-glycosides. Challenging aspects in the use of glycosyltransferases *in vitro* are their poor stability and the expensive or unavailable sugar-donor (Slámová et al. 2018). In a whole-cell biotransformation the glycosyltransferase used for the biocatalytic reaction is expressed recombinant by the host after induction with IPTG and the activated sugars are provided over the cellular glucose or rhamnose pathway (Fig. 1.5). The biotransformation of flavonoid glycosides in a whole-cell fermentation process is an efficient alternative to chemical synthesis. There is a variety of chemical glycosylation reactions, but no standard method for efficient chemical synthesis of different glycosidic linkages (Sun et al. 2014), whereas in whole-cell biotransformation it is supposed to be possible to transfer different sugar-donors to all available hydroxyl groups of

various polyphenols. Problems in chemical synthesis are that many flavonoid derivatives are poorly soluble in conventional glycosylation solvents and fragile under acidic and basic conditions (Sun et al. 2014). Also the phenolic hydroxyl groups of the flavonoid aglycone are less nucleophilic than aliphatic alcohols. Additionally, electron-withdrawing substituents and intramolecular hydrogen bonds decrease the reactivity of the phenolic hydroxyl groups even more (Sun et al. 2014). This makes the chemical glycosylation difficult.

In this work *E. coli* strains carrying GT1-family glycosyltransferases were used for the whole-cell biotransformation of flavonoids. The enzymes used in this study are able to glycosylate flavonoids by using dTDP-rhamnose and transferring the sugar residues to hydroxyl groups at different positions of the polyphenol (Fig. 1.5).

A specific feature of the used glycosyltransferases is that they are able to rhamnosylate the 5-O-position of the flavonoid. The 5-O-position is an unusual glycosidic linkage, which doesn't commonly occur in nature and is a challenging target in chemical synthesis, since the C-5 hydroxyl group forms intramolecular hydrogen bonds with the adjacent C-4 carbonyl group (Liao et al. 2016, Sun et al. 2014).

The formation of dTDP-rhamnose in the cells can be enhanced by the overexpression of the relevant enzymes of the dTDP-rhamnose synthesis pathway to improve the glycosylation rate (Fig. 1.5). The activated rhamnose, dTDP-L-rhamnose, is synthesized from deoxythymidine triphosphate (dTTP) and glucose-1-phosphate (G-1-P). Thymidine triphosphate is formed from thymidine by three successive ATP-dependent phosphorylations catalyzed by the enzymes thymidine kinase (TK), thymidylate kinase (TMK), and nucleotide diphosphate kinase (NDK) (White-Phillip et al. 2009). In the first reaction of the dTDP-rhamnose synthesis pathway, G-1-P thymidylyltransferase (RmlA) transfers dTTP to G-1-P. Then the dTDP-D-glucose 4,6-dehydratase (RmlB) catalyzes the oxidation and dehydration of dTDP-D-glucose to form dTDP-4-keto-6-deoxy-D-glucose. The dTDP-4-dehydrorhamnose 3,5-epimerase (RmlC) converts dTDP-4-keto-6-deoxy-D-glucose to dTDP-4-keto-L-rhamnose, which is finally reduced to dTDP-L-rhamnose by the dTDP-4-dehydrorhamnose reductase (RmlD) (Teramoto et al. 2012).

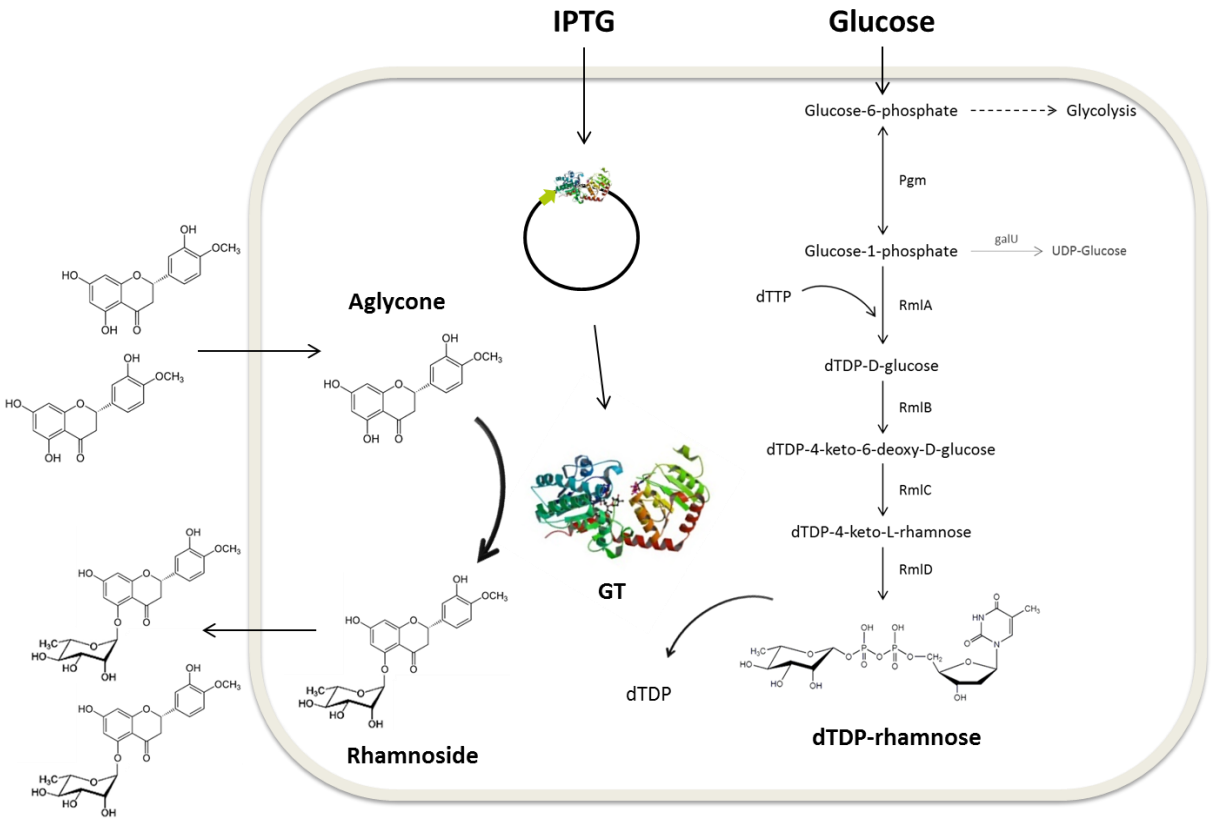

Figure 1.5: Whole-cell rhamnosylation of flavonoids in *E. coli*. The production of the recombinant glycosyltransferase (GT) is induced by IPTG. The GT transfers dTDP-rhamnose to the free hydroxyl-groups of the flavonoid and is able to attach the 5-O-position. For cell growth, but also for the co-factor dTDP-rhamnose, the cell needs glucose as carbon source.

1.6 Outer membrane protein TolC

In this work the overexpression of the outer membrane protein TolC was implemented for improved production of the flavonoid-rhamnoside N5R. TolC is a membrane channel that is involved in the export of small molecules and toxins across the outer membrane of gram-negative bacteria like *E. coli*. In whole-cell biotransformation the glycosylated flavonoids are transported out of the cell and as an extracellular product they can easily be separated from the cells for further purification. An overexpression of TolC may enhance the transport of flavonoid-glycosides into the supernatant.

TolC consists of a trimeric structure comprising an outer membrane beta-barrel and an alpha-helical barrel that extends into the periplasm (Fig. 1.6). The part of TolC that is embedded in the outer membrane is a 12-stranded beta-barrel, which is made from an oligomeric structure where each protomer constitutes only a third of the beta-strands. The periplasmic part is

almost entirely made of alpha-helices. The helices are up to 100 Å long and form a cylindrical architecture, which is dense packed with inwards curved coiled-coil helices and nearly sealed (Fig. 1.6, A). For the passage of large molecules up to 160 kDa TolC undergoes a conformational transition to form a tunnel entrance (Fig. 1.6, B) (Federici et al. 2004, Zgurskaya et al. 2011).

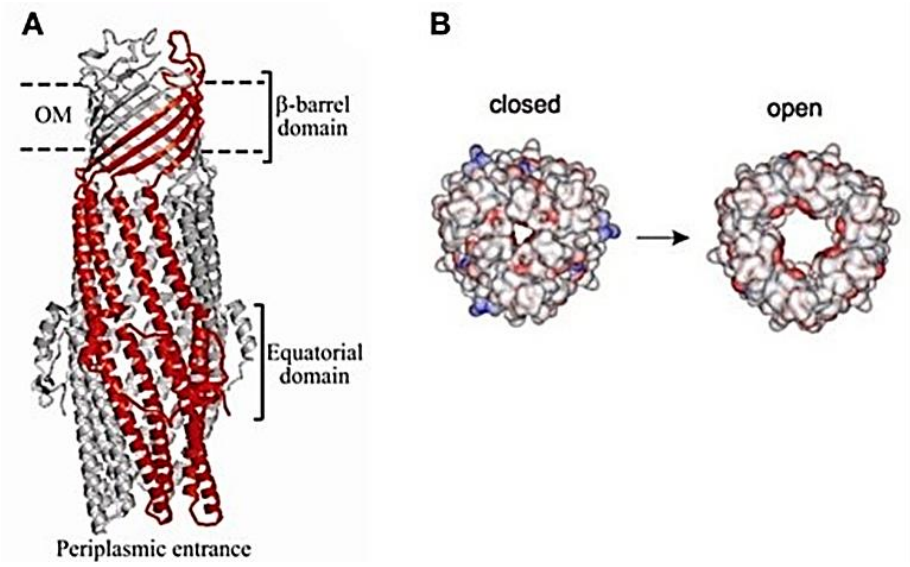

Figure 1.6: Structure of TolC. (A) Ribbon representation of TolC homotrimer. One monomer is highlighted in red. (B) The proposed mechanism of TolC transition into the open state. Space-filled model visualization of the closed and modeled open state of the tunnel entrance, viewed from the periplasm. (Figure from Zgurskaya et al. 2011, modified).

Normally, target compounds that are produced in recombinant *E. coli* cells accumulate intracellularly and even if the product is secreted by the cells, like glycosylated flavonoids, high production rates can lead to high levels of product concentration in the cells where the efflux is saturated. Overexpression of multi-drug efflux pumps can increase the efflux of the product (Zhang et al. 2016).

Multi-drug efflux pumps expressed by gram-negative bacteria are usually composed of three subunits. The inner and outer subunits are linked by a periplasmic accessory protein. The inner membrane unit is a transport protein, which binds the substrate from within the phospholipid bilayer of the inner membrane or from the cytoplasm and exports it through the outer membrane channel TolC (Fig. 1.7, Piddock 2006).

In gram-negative bacteria there are three families of efflux transporters: the resistance nodulation division (RND) family, the ATP-binding cassette (ABC) superfamily and the

major facilitator superfamily (MFS) (Fig. 1.7, Piddock 2006). Efflux through MFS and RND family transporters is driven by proton motive force, whereas the efflux of ABC pumps is driven by ATP hydrolysis. ABC family transporters (e.g. MacAB-TolC) can transport macrolides like many antibiotics and drugs across the cellular membrane. MFS transporters (e.g. EmrAB- or EmrKY-TolC) are capable of transporting small hydrophobic compounds and RND transporters (e.g. AcrAB- or AcrAD-TolC) can export various drugs and other molecules out of the cell (Piddock 2006, Zhang et al. 2016).

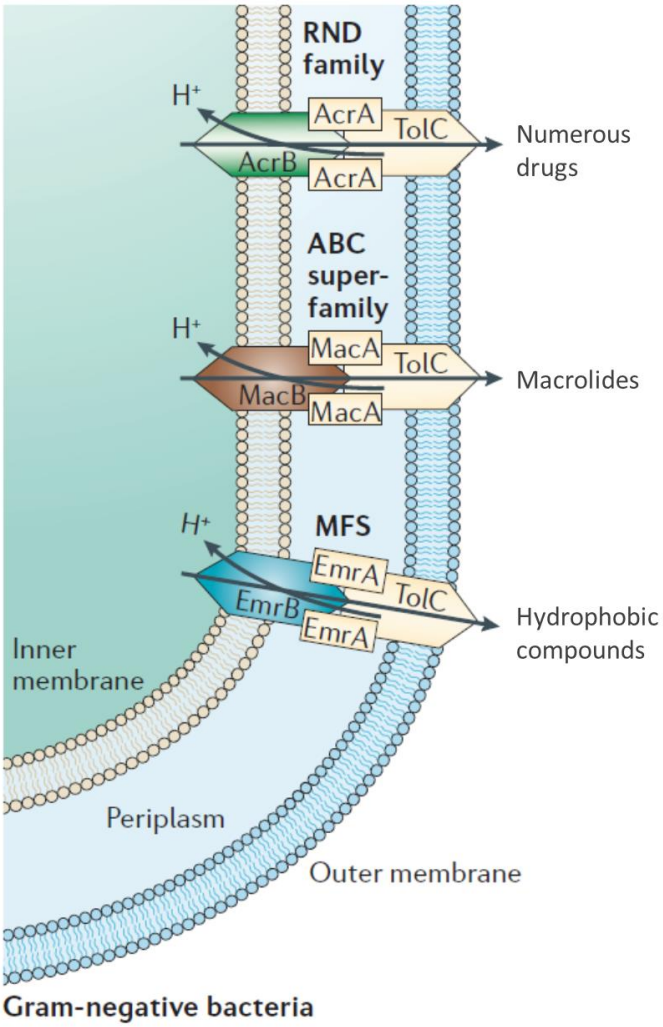

Figure 1.7: Multidrug-resistance efflux pumps. There are three families of multidrug-resistance efflux pumps in gram-negative bacteria: the resistance nodulation division (RND) family, the ATP-binding cassette (ABC) superfamily and the major facilitator superfamily (MFS). For each family a common example of the individual proteins are shown. The outer membrane protein is typically TolC. (Figure from Piddock 2006, modified).

1.7 Bioprocess engineering

In recent years, industrial bioprocesses became more important due to an increasing amount of biotechnological products such as food supplements, pharmaceuticals, cosmetics or fine chemicals. The field of bioprocess engineering includes the development, optimization and operation of manufacturing processes that uses whole cells or biological components (e.g. enzymes) to produce biotechnological products. Therefore, a detailed understanding of the complex mechanism of cell growth and product formation is necessary. On- and off-line monitoring of the bioprocess enables large amounts of data to analyze the cell metabolism, substrate consumption and product formation. For development and optimization of bioprocesses mathematical models play an important role. These models help to understand complex interactions between microorganisms and their environment in a bioreactor.

1.7.1 Microbial growth kinetics

An important parameter in microbial fermentation is the growth rate, which describes the change of biomass concentration c_X over time t. Under non-limited conditions the growth rate is proportional to the biomass (Chmiel 2011):

$$\frac{dc_X}{dt} = \mu \cdot c_X \tag{3.1}$$

c_X: biomass, g L^{-1}
t: time, h
μ: specific growth rate, h^{-1}

The specific growth rate μ is defined as:

$$\mu = \frac{1}{c_X} \cdot \frac{dc_X}{dt} \tag{3.2}$$

In defined medium the growth rate depends on one substrate, normally the carbon source. The correlation of the growth-limited substrate c_S and the specific growth rate μ can be described by the Monod equation (Chmiel 2011):

$$\mu = \mu_{max} \cdot \frac{c_S}{c_S + K_S} \tag{3.3}$$

μ_{max}: maximal specific growth rate, h^{-1}
c_S: substrate concentration, g L^{-1}
K_S: saturation constant of the limiting substrate, g L^{-1}

The maximal specific growth rate μ_{max} is reached when the substrate concentration c_S is much higher than the saturation constant K_S, which is defined as the substrate concentration where the specific growth rate μ is half the maximal specific growth rate μ_{max}.

The definition of production rate and substrate uptake rate are similar to the growth rate (Chmiel 2011):

$$\frac{dc_P}{dt} = q_P \cdot c_X \tag{3.4}$$

c_P: product concentration, g L^{-1}
t: time, h
q_P: specific production rate, g g^{-1} h^{-1}
c_X: biomass, g L^{-1}

$$\frac{dc_S}{dt} = q_S \cdot c_X \tag{3.5}$$

c_S: substrate concentration, g L^{-1}
t: time, h
q_S: specific substrate uptake rate, g g^{-1} h^{-1}
c_X: biomass, g L^{-1}

The substrate concentration c_S can be put into correlation with the biomass c_X over the biomass yield $Y_{X/S}$, which is defined as the produced biomass per utilized substrate (Chmiel 2011):

$$Y_{X/S} = \frac{dc_X}{dc_S} = \frac{\mu}{q_S} \tag{3.6}$$

$Y_{X/S}$: biomass yield, g g^{-1}

For cell growth only, the growth rate and the substrate uptake rate are described by the biomass yield. This can be extended by the term of substrate utilization for the maintenance metabolism m_S and for production $q_{S/P}$ (Chmiel 2011):

$$q_S = \frac{\mu}{Y_{X/S}} \tag{3.7}$$

$$q_S = \frac{\mu}{Y_{X/S}} + m_S + q_{S/P} \tag{3.8}$$

m_S: substrate uptake for maintenance metabolism, g g^{-1} h^{-1}
$q_{S/P}$: substrate uptake for production, g g^{-1} h^{-1}

The production yield $Y_{P/S}$, product formation per utilized substrate, or cell-specific production yield $Y_{P/X}$, is an important factor for the development of a cost-effective production process (Chmiel 2011):

$$Y_{P/S} = \frac{dc_P}{dc_S} = \frac{q_P}{q_S} \tag{3.9}$$

$$Y_{P/X} = \frac{c_P}{c_X} \tag{3.10}$$

The aim of bioprocess development and optimization is to reach high cell densities with high specific production yields within minimum use of substrate and low costs for the culture medium.

1.7.2 Mass balance of ideal stirred tank bioreactors

An ideal bioreactor is defined as a bounded volume, which is perfectly mixed with homogeneous conditions throughout the system. Bioreactors can be operated as a closed system (batch reactor), where no mass enters or leaves, a semi-open system (fed-batch), where mass enters but doesn't leave, and an open system (continuous flow), where mass enters and leaves (Chmiel 2011).

The stirred tank bioreactor is the most commonly used type of bioreactors. It is shown schematically in Fig. 1.8. It is a tank with a rotating shaft for mixing and a height/diameter proportion of 2 to 3 for an optimal ratio of surface to volume. Air is pumped into the bioreactor over a sparger at the bottom of the reactor near to the stirrer, so that the supplied oxygen has a longer retention time and can be better exploited. A typical stirrer type for fermentations of microorganisms is the Rushton turbine, a radial flow impeller (Chmiel 2011).

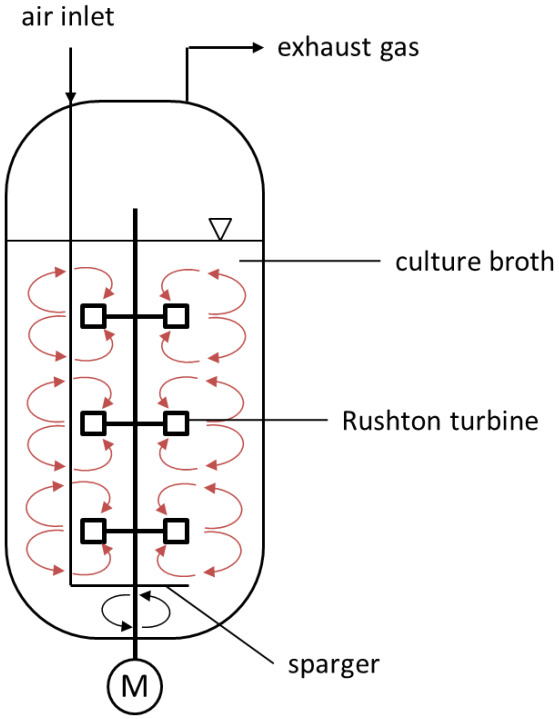

Figure 1.8: Schematically diagram of a stirred tank bioreactor (STR) with Rushton turbines for the fermentation of microorganisms (modified after Chmiel 2011).

After Chmiel (2011) the mass balance equation for an ideal stirred tank reactor (STR) can be described as:

Mass change of a component over the time in the system	=	Fed mass of a component over the time in the system	-	Removed mass of a component over the time in the system	+	Transformed mass of a component over the time in the system

or

$$\frac{dm}{dt} = \frac{d[c \cdot V]}{dt} = F_{in} \cdot c_{in} - F_{out} \cdot c_{out} + r \cdot V \quad (3.11)$$

m: mass of the component in the bioreactor
V: volume of the bioreactor, L
c: concentration of the component, g L^{-1}
F: flow, L h^{-1}
r: reaction rate, g L^{-1} h^{-1}

1.7.2.1 Batch process

In a batch process after inoculation of the culture medium no liquid is supplied or released from the bioreactor, with the exception of small amounts of acid or base for pH regulation and anti-foam. Gassing and exhaust air are excluded. So the flows F_{in} and F_{out} are zero and the reactor volume V stays constant. During cell growth the concentration of utilized substrates, cells and product(s) are changing over the time. Based on these assumptions the mass balance equation (3.11) can be shortened to the following concentration balance (Chmiel 2011):

$$\frac{dc_i}{dt} = r_i \quad (3.12)$$

After the Monod model the cell growth in a batch fermenter undergoes four different growth phases (Fig. 1.9). First after inoculation the cells are in a short lag phase (phase I) for adaptation to their environment and then start to grow (phase II).

Without any limitation or inhibition the growth rate μ is maximal and the cell growth is exponential (Chmiel 2011):

$$c_X = c_{X,0} \cdot e^{(\mu_{max} \cdot t)} \quad (3.13)$$

$c_{X,0}$: initial biomass concentration, g L^{-1}

Due to consumption of the carbon source (and other nutrients) and production of metabolites the cell growth is limited and/or inhibited. The growth rate decreases and the exponential growth phase ends. In the stationary phase (phase III) the growth rate and the mortality rate are equal and the biomass concentration is constant. After a certain time the substrate is depleted and the mortality rate becomes greater than the growth rate. The biomass concentration decreases (phase IV).

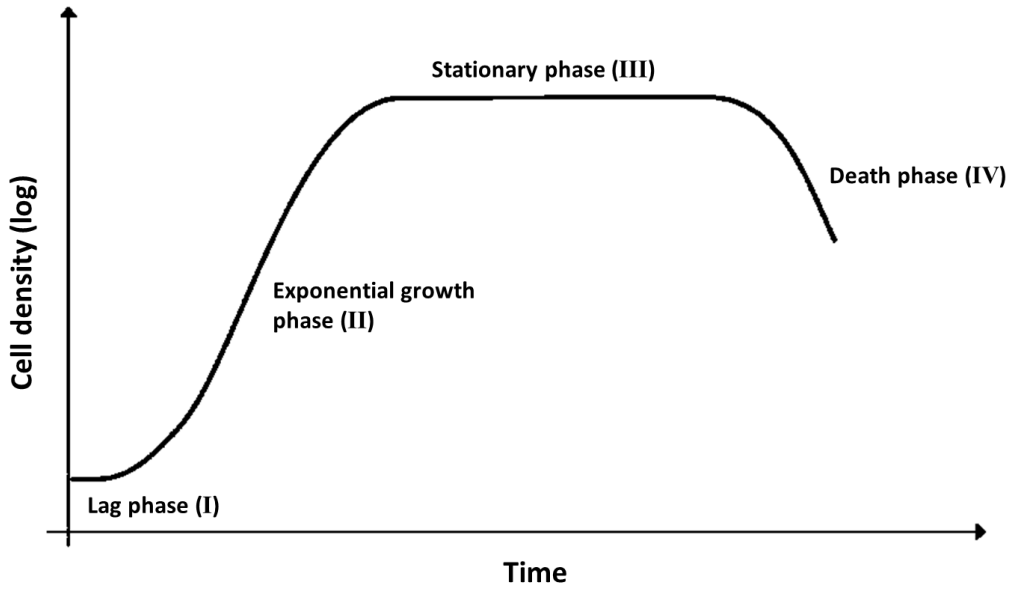

Figure 1.9: Phases of cell growth in microbial batch cultures (modified after Monod 1949).

In industrial processes batch cultures are often used as pre-culture for inoculation of the main culture and are harvested during the exponential growth phase for high cell viability.

1.7.2.2 Continuous process

In continuous cultivations fresh medium is added to the bioreactor and culture broth is removed from the bioreactor at the same rate. So the reactor volume is kept constant over the cultivation time (steady state) and the biomass concentration c_X, substrate concentration c_S and product concentration c_P are constant (Chmiel 2011). The mass balance equation (3.11) can be reformulated into following equation:

$$\frac{d[c \cdot V]}{dt} = 0 = F_{in} \cdot c_{in} - F_{out} \cdot c_{out} + r \cdot V \quad (3.14)$$

In a steady state with constant volume the flows in and out of the reactor are $F_{in} = F_{out} = F$ and the specific flow is defined as the dilutation rate D (Chmiel 2011):

$$D = \frac{F}{V} \quad (3.15)$$

This results in the following mass balance for steady state (Chmiel 2011):

$$r = D \cdot (c_{out} - c_{in}) \quad (3.16)$$

Under these conditions the process time can be extended. This improves the process efficiency due to reduced operation costs and reactor downtimes for cleaning and sterilization.

1.7.2.3 Fed-batch process

Fed-batch fermentations are semi-open and combine the simplicity of a batch with the advantages of extended process times like in continuous cultures. In a fed-batch a feed-solution with usually highly concentrated substrate is added to the culture.

So the culture volume is not constant and $F_{in} > 0$, but $F_{out} = 0$. This results in the following equation (Chmiel 2011):

$$\frac{dm}{dt} = \frac{d[c \cdot V]}{dt} = c \cdot \frac{dV}{dt} + V \cdot \frac{dc}{dt} = F_{in} \cdot c_{in} + r \cdot V \quad (3.17)$$

The volume inflow F_{in} can be equated to the volume change in the bioreactor over the time:

$$F_{in} = \frac{dV}{dt} \quad (3.18)$$

$$\frac{dc}{dt} = \frac{F_{in}}{V} \cdot (c_{in} - c) + r \tag{3.19}$$

Fed-batch fermentations are often used for industrial production processes for achievement of high cell densities. To avoid overflow metabolism (accumulation of partially oxidized catabolites such as acetate and ethanol) due to excess of carbon source and high oxygen demand due to unlimited growth, the fermentation is controlled by feeding the carbon source to achieve C-limited growth. Normally the fermentation starts with low concentration of the limiting substrate (e.g. glucose) and after consumption the substrate is fed to the culture, so that the substrate concentration in the culture is nearly zero, $\frac{dc_S}{dt} = 0$ (Chmiel 2011).

This results in:

$$F_{in} = \frac{V \cdot r_S}{(c_{S,in} - c_S)} \tag{3.20}$$

Under substrate-limited growth conditions the growth rate is smaller than μ_{max} and the substrate concentration c_S in the bioreactor is significantly smaller than the concentration in the feed $c_{S,in}$. So c_S is negligible and can be ignored. With $r_S = \frac{dc_S}{dt} = q_S \cdot c_X$ (3.5), $q_S = \frac{\mu}{Y_{X/S}}$ (3.7) and $c_X = c_{X,0} \cdot e^{(\mu \cdot t)}$ (3.13), an exponential feed profile can be calculated by following equation (Chmiel 2011):

$$F_{in} = \frac{\mu}{c_{S,in} \cdot Y_{X/S}} \cdot V_0 \cdot c_{X,0} \cdot e^{(\mu \cdot t)} \tag{3.21}$$

V_0: volume of the bioreactor at the end of batch phase (feed start), L
$c_{X,0}$: biomass concentration at the end of batch phase (feed start), g L^{-1}

The glucose-limited fed-batch is a simple strategy to obtain high cell densities and increase volumetric productivity due to extended cultivation periods and therefore the most commonly used standard process in industrial scale fermentations.

1.7.2.4 Oxygen mass transfer in bioreactors

High cell density fermentations usually have a high oxygen demand. Due to the low solubility of oxygen and insufficient mixing in large scale fermentation processes, the oxygen supply is one of the most important process parameters in aerobic bioprocesses. In bioreactors the oxygen is transferred from air bubbles dispersed into the liquid culture medium.

The oxygen uptake rate (OUR) is defined as (Chmiel 2011):

$$OUR = q_{O_2} \cdot c_X \tag{3.22}$$

q_{O2}: specific oxygen uptake rate, g g^{-1} h^{-1}
c_X: biomass concentration, g L^{-1}

After the two-film theory of Lewis and Whitman (1924) the oxygen transfer rate (OTR) can be described by the concentration gradient in the liquid film at the phase boundary interface between the gas and the liquid ($c^*_{O2,L} - c_{O2,L}$), as well as the diffusion coefficient through the liquid film k_L and the specific gas-liquid interface area a (Chmiel 2011):

$$OTR = k_L a \cdot (c^*_{O2,L} - c_{O2,L}) \tag{3.23}$$

k_La: volumetric oxygen transfer coefficient, h^{-1}
$c^*_{O2,L}$: oxygen concentration in liquid at liquid-gas interface, g L^{-1}
$c_{O2,L}$: oxygen concentration in liquid phase, g L^{-1}

The volumetric oxygen transfer coefficient k_La is an important value for the oxygen supply of cell cultures. It is dependent on the bioreactor characteristics and can be useful for the comparison of different bioreactors regarding the oxygen transfer, e.g. for scale-up of fermentation processes from a small bioreactor in laboratory scale to a large fermenter in production scale (Chmiel 2011).

1.8 Downstream processing

The downstream processing (DSP) follows after the fermentation process (USP) for purification of the product. After harvest of the culture broth the further steps in the DSP are depending on the specific product and its application.

1.8.1 Tangential flow filtration

In this work after production of glycosylated flavonoids in an *E. coli* fermentation, the cells had to be separated from the supernatant since the flavonoid-glycosides are an extracellular product. This was done by tangential flow filtration through a 0.2 µm filter membrane. Tangential flow filtration (TFF) or cross-flow filtration is a rapid and efficient separation method in biotechnological industry. It can be used for concentration, diafiltration, and separation of large from small biomolecules, for removal of cells from fermentation broths or to clarify cell lysates (*https://laboratory.pall.com/content/dam/pall/laboratory/literature-library/non-gated/id-34212.pdf* – retrieved March 2019). Depending on the pore size of the membrane, it can be classified in a microfiltration and an ultrafiltration process. Microfiltration with pore sizes between 0.1 µm and 10 µm is normally used for clarification or cell harvesting. Ultrafiltration membranes with smaller pore sizes than 0.1 µm are used for concentrating and desalting processes (*https://laboratory.pall.com/content/dam/pall/laboratory/literature-library/non-gated/id-34212.pdf* – retrieved March 2019).

The principle of TFF is that the sample fluid flows through a feed channel across the surface of the membrane as well as through the membrane. The crossflow prevents the surface from larger particles that form a membrane clogging gel that can cause fouling. This makes the TFF faster and more efficient than the Dead-end filtration. Smaller particles can move through the membrane pores. The flow through the membrane (permeate) is separated, while the retentate is recirculated back to the feed reservoir and mixed with the sample fluid (*https://laboratory.pall.com/content/dam/pall/laboratory/literature-library/non-gated/id-34212.pdf* – retrieved March 2019).

One important process variable in tangential flow filtration is the transmembrane pressure (TMP). The TMP is the force that drives fluid containing permeable particles through the membrane. The fluid flowing through the feed channel creates a pressure drop in the membrane between the feed (membrane inlet) and the retentate (membrane outlet). This pressure is the TMP:

$$\mathrm{TMP} = \left(\frac{\mathrm{P_{Feed} - P_{Retentate}}}{2}\right) - \mathrm{P_{Permeate}} \quad (3.24)$$

The TMP can be regulated by the crossflow rate or by constricting the tubing of the retentate to reduce the retantate flow. For an efficient TFF process the TMP and the crossflow rate should be regulated to prevent the membrane from fouling and allow a greater volume of product to be processed per unit area of the membrane surface (*https://laboratory.pall.com/content/dam/pall/laboratory/literature-library/non-gated/id-34212.pdf* – retrieved March 2019).

1.8.2 Reversed-phase HPLC

High performance liquid chromatography (HPLC) is a method of high versatility and sensitivity for analytical approaches or purification of molecules. Instead of polar stationary phases (normal-phase HPLC), in reversed-phase HPLC silica-bonded non-polar stationary phases are used for the separation of molecules due to their polarity (Horváth 1981). Reversed-phase HPLC has been used in this project for the analytical and preparative separation of small molecule hydrophobic polyphenols and polyphenol-glycosides.

Reversed-phase chromatography can be applied for a variety of compounds spanning a wide range of size, polarity, and iconicity and therefore has proved to be the method of choice for the analysis and purification of biological samples (Horváth 1981, Poole 2019).

The most commonly used stationary phases in reversed-phase chromatography are modified silica gels with C8- or C18-chains, which are highly hydrophobic. The mobile phase is normally a mixture of water or aqueous buffer solution and an organic solvent like acetonitrile or methanol. The retention of molecules depends on their polarity, which means their solubility in the polar mobile phase and their hydrophobic interaction to the non-polar stationary phase (Horváth 1981).

Still, after years of development the retention mechanism for reversed-phase HPLC remains a matter of conjecture (Poole 2019). Several variable factors that affect the retention of molecules in reversed-phase HPLC do not allow a simple mathematical description of the retention mechanism and it is not certain whether the distribution of compounds between the mobile phase and the stationary phase is a partition or adsorption process or a combination of both (Poole 2019, Poole and Lenca 2017). So there are many different models trying to

describe the retention mechanism of reversed-phase chromatography (Horváth 1981, Melander and Horváth 1984, Poole 2019).

1.8.3 Solid-phase extraction

Solid-phase extraction is similar to HPLC a separation method, where a liquid sample passes through a sorbent. Unlike HPLC, which is operated under high pressure up to 400 bar, solid-phase extraction is used under much lower pressures of 5 to 20 bar depending on the size of the column (*https://www.mn-net.com/tabid/10362/default.aspx* – retrieved March 2019).
Within the framework of this work, reversed-phase material was used as sorbent in flash chromatography to purify glycosylated flavonoids. Reversed-phase materials are suitable for the separation of hydrophobic compounds like flavonoids. The target substance is retained on the sorbent and can be eluted in a small volume of the more polar organic solvent-water mixture, so that the substance is concentrated (Marce´ and Borrull 2000).

1.8.4 Lyophilization

Lyophilization (or freeze-drying) is a common process for making solid pharmaceutical and biological products (Rey and May 2010). The lyophilization process consists of two major steps, the freezing of the aqueous product solution and the drying under vacuum (divided in primary drying and secondary drying). During the freezing step the liquid sample becomes solid, either crystalline, amorphous, or glass. In the next step, the primary drying, the sublimation takes place. The frozen material is placed under vacuum and thereby progressively heated to deliver enough energy for the ice to sublimate (Rey 2010). In this critical step a correct balance between heat input and water sublimation is needed, so that drying the frozen material can proceed without adverse reactions such as back melting, puffing, or collapse (Rey 2010). The secondary drying, where all frozen water is removed, is the desorption phase. In this step the sample is exposed to temperatures above zero and a higher vacuum for extraction of bound water (Rey 2010).
After lyophilization the product remains unchanged as a stable solid. It is a preferred method for gentle processing of temperature-sensitive substances (Rey 2010).

1.9 State of research and intention of this work

In this work a fermentation process with downstream part for product separation was developed for production of the flavonoid-glycosides of hesperetin and naringenin in recombinant *E. coli* with glycosyltransferase family 1 GTs. Enzymes of the GT family 1 catalyze the glycosylation of small hydrophobic molecules like polyphenols (Bowles 2006). The enzymatic glycosylation of polyphenols by GTs is an efficient alternative to difficult chemical glycosylation reactions (Sun et al. 2014). Polyphenols have a low water solubility and therefore a low bioavailability, which is a great disadvantage in cosmetic or pharmaceutical applications. The glycosylation enhanced their bioavailability (Simkhada et al. 2010, Ahn et al. 2009, Bowles et al. 2005).

In previous work could be shown that metagenome-derived family 1 GTs from the sediment of the river Elbe can be used to glycosylate flavonoids in a whole-cell biotransformation in *E. coli* (Rabausch et al. 2013). Rabausch *et al.* had the assumption that the enzyme GtfC transfers dTDP-activated sugars, e.g., dTDP-rhamnoside. Results showed that glucose, rhamnose, and a third sugar residue (molecular weight of 446) were transferred by GtfC in biotransformations in *E. coli* cells. As part of the dTDP-sugar biosynthesis pathway the activated sugars dTDP-α-D-glucose, dTDP-4-keto-6-deoxy-α-D-glucose, dTDP-4-keto-β-L-rhamnose, and dTDP-β-L-rhamnose are present in *E. coli* and are potentially donors for the GtfC in whole-cell biotransformation (Rabausch et al. 2013).

The enzyme GtfC was used during this work for the glycosylation of the flavonoids hesperetin and naringenin. Products of the biotransformation with GtfC are the rhamnosides hesperetin-5-O-α-L-rhamnoside and naringenin-5-O-α-L-rhamnoside, as well as hesperetin-3'-O-α-L-rhamnoside and naringenin-4'-O-α-L-rhamnoside. Additionally the flavones chrysin and diosmetin as well as the isoflavone biochanin A were rhamnosylated with GtfC to characterize the glycosylation positions at different substrates. It could be shown that GtfC is able to rhamnosylate the 5-O-position, which is an unusual modification in nature (Sun et al. 2014). The produced novel flavonoid-5-O-rhamnosides are to my best knowledge not described so far. Most glycosylations of polyphenols are at the 3-O-position (Bowles et al. 2005, Ko et al. 2006, Ahn et al. 2009, Simkhada et al. 2010, Kim et al. 2012, de Bruyn et al. 2015a).

The production titers in whole-cell biotransformations were previously very low (Tab. 1.1). As host for the glycosylation of flavonoids usually metabolic engineered *E. coli* strains are used, overexpressing the activated sugar and the recombinant GT. Most groups worked with UDP-glycosyltransferases from *Arabidopsis thaliana* (Tab. 1.1). Some have overexpressed

biosynthetic gene clusters not only in order to increase the intracellular level of activated sugars, but also to synthesize activated sugars that are normally not available in *E. coli*, like UDP-xylose (Simkhada et al. 2009, Pandey et al. 2013, Han et al. 2014). In most approaches the generation of glucose 1-phosphate as precursor for UDP-glucose is optimized by gene knockout of metabolic reactions and the pool of UDP-glucose is increased by overexpression of *galU* (Simkhada et al. 2009, Pandey et al. 2013).

Table 1.1: Overview of flavonoid glycosylation by glycosyltransferases of family GT 1 in whole-cell biotransformation in *E. coli* – state of the art. Production titers beyond 1 g/L are bolded.

Product	GT	Source	Aglycone	Activated sugar	Titer [g/L]	Reference
Quercetin-3-O-glucoside	UGT73B3	*Arabidopsis thaliana*	Quercetin	UDP-glucose	0.099	Lim et al. 2004
Quercetin-3-O-rhamnoside	UGT78D1	*Arabidopsis thaliana*	Quercetin	UDP-rhamnose	0.184	Lim et al. 2006
Genistein-7-O-glucoside	UGT71G1	*Medicago truncatula*	Genistein	UDP-glucose	0.018	He et al. 2008
Biochanin-7-O-glucoside	UGT71G1	*Medicago truncatula*	Biochanin	UDP-glucose	0.013	
Quercetin-3-O-glucoside	UGT71G1	*Medicago truncatula*	Quercetin	UDP-glucose	0.02	
Kaempferol-3-O-glucoside	UGT71G1	*Medicago truncatula*	Kaempferol	UDP-glucose	0.019	
Luteolin-4'-O-glucoside	UGT73C8	*Medicago truncatula*	Luteolin	UDP-glucose	0.016	
Luteolin-7-O-glucoside	UGT73C8	*Medicago truncatula*	Luteolin	UDP-glucose	0.009	
Naringenin-7-O-xyloside	ArGT4	*Arabidopsis thaliana*	Naringenin	UDP-xylose	-	Simkhada et al. 2009
Quercetin-3-O-rhamnoside	ArGT3	*Arabidopsis thaliana*	Quercetin	TDP-rhamnose	0.024	Simkhada et al. 2010
Kaempferol-3-O-rhamnoside	ArGT3	*Arabidopsis thaliana*	Kaempferol	TDP-rhamnose	0.013	
Quercetin-3-O-deoxyalloside	ArGT3	*Arabidopsis thaliana*	Quercetin	TDP-6-deoxyallose	-	
Quercetin-3-O-rhamnoside	UGT78D1	*Arabidopsis thaliana*	Quercetin	UDP-rhamnose	0.15	Kim et al. 2012
Kaempferol-3-O-rhamnoside	UGT78D1	*Arabidopsis thaliana*	Kaempferol	UDP-rhamnose	0.2	
Quercetin-3-O-deoxytaloside	UGT78D1	*Arabidopsis thaliana*	Quercetin	TDP-6-deoxytalose	0.098	Yoon et al. 2012
Kaempferol-3-O-glucoside	UGT78D2	*Arabidopsis thaliana*	Naringenin	UDP-glucose	0.023	Malla et al. 2013
Kaempferol-3-O-glucoside	UGT78K1	*Glycine max*	Naringenin	UDP-glucose	0.109	
Quercetin-3-O-xyloside	ArGT3	*Arabidopsis thaliana*	Quercetin	UDP-xylose	0.043	Pandey et al. 2013
Quercetin-3-O-glucoside-7-O-rhamnoside	UGT89C1	*Arabidopsis thaliana*	Quercetin-3-O-glucoside	UDP-rhamnose	0.02	Roepke et al. 2013
Myricetin-3-O-rhamnoside	ArGT3	*Arabidopsis thaliana*	Myricetin	TDP-rhamnose	0.026	Thuan et al. 2013a
Apigenin-7-O-glucoside	ArGT	*Arabidopsis thaliana*	Apigenin	UDP-glucose	0.039	Thuan et al. 2013b
Baicalein-7-O-glucoside	ArGT	*Arabidopsis thaliana*	Baicalin	UDP-glucose	0.033	
Quercetin-3-O-xyloside	UGT78D3	*Arabidopsis thaliana*	Quercetin	UDP-xylose	0.15	Han et al. 2014
Quercetin-3-O-arabinoside	UGT78D3	*Arabidopsis thaliana*	Quercetin	UDP-arabinose	0.158	
Quercetin-3-O-galactoside	F3GT	*Petunia hybrida*	Quercetin	UDP-galactose	0.94	De Bruyn et al. 2015b
Kaempferol-3-O-galactoside	F3GT	*Petunia hybrida*	Kaempferol	UDP-galactose	0.084	
Myricetin-3-O-galactoside	F3GT	*Petunia hybrida*	Myricetin	UDP-galactose	0.052	
Morin-3-O-galactoside	F3GT	*Petunia hybrida*	Morin	UDP-galactose	0.034	
Fisetin-3-O-galactoside	F3GT	*Petunia hybrida*	Fisetin	UDP-galactose	0.134	
Quercetin-3-O-rhamnoside	RhaGT	*Arabidopsis thaliana*	Quercetin	UDP-rhamnose	**1.176**	
Kaempferol-3-O-rhamnoside	RhaGT	*Arabidopsis thaliana*	Kaempferol	UDP-rhamnose	0.416	
Myricetin-3-O-rhamnoside	RhaGT	*Arabidopsis thaliana*	Myricetin	UDP-rhamnose	0.072	
Morin-3-O-rhamnoside	RhaGT	*Arabidopsis thaliana*	Morin	UDP-rhamnose	0.116	
Fisetin-3-O-rhamnoside	RhaGT	*Arabidopsis thaliana*	Fisetin	UDP-rhamnose	0.403	
Quercetin-3-O-galactoside	PhUGT	*Petunia hybrid*	Quercetin	UDP-galactose	0.280	Kim et al. 2015
Quercetin-3-O-glucuronide	AmUGT10	*Antirrhinum majus* or	Quercetin	UDP-glucuronic acid	0.687	
Luteolin-7-O-glucuronide	or VvUGT	*Vitis vinifera*	Luteolin	UDP-glucuronic acid	0.3	
Fisetin-3-O-glucoside	UGT78K1	*Glycine max*	Fisetin	UDP-glucose	0.393	Parajuli et al. 2015
Fisetin-3-O-rhamnoside	ArGT3	*Arabidopsis thaliana*	Fisetin	TDP-rhamnose	0.342	
Kaempferol-3-O-glucoside	UGT78D2	*Arabidopsis thaliana*	Kaempferol	UDP-glucose	**3.6**	Pei et al. 2016
Taxifolin-3-O-rhamnoside	ArGT3	*Arabidopsis thaliana*	Taxifolin	TDP-rhamnose	0.022	Thuan et al. 2017
Quercetin-3-O-rhamnoside	GtfC	metagenome-derived	Quercetin	TDP-rhamnose	**4.32**	Ruprecht et al. 2019
Hesperetin-3'-O-rhamnoside	GtfC	metagenome-derived	Hesperetin	TDP-rhamnose	**2.36**	
Kaempferol-3-O-rhamnoside	GtfC	metagenome-derived	Kaempferol	TDP-rhamnose	**1.92**	
Naringenin-5-O-rhamnoside	GtfC	metagenome-derived	Naringenin	TDP-rhamnose	**1.217**	Data from this work
Hesperetin-3'-O-rhamnoside	GtfC	metagenome-derived	Hesperetin	TDP-rhamnose	0.599	
Hesperetin-5-O-rhamnoside	GtfD	*Dyadobacter fermentans*	Hesperetin	TDP-rhamnose	**2.893**	
Naringenin-5-O-rhamnoside	GtfD	*Dyadobacter fermentans*	Naringenin	TDP-rhamnose	**2.631**	
Naringenin-4'-O-rhamnoside	GtfD	*Dyadobacter fermentans*	Naringenin	TDP-rhamnose	0.137	

De Bruyn *et al.* developed a growth coupled system for selective galactosylation and rhamnosylation by using an alternative sucrose metabolism for an increased glucose 1-phosphate synthesis as precursor for UDP-glucose. Sucrose is fed as carbon source to the fermentation and can be degraded by a sucrose phosphorylase into fructose to be used for growth and glucose 1-phosphate as precursor for UDP-glucose (De Bruyn et al. 2015b). With this strategy production titers of 1 g/L could be reached (Tab. 1.1, de Bruyn et al. 2015b).
Pei *et al.* also used a growth coupled glycosylation system on sucrose as carbon source with an optimized UDP-glucose synthesis pathway by integration of the enzymes sucrose permease, sucrose phosphorylase, sucrose phosphorylase, and uridylyltransferase, constantly producing glucose 1-phosphate for glycosylation of kaempferol to kaempferol-3-O-glucoside (Pei et al. 2016). Maximal production in this approach was 3.6 g/L (Tab. 1.1, Pei et al. 2016).

Within the scope of this work a fermentation process for production of flavonoid-rhamnosides in recombinant *E. coli* Rosetta gami 2 (DE3) strains overexpressing metagenome-derived GtfC was developed. The aim was to optimize the fermentation process to reach production titers above 1 g/L for naringenin- and hesperetin-5-O-rhamnosides. After glycosylation with GtfC wasn't sufficient for hesperetin-5-O-rhamnoside production, the enzyme GtfD from *Dyadobacter fermentans* was used and showed higher production titers above 2.5 g/L not only in hesperetin-5-O-rhamnoside production, but also in naringenin-5-O-rhamnoside production (Tab. 1.1). In parallel work Constantin Ruprecht developed a growth coupled glycosylation system with the glycosyltransferase GtfC in engineered *E. coli* K-12 MG1655 using dextrins of starch as carbon source. This enabled the production of flavonoid-3-O-rhamnosides in g/L scale (Tab. 1.1, Ruprecht et al. 2019).

2 Material & Methods

2.1 *Escherichia coli* strains and vectors

E. coli strains used in this work for biotransformation of flavonoids with glycosyltransferase GtfC or GtfD are listed in table 2.1. GtfC derived from a metagenomic library of the river Elbe (Rabausch et al. 2013) and GtfD is a glycosyltransferase from *Dyadobacter fermentans* (NCBI WP_015811417.1) (for protein sequences see appendix, A2).

Strains were constructed with Rosetta-gami 2 (DE3) competent cells from Novagen, except the MG1655 Δ*pgi* Δ*galU* Δ*rec::Mhex* constructed by Constantin Ruprecht from the wild type strain K12 MG1655 from DSMZ (No. 18039).

Table 2.1: *E. coli* strains and plasmids (plasmid maps see appendix, A3).

***E. coli* Strains**	**Genotype**	**Reference**
Rosetta gami 2 (DE3)	Δ(*ara-leu*)*7697* Δ*lacX74* Δ*phoA Pvu*II *phoR araD139 ahpC galE galK rpsL* (DE3) F'[*lac*$^+$ *lacI*^{q} *pro*] *gor522*::Tn*10 trxB* pRARE2 (Cam^R, Str^R, Tet^R)	Novagen
Rosetta gami GTC	Rosetta gami 2 (DE3), pET-19b::*gtfC* , pRSFDuet-1::*tmk* ::*ndk* , pCDFDuet-1::*rmlA* ::*rmlC*	within the project
Rosetta gami GTCopt	Rosetta gami 2 (DE3), pET-19b::*gtfC(opt)* , pRSFDuet-1::*tmk* ::*ndk* pCDFDuet-1::*rmlA* ::*rmlC*	within the project
Rosetta gami GTDopt	Rosetta gami 2 (DE3), pET-19b::*gtfD(opt)* , pRSFDuet-1::*tmk* ::*ndk* pCDFDuet-1::*rmlA* ::*rmlC*	within the project
K12 MG1655	F$^-$, lambda$^-$, *rph-1*	DMSZ
MG1655 pgi galU Mhex	K12 MG1655, Δ*pgi* Δ*galU* Δ*rec* ::*Mhex*	within the project
MG1655 pgi galU Mhex GTD	K12 MG1655, Δ*pgi* Δ*galU* Δ*rec* ::*Mhex* , pTrcHisA::*gtfD(opt)*	within the project
MG1655 pgi galU Mhex GTD TolC	K12 MG1655, Δ*pgi* Δ*galU* Δ*rec* ::*Mhex* , pTrcHisA::*gtfD(opt)* , pRSF-malZp::*tolC*	within the project
Plasmids	**Characteristics**	**Reference**
pET-19b	pBR322 origin, AmpR, *lacI* , T7 promotor	Novagen
pET-19b::*gtfC*	expression of GtfC under control of T7*lac*	within the project
pET-19b::*gtfC(opt)*	expression of codon optimized GtfC under control of T7*lac*	within the project
pET-19b::*gtfD(opt)*	expression of codon optimized GtfD under control of T7*lac*	within the project
pRSFDuet-1	RSF origin (RSF1030-derived), KanR, *lacI* , T7 promotor-1 and -2	Novagen
pRSFDuet-1::*tmk* ::*ndk*	coexpression of Tmk and Ndk under control of T7*lac*	within the project
pCDFDuet-1	CDF origin (CloDF13-derived), SmR, *lacI* , T7 promotor-1 and -2	Novagen
pCDFDuet-1::*rmlA* ::*rmlC*	coexpression of RmlA and RmlC under control of T7*lac*	within the project
pTrcHisA	pBR322 origin, AmpR, *lacI* , *trc* promotor	Invitrogen
pTrcHisA::*gtfD(opt)*	expression of codon optimized GtfD under control of *trc*	within the project
pRSF-malZp	RSF origin, KanR, *malZ* promotor	within the project
pRSF-malZp::*tolC*	expression of TolC under control of *malZ*	this work

2.2 Molecular biological methods

2.2.1 Plasmid isolation with the Presto™ Mini Plasmid Kit

Plasmid isolation was performed with the Presto™ Mini Plasmid Kit (Geneaid). Buffers and column were provided within the kit and were used as described in the manual. Cells from a small overnight culture were harvested by centrifugation of 1.5 mL of the culture at 14000 g for 1 minute at room temperature. The pellet was resuspended in 200 µL PD1 buffer containing RNase and 2 µL of TrueBlue lysis buffer. For cell lysis 200 µL PD2 buffer was added to the resuspended cells and mixed gently by inverting the tube 10 times. After 2 minutes at room temperature to ensure the lysate is homogeneous, 300 µL PD3 buffer was added for neutralization. The tube was immediately mixed by inverting 10 times and then centrifuged at 14000 g for 3 minutes at room temperature. Afterwards the supernatant was transferred onto the PDH column for DNA binding and centrifuged for 30 seconds at room temperature. The flow-through was discarded and the column was washed with 600 µL of wash buffer for plasmid DNA purification and then centrifuged at 14000 g for 30 seconds at room temperature. The flow-through was discarded. To dry the column matrix, the column was centrifuged at 14000 g for 3 minutes at room temperature. Then the purified plasmid DNA was eluted with 30 µL elution buffer (10 mM Tris-HCl, pH 8.5) by incubation at room temperature for 2 minutes to ensure complete absorption and then centrifugation for 2 minutes at 14000 g. The isolated plasmid was stored at -20°C. Plasmid DNA quantity and integrity were checked by agarose gel electrophoresis (2.2.7).

2.2.2 Polymerase chain reaction (PCR)

Polymerase chain reaction (PCR) was used within this work for amplification of the DNA fragment of the outer membrane protein TolC with genomic DNA of *E. coli* K12 MG1655 as template. The PCR product was analyzed using agarose gel electrophoresis (2.2.7) and further purified by GenepHlow™ PCR clean-up kit (2.2.8).

PCR was performed in a thermocycler with the *Pfu* DNA Polymerase, which is a fast and high fidelity DNA polymerase with proofreading activity. The applied primers with the respective melting temperature (T_m) are listed in table 2.2.

Table 2.2: PCR primers.

Primer	Sequence (5'-3')	T_m
FW_tolC_NcoI	ATACCATGGGCATGAAGAAATTGCTCCCCATTCT	68.3°C
RV_tolC_BamHI	TTCGGATCCTCAGTTACGGAAAGGGTTATGACC	69.5°C

The PCR reaction assay consisted of the following ingredients (Tab. 2.3):

Table 2.3: 50 µL PCR assay.

H_2O (demineralized)	38.5 µl
Pfu polymerase buffer (10x)	5 µl
dNTPs (100 mM) (dATP, dCTP, dGTP, dTTP)	2 µl
Forward primer (10 mM)	1 µl
Reverse primer (10 mM)	1 µl
Template DNA	1 µl
Pfu polymerase	0.5 µl

The performed PCR program of the Thermo-Cycler is shown in table 2.4.

Table 2.4: PCR conditions.

Initial denaturation	95°C	2 min	
Denaturation	95°C	30 sec	
Annealing	50°C	30 sec	x 30 cycles
Elongation	68°C	55 sec	
Final elongation	68°C	5 min	

2.2.3 Ligation

For ligation of a specific DNA fragment into a vector the ends of the vector and the PCR product were prepared with restriction enzymes. For the ligation of the tolC-fragment into pRSF-malZp the restriction enzymes NcoI and BamHI were used for restriction digestion. The digested DNA was analyzed by agarose gel electrophoresis (2.2.7) and then purified by gel extraction with the GenepHlow™ gel extraction kit (2.2.9).

The ligation was performed with the reaction mixture shown in table 2.5, incubating overnight at 4°C.

Table 2.5: 10 µL ligation reaction mixture.

Plasmid	1 µl
Insert (molar ratio insert:vector 1:1, 3:1, 5:1)	1, 3, 5 µl
Ligation buffer (10x)	1 µl
T4 DNA ligase	1 µl
H_2O (demineralized)	ad 10 µl

The ligation product was then transformed into *E. coli* DH5α competent cells via heat shock (2.2.4).

2.2.4 Heat shock transformation

For heat shock transformation 5 µL of the ligation product was added to 100 µL competent *E. coli* DH5α cells and incubated for 30 minutes on ice. The heat shock was performed at 42°C for 45 seconds. After that the cells were incubated on ice for 2 minutes before 250 µL SOC medium was added and cells were incubated for 45 minutes at 37°C.

The cells were plated on agar plates containing the appropriate antibiotic (kanamycin for the pRSF-malZp) and incubated overnight at 37°C. Potentially positive clones were analyzed by colony PCR (2.2.5).

2.2.5 Colony PCR

Colony PCR was performed to verify potential positive clones after transformation. The respective colonies were picked, suspended in 20 µL demineralized water and then heated up at 98°C. 1 µL of this suspension was added to the PCR reaction as template. The DCS polymerase was used and colony PCR was performed after the following reaction mixture (Tab. 2.6) and conditions (Tab. 2.7).

Table 2.6: 50 µL colony PCR assay.

H_2O (demineralized)	36.7 µl
Buffer B (10x)	5 µl
$MgCl_2$	3 µl
dNTPs (100 mM) (dATP, dCTP, dGTP, dTTP)	2 µl
Forward primer (10 mM)	1 µl
Reverse primer (10 mM)	1 µl
Template	1 µl
DCS polymerase	0.3 µl

Table 2.7: Colony PCR conditions.

Initial denaturation	95°C	2 min	
Denaturation	95°C	30 sec	
Annealing	50°C	30 sec	x 30 cycles
Elongation	72°C	1,5 min	
Final elongation	72°C	5 min	

2.2.6 Electroporation

Electroporation was performed with the Gene Pulser Xcell™ electroporation system (BioRad) for transformation of the plasmids pTrcHisA::*gtfD(opt)* and pRSF-malZp::*tolC* into *E. coli* K12 MG1655 Δ*pgi* Δ*galU* Δ*rec*::*Mhex*. For electroporation cells had to be in the exponential growth phase. Therefore cells were cultivated for 3 hours at 37°C and then 1.5 mL was harvested by centrifugation at 14000 g for 30 seconds at 2°C. All working steps were to proceed on ice. The pellet was washed three times with 1 mL glycerol (10%) and then centrifuged for 30 seconds at 2°C. Then the pellet was suspended in 50 µL glycerol (10%) and transferred into a electroporation cuvette. 1 µL of the respective plasmids were added and electroporation was performed at following conditions with 5 ms puls: 1350 V, 10 µF, 600 Ω. After that the cells were incubated in SOC medium for 2 hours at 37°C and then plated on LB agar plates for incubation overnight. Potential positive clones were picked and analyzed by colony PCR.

2.2.7 Agarose gel electrophoresis

Agarose gel electrophoresis was performed to analyze the size, quantity and integrity of DNA. Samples were supplemented with loading dye and loaded onto an agarose gel (0.8% (w/v) in TAE buffer (40 mM Tris, 20 mM acetic acid, and 1 mM EDTA)) placed in an electrophoresis gel chamber filled with TAE buffer. DNA fragments were separated at 120 V for 25 minutes. After that agarose gels were stained in ethidium bromide for 10 minutes and washed in water to remove excessive ethidium bromide. Visualization and documentation were carried out at the Molecular Imager® Gel Doc™ XR System (BioRad). The size of DNA fragments was determined by comparison with the GeneRuler™ 1 kb DNA Ladder (Thermo Scientific).

2.2.8 Purification of DNA with the GenepHlow™ PCR clean-up kit

DNA fragments were purified using the GenepHlow™ Gel/PCR Kit (Geneaid) according to the PCR clean-up protocol. All buffers were supplied within the kit.
For sample preparation 50 µL of a PCR reaction product was mixed with 5 volumes of the Gel/PCR buffer and then transferred onto the DFH column for DNA binding and centrifuged for 30 seconds at 14000 g. The flow-through was discarded and the column was washed by adding 600 µL wash buffer and letting stand for 1 minute. After centrifugation at 14000 g for 30 seconds and discarding the flow-through, the column was centrifuged for further 3 minutes to dry the column matrix. Purified DNA fragments were eluted with 20 µL elution buffer into a new sterile tube by incubation at room temperature for 2 minutes and centrifugation for 2 minutes at 14000 g. The purified PCR product was analyzed by agarose gel electrophoresis (2.2.7) and stored at 4°C until further use.

2.2.9 Gel extraction of DNA with the GenepHlow™ gel extraction kit

To purify single DNA bands from agarose gels (2.2.7) the GenepHlow™ Gel/PCR Kit (Geneaid) was used according to the gel extraction protocol. All buffers were supplied within the kit. The gel slice containing the DNA fragment was cut out the agarose gel with a scalpel and mixed with 500 µL of the Gel/PCR buffer. The sample mixture was incubated at 60°C for 10 minutes until the gel slice was completely dissolved. 800 µL of the sample mixture was transferred to the DFH Column to bind the DNA and centrifuged at 14000 g for 30 seconds. The flow-through was discarded and the column was washed. Therefore first 400 µL of W1

buffer was transferred to the DFH Column. After centrifugation at 14000 g for 30 seconds the flow-through was discarded and 600 µL of wash buffer was added into the DFH Column. The column had to be incubated in wash buffer for 1 minute and was then centrifuged at 14000 g for 30 seconds. To dry the column matrix after the washing, the column was centrifuged for 3 minutes at 14000 g. The column was transferred into a sterile tube and the purified DNA was eluted in 25 µL elution buffer by incubation at room temperature for 2 minutes and centrifugation for 2 minutes at 14000 g. The purified DNA fragment was stored at 4°C until further use.

2.2.10 Sequencing

Samples were sent to Eurofins Genomics for Sanger sequencing (Sanger et al. 1977). Therefore the plasmid DNA was purified (2.2.1) and then divided into two equal parts of 15 µL and premixed with 2 µL of the forward and reverse primer, respectively.

2.3 Media and feed solutions

The following media were used within this work for cultivation (Tab. 2.8).

Table 2.8: Culture media used within this study.

Medium	Component	Concentration	Supplier
SOC medium	Tryptone/ peptone	20 g/L	Roth
	Yeast extract	5 g/L	Roth
	Magnesium sulfate	4.8 g/L	Roth
	Glucose	3.6 g/L	Roth
	Sodium chloride	0.5 g/L	Roth
	Potassium chloride	0.188 g/L	Roth
Lysogeny broth (LB) medium	Yeast extract	5 g/L	Roth
	Tryptone/ peptone	10 g/L	Roth
	Sodium chloride	5 g/L	Roth
Terrific broth (TB) medium	Casein (enzymatically digested)	12 g/L	Roth
	Yeast extract	24 g/L	Roth
	K_2HPO_4	12.54 g/L	Roth
	KH_2PO_4	2.31 g/L	Roth
	50.8 g premixed powder + 4 mL/L glycerol		

M29 medium	Glucose	4 g/L	Roth
	Glycerol	10 g/L	Roth
	Magnesium sulfate	0.06 g/L	Roth
	Calcium chloride	0.017 g/L	Roth
	Sodium chloride	0.5 g/L	Roth
	Ammonium chloride	1.34 g/L	Merck
	K_2HPO_4	23.7 g/L	Merck
	KH_2PO_4	7.3 g/L	Merck
	Yeast extract	2.5 g/L	Roth
	Casein hydrolysate	2 g/L	Roth

For fed-batch cultivation the following feed solutions were used (Tab. 2.9).

Table 2.9: Feed solution used for fed-batch fermentations.

Feed	Component	Concentration	Supplier
Feed solution for use with TB medium	Glucose	500 g/L	Roth
	Magnesium sulfate	10 g/L	Roth
Feed solution for use with M29 medium	Glucose	500 g/L	Roth
	Magnesium sulfate	20 g/L	Roth
	Ammonium chloride	60 g/L	Merck
	Casein hydrolysate	4 g/L	Roth

In table 2.10 other supplements to the culture medium are listed.

Table 2.10: Supplements and titration solutions.

Component	Concentration in stock solution	Concentration in culture medium	Supplier
Anti-foam SE-15	10 %	varied	Sigma
IPTG	100mM	100 µM	Sigma
pH titration			
NH_3	25%	varied	Roth
NaOH	1 M	varied	Roth
H_3PO_4	1 M	varied	Roth
Antibiotics			
Ampicillin	100 g/L	100 mg/L	Roth
Kanamycin	50 g/L	50 mg/L	Roth
Streptomycin	25 g/L	25 mg/L	Roth
Spectinomycin	25 g/L	25 mg/L	Sigma

2.4 Fermentation (USP)

2.4.1 Cultivation in shake flasks

2.4.1.1 Biotransformation with *E. coli* Rosetta gami 2 (DE3)

For biotransformation in shake flasks Rosetta gami 2 (DE3) strains harboring a glycosyltransferase were inoculated from an overnight culture to an optical density (OD_{600}) of 0.1 in terrific broth medium (TB) containing the appropriate antibiotics and cultivated at 150 rpm and 28°C. After an OD_{600} of 1 was reached, the expression of the glycosyltransferase was induced with 100 µM Isopropyl β–D–1–thiogalacto-pyranoside (IPTG) and 1 g/L of the flavonoid-precursor was added to the culture. The biotransformation lasted 48 hours. Then the culture could be harvested for further HPLC purification of the produced flavonoid-glycosides (2.6.2) by centrifugation and sterile filtration of the supernatant. The concentration of the flavonoid-glycosides during fermentation was analyzed by HPLC (2.5.2) and/or UHPLC-MS-MS (2.5.3).

2.4.1.2 Biotransformation with *E. coli* MG1655 Δ*pgi*, Δ*galU*, Δ*rec::Mhex*

Fermentation of MG1655 Δ*pgi*, Δ*galU*, Δ*rec::Mhex* was carried out on dextrin (5%) for autoinduction of the expression of *gtfD* on pTrcHisA and *tolC* on pRSF-malZp. The flavonoid-precursor naringenin was added at the beginning of the fermentation with concentration of 5 g/L and the cultivation was performed as described above, but without addition of IPTG. Biotransformation lasted 72 hours. After every 24 hours a sample was taken for UHPLC-MS-MS (2.5.3) and solid dextrin (5%) was added.

2.4.2 Cultivation in benchtop parallel bioreactor system

Cultivations for parameter characterization and process development were carried out in benchtop 2-liter stirred tank bioreactors of the DASGIP® parallel bioreactor system (Eppendorf) (Fig. 2.1).

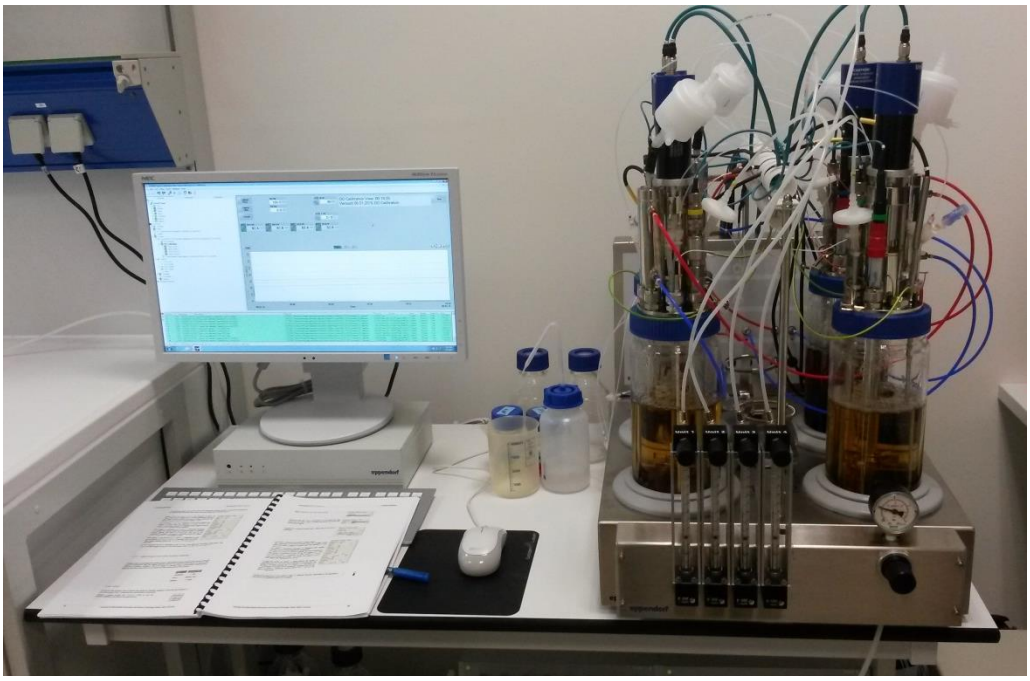

Figure 2.1: DASGIP® parallel bioreactor system (Eppendorf) with four 2-litre stirred tank bioreactors.

For biotransformations of flavonoids 0.5 liter-scale terrific broth (TB) medium containing the appropriate antibiotics was inoculated with *E. coli* cells of an overnight preculture in shake flasks (150 rpm, 28°C) to an OD_{600} of 0.1 and cells were grown at constant conditions of pH 7, a temperature of 28 °C and a stirrer controlled dissolved oxygen (DO) of 30 %. The pH was controlled using 25 % ammonia and 1 M phosphoric acid. To avoid foaming the addition of anti-foam SE-15 (Sigma) was triggered by a level sensor. The expression of the glycosyltransferase was induced by addition of 100 µM IPTG and 500 mg of the flavonoid-precursor was supplemented. During fermentation samples were taken for HPLC (2.5.2) and/or UHPLC-MS-MS (2.5.3) and every 24 hours 500 mg of the precursor was added.

In a fed-batch process for high cell densities a feeding solution containing glucose (feed composition see chapter 2.3) was exponentially added, triggered by rising dissolved oxygen ("hunger peak"). After an increase of the dissolved oxygen above 40 % the exponential feed ($y=e^{0.1*t}$) was started. When a feed rate of 3 mL/h was reached, the feed was continued at a constant feed rate of 3 mL/h.

2.4.3 Cultivation in 10 liter-scale stirring tank bioreactor

Production of glycosylated flavonoids in liter-scale was performed in a 10-liter stirred tank benchtop glas-fermenter BioFlo® 320 (Eppendorf) (Fig. 2.2).

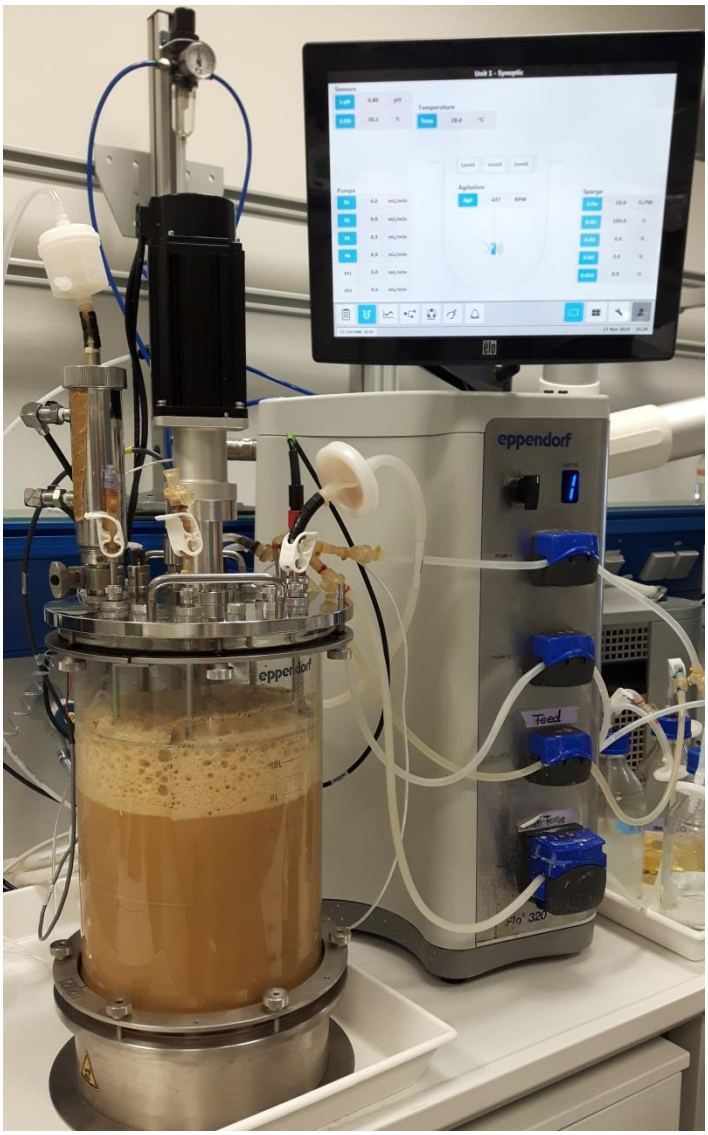

Figure 2.2: BioFlo® 320 bioreactor system (Eppendorf).

Biotransformation procedure and fermentation parameters were the same as described above for the 2-liter bioreactors. The working volume of 5 liter was inoculated with 10 % of the volume of an overnight preculture in shake flasks (150 rpm, 28°C). The glucose feeding was scaled-up to a 10-fold higher feed rate ($y=10\ e^{0.1*t}$, until constant feed rate of 30 mL/h). With start of the fed-batch phase the expression of the glycosyltransferase was induced by addition of 100 µM IPTG and 25 g of the precursor (5 g/L). During fermentation samples were taken for UHPLC-MS-MS (2.5.3). The fermentation broth was harvested over a tangential flow filtration (2.6.1) for further purification of the produced flavonoid-glycosides (for down-stream methods see chapter 2.6).

2.5 Analytical methods

2.5.1 Measurement of the optical density for cell growth

The optical density (OD) was measured with a spectrophotometer at a wavelength of 600 nm. The fermentation samples were measured against the culture medium (blank) and were diluted with the medium for absorption within a measuring range between 0.1 and 0.6.

2.5.2 Quantification of flavonoid-glycosides using HPLC

Flavonoid-glycoside concentrations were determined by analytical high pressure liquid chromatography (HPLC). For sample preparation the cells were removed by centrifugation. To avoid loss of adsorbed product to filter matrices, the samples were not sterile-filtrated. Appropriate diluted samples were loaded on an Agilent ZORBAX SB-C18 column (4.6 mm internal diameter x 250 mm length, 5 µm particle size) at a Hitachi Elite LaChrome HPLC system. Analysis was performed with a step gradient of acetonitrile (A) and water with 0.1 % trifluoroacetic acid (B) at a constant flow rate of 1 mL/min over 63 minutes (Fig. 2.3). Detection was done at a wavelength of 254 nm.

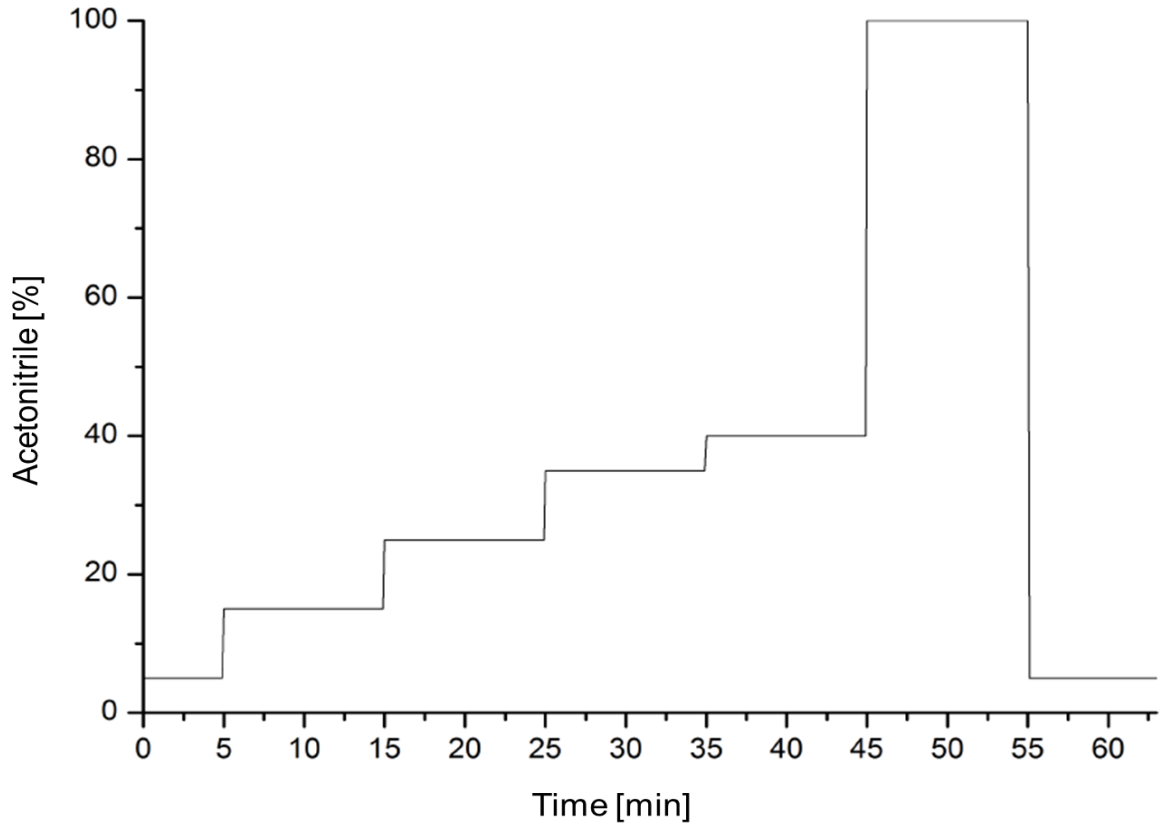

Figure 2.3: HPLC method for quantification of flavonoid-glycosides at constant flow rate of 1 mL/min with step gradient of acetonitrile (A) and water with 0.1 % trifluoroacetic acid (B): 1. 0 min 5:95 (A:B), 2. 5 min 15:85, 3. 15 min 25:75, 4. 25 min 35:65, 5. 35 min 40:60, 6. 45 min 100:0, 7. 55 min 5:95.

2.5.3 Determination of flavonoid-glycoside using UHPLC-MS-MS

For quantification and identification of flavonoid-glycosides an ultra-high pressure liquid chromatography (UHPLC) coupled to tandem mass spectrometry (MS/MS) was used. Sample preparation was the same as for HPLC (see 2.5.2). UHPLC analysis was carried out at a Thermo Scientific UltiMate 3000 system with a NUCLEOSHELL RP18 EC100 column (2 mm internal diameter x 100 mm length, 2.7 µm particle size) from Macherey-Nagel. Acetonitrile (A) and water with 0.05 % formic acid (B) were used as eluents in a linear gradient over 9 minutes (Fig. 2.4). The flow rate was constant at 0.5 mL/min and the detection was at 254 nm.

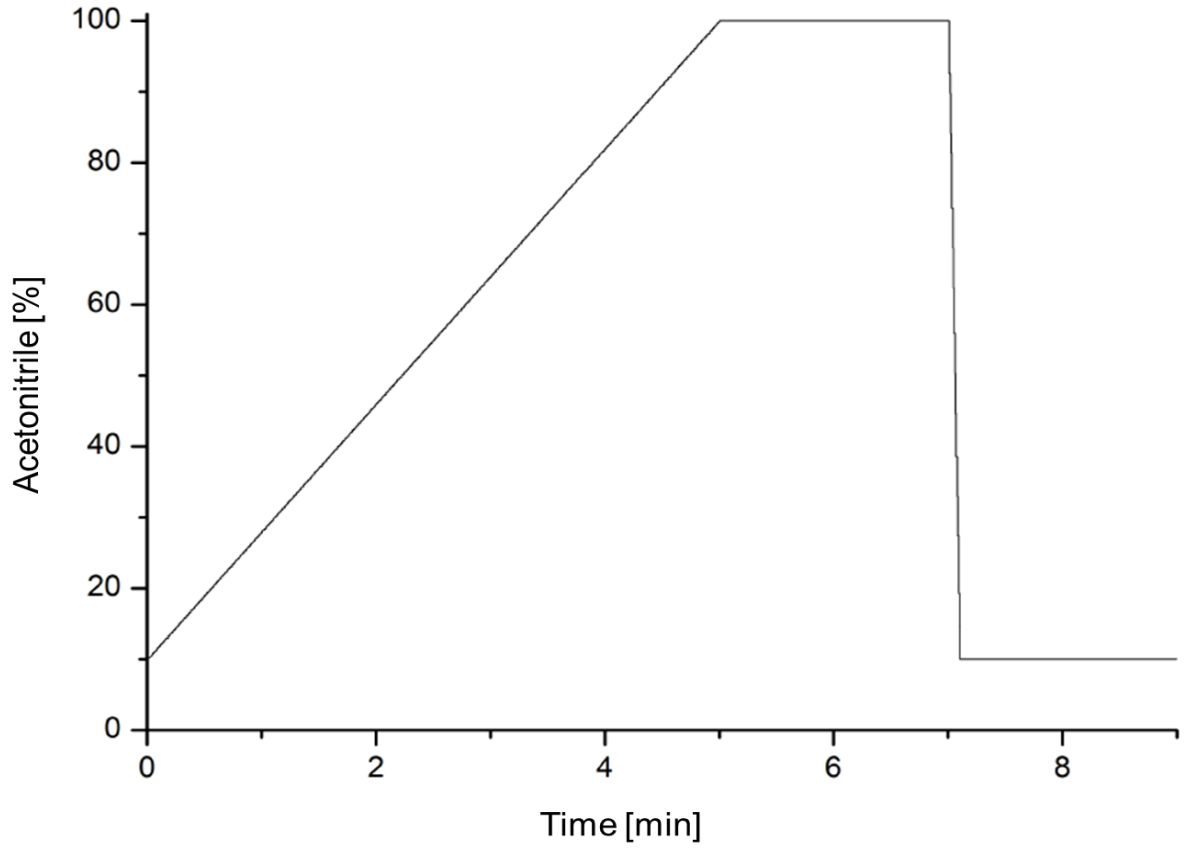

Figure 2.4: UHPLC method for quantification of flavonoid-glycosides at constant flow rate of 0.5 mL/min with linear gradient of acetonitrile (A) and water with 0.05 % formic acid (B): 1. 0 min 10:90 (A:B), 2. 5 min 100:0, 3. 7 min 100:0, 4. 7.1 min 10:90, 5. 9 min 10:90.

After UHPLC the eluted samples were injected into the Bruker Daltonics micrOTOF-Q mass spectrometer with electrospray ionization and fragmented for detection by tandem mass spectrometry with a collision energy of 10 eV.

2.5.4 NMR spectroscopy

Produced flavonoid-glycosides were confirmed by ^{1}H and ^{13}C NMR spectroscopy. Therefore the purified glycosides were sent to Dr. Erhard Haupt at the Institute of Inorganic and Applied Chemistry of the University of Hamburg.

2.6 Down-stream methods (DSP)

2.6.1 Tangential flow filtration

For harvest and clarification of the fermentation broth a tangential flow filtration (TFF) was applied by use of a Centramate™ 500 S benchtop tangential flow filtration system (Pall) with Pall Supor polyethersulfone (PES) membrane cassettes (pore size 0.2 µm).

2.6.2 HPLC purification of flavonoid-rhamnosides

Flavonoid-rhamnosides were purified by HPLC using an Agilent 1260 Infinity II Preparative LC System with a SB-C18 column (21.2 mm internal diameter x 250 mm length, 7 µm particle size) or for larger scales the Agilent Varian PrepStart SD-1 HPLC system with a Macherey-Nagel reversed phase C18Htec column (50 mm internal diameter x 250 mm length, 7 µm particle size). The sterile filtrated permeate was loaded onto the column with a constant flow rate of 20 mL/min (SB-C18 21.2 x 250 mm) or 100 mL/min (C18Htec 50 x 250 mm) and then eluted with the same flow rate by an acetonitrile (A) and water with 0.05 % formic acid (B) step gradient: 1. 0 – 5 min 10:90 (A:B), 2. 5.1 – 15 min 25:75, 3. 15.1 – 25 min 40:60, 4. 25.1 – 30 min 100:0, 5. 30.1 – 40 min 10:90. HPLC fractions were collected and product fractions were analyzed by UHPLC-MS-MS (2.5.3). The product fractions were evaporated for solvent removal (2.6.4) and lyophilized (2.6.5).

2.6.3 SPE flash chromatography

For purification of flavonoid-rhamnosides by solid phase extraction (SPE) a Büchi Pump-Manager C-615 flash chromatography system with CHROMABOND Flash RS C18 cartridges (330 g or 800 g, max. 12 bar) was used. Sterile filtrated fermentation broth (5 to 10

liter) was loaded onto the flash cartridge and eluted with a flow rate of 200 mL/min. Elution was performed with a step gradient of acetone (A) and water with 0.05% formic acid (B) with two column-volumes of each step: 10 % (A), 25 % (A), 40 % (A) and 100 % (A). The steps were collected as fractions and analyzed by UHPLC-MS-MS (2.5.3). Fractions with 25 % and 40 % acetone were the product fractions, which were evaporated for solvent removal (2.6.4) and lyophilized (2.6.5).

2.6.4 Evaporation

For solvent (acetonitrile or acetone) removal the HPLC or SPE product fractions were evaporated using a Büchi Syncore® Polyvap parallel evaporator with 6 vessels for working volumes up to 250 mL. To avoid product degradation evaporation was performed at a temperature of 40 °C and 75 mbar until the sample was solvent-free and could be frozen at −80 °C for lyophilisation (2.6.5).

2.6.5 Lyophilisation

The aqueous product fractions were frozen at −80 °C and lyophilized in a Christ Freeze dryer Alpha 2-4 LSCplus. To accelerate the freeze-drying process, the surface to volume ratio had to be as great as possible. After lyophilisation the product remains as a fluffy, amorphous powder.

3 Results & Discussion

3.1 Production of flavonoid-rhamnosides with GtfC

An *E. coli* Rosetta gami 2 (DE3) strain carrying the metagenome-derived glycosyltransferase GtfC was used for the whole cell biotransformation of various flavonoids. GtfC is able to glycosylate flavonoids by using dTDP-rhamnose and transferring the sugar residue to hydroxyl groups (-OH) at different positions of the polyphenolic scaffold. To characterize the O-positions, which can be addressed by GtfC, the flavonoids chrysin, diosmetin, biochanin A, hesperetin, and naringenin were rhamnosylated. Biotransformations were performed in shake flasks with a working volume of 1 L. *E. coli* Rosetta gami 2 (DE3) carrying GtfC was incubated overnight in LB medium at 28 °C. Before induction with 100 mM IPTG and addition of 400 µM of the flavonoid, cell suspension was centrifuged at 7000 rpm for 10 minutes and pellet was suspended in phosphate buffer, pH 7 with 1 % glucose. Conversion of the flavonoids took place in phosphate buffer at 17 °C.

NMR results of the HPLC-purified products showed that GtfC is able to produce 5-O-rhamnosides of flavones (chrysin, diosmetin), isoflavones (biochanin A) and flavanones (hesperetin, naringenin) (NMR data see appendix, A5), although the 5-O-position is normally not addressed by glycosyltransferases (Liao et al. 2016, Sun et al. 2014). HPLC purification of the different flavonoid rhamnosides was done by Dr. Henning Rosenfeld and NMR spectroscopy was done at the Institute of Inorganic and Applied Chemistry by Dr. Erhard Haupt. The identified products of GtfC are listed in the following table (Tab. 3.1). These novel rhamnosides are to my best knowledge not described so far.

GtfC can glycosylate the 5-O-position, but it is not always the preferred position. When the 3'-O-position is available (diosmetin, hesperetin), GtfC prefers the 3'-O-position over the 5-O-position and produces the 3'-O-rhamnoside as main product. When only the 7-O-position is available (biochanin A, chrysin) or additionally the 4'-O-position (naringenin), GtfC produces the 5-O-rhamnoside as main product (data see appendix, A6).

Table 3.1: Rhamnosylation products of GtfC in whole cell biotransformation with *E. coli* Rosetta gami 2 (DE3) identified by NMR. The main product preferred by GtfC is underlined. (NMR spectroscopy was done by Erhard Haupt at the Institute of Inorganic and Applied Chemistry, University of Hamburg).

Flavonoid precursor	NMR-identified rhamnosides
Biochanin A	5-O-rhamnoside 5,7-di-O-rhamnoside
Chrysin	5-O-rhamnoside 5,7-di-O-rhamnoside
Diosmetin	3'-O-rhamnoside 5-O-rhamnoside
Hesperetin	3'-O-rhamnoside 5-O-rhamnoside
Naringenin	5-O-rhamnoside 4'-O-rhamnoside

3.1.1 Biotransformation of Naringenin with GtfC

For the biotransformation of naringenin to naringenin-5-O-rhamnoside (N5R) the two process parameters, temperature and pH, were characterized. Biotransformations were performed in 1 L bench-top parallel bioreactors in a fed-batch process (constant feeding of 50 % glucose (3 mL/L/h) after an increase of the dissolved oxygen above 40 %) at a regulated pO_2 of 30 % in terrify broth medium for 24 h. The optimal temperature for *E. coli* fermentation is known to be at 37 °C, but the temperature optimum of GtfC is unknown, since no kinetic studies for enzyme characterization could be done because the needed co-factor, dTDP-rhamnose, is commercially not available. At temperatures around 37 °C protein expression under the control of the T7 promoter often results in incomplete folding processes that usually ends with accumulation of the recombinant protein as insoluble aggregates (inclusion bodies). To reduce the accumulation of inclusion bodies in the cytoplasm, a common strategy is the cultivation at lower temperatures during induction and production phase (De Groot and Ventura 2006, Sørensen and Mortensen 2005).

Results showed that the temperature optimum for the whole-cell biotransformation is 28 °C (Fig. 3.1 A). At this temperature the cells are still able to grow fast enough and the enzymatic rhamnosylation reaction works. Also 28 °C seems to be low enough to produce the glycosyltransferase in its active form (but the actual amount of inclusion bodies at this

temperature is not known). The productivity is significantly lower when temperatures are higher than 30°C, even if the cells are grown much better. At lower temperatures the cells are grown very slowly. This means fewer enzymes in the culture and less product. The optimal pH range is characterized to be slightly alkaline at pH 7 to 8. (Fig. 3.1 B).

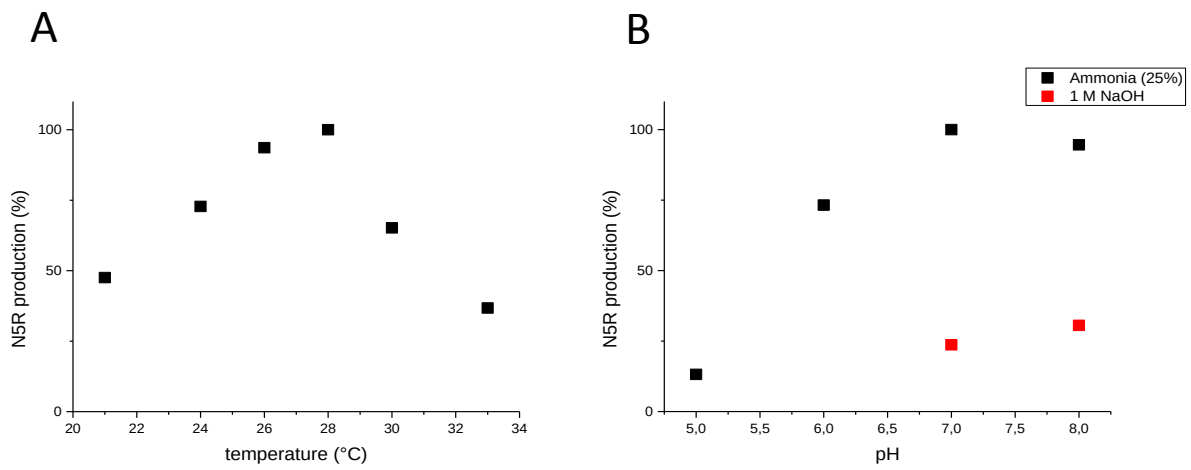

Figure 3.1: Characterization of the process parameters temperature and pH for the production of N5R. The optimal temperature is around 28°C (A) and the pH shows an optimum in the neutral to slightly alkaline range (B). For the pH regulation in the bioreactor ammonia (25%) and NaOH (1 M) were tested. With ammonia much higher N5R concentration could be reached. (Standard deviation is missing because only done once).

When *E. coli* grows on glucose the pH drifts into the acidic range, so during fermentation the pH has to be regulated by the addition of a concentrated base like sodium hydroxide or ammonia. Ammonia also provides a nitrogen source and has impact on the cell growth. That's why much higher product concentrations are reached with ammonia (Fig. 3.1 B).

3.3.2 Fed-batch for high cell density fermentation

To increase the productivity a fed-batch process with an exponential feeding profile for high cell density fermentation was developed. During batch fermentation the nutrients are consumed from the growing cells and become a limiting factor for cell viability and further cell growth. With decreasing cell viability the production rate is stagnating and degradation of the product is possible. So the essential nutrients have to be fed to the culture in a fed-batch process to extend the exponential growth phase for higher cell densities and to maintain high cell viability over the production phase. As it could be seen in Figure 3.2 the growth rate is stagnating after 7 hours of growth and the OD remains under 10 (without feed). In fed-batch

the growth phase can be extended to an OD of 60 with use of 25% ammonia for pH regulation instead of 1M sodium hydroxide solution (Fig. 3.2 and 3.3). With NaOH an OD of only 43 has been achieved after 28 hours (Fig. 3.2). As previously mentioned ammonia functions as nitrogen source and promotes the cell growth.

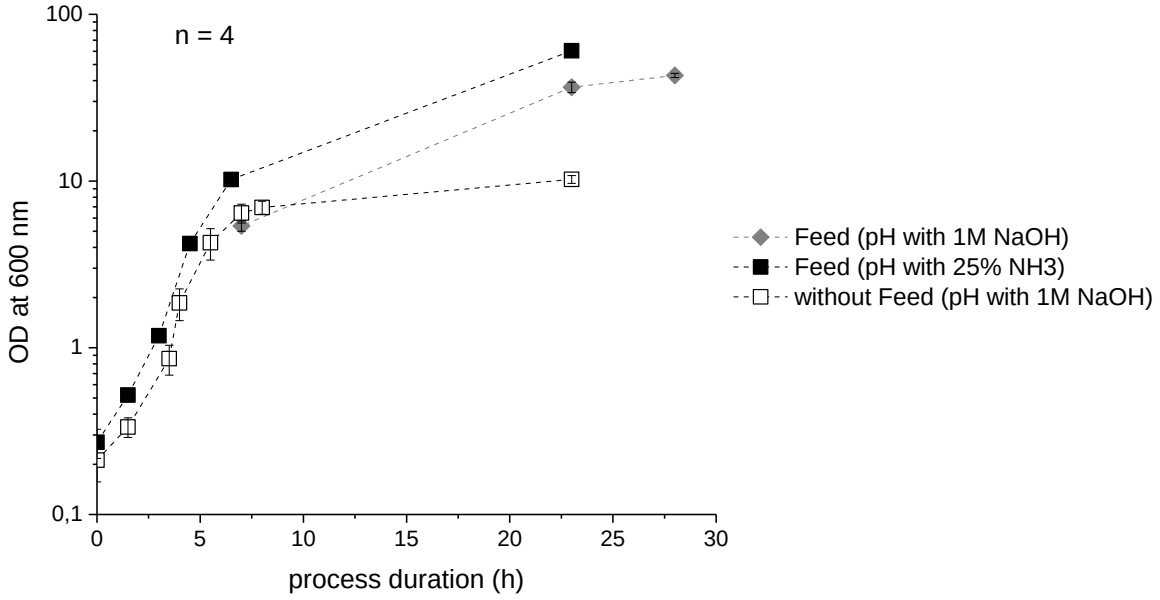

Figure 3.2: Cell growth during a fed-batch with exponential feed with 1M NaOH for pH regulation and a fed-batch with 25% ammonia for pH regulation in comparison to the cell growth of a batch fermentation with 1M NaOH. The OD at 600 nm is plotted over the process duration.

The main feed-compound is glucose as carbon-source, but also magnesium is important for growth of *E. coli* (Lusk et al. 1968). In complex media like terrific broth (TB) cell growth is magnesium limited, which leads the culture to enter stationary phase before the glucose is fully consumed during exponential growth. So supplementation of magnesium is necessary for *E. coli* to use the glucose for cell growth (Christensen et al. 2017). Compared to a feed with only glucose (OD_{600} of 7.9), the cell growth increases with magnesium added to the feeding solution and an OD_{600} of 36.5 could be reached (Fig. 3.3). Without magnesium in the feed the cell growth was even 22% lower than without a feed (Figure 3.2 and 3.3). With magnesium and ammonia for pH regulation an 87% higher OD_{600} of 60.5 could be reached (Figure 3.3). A higher cell density has positive impact on the production, because more cells mean a higher production of the recombinant glycosyltransferase and an increased glycosylation of the added precursor, which results in higher production titers (mg/L).

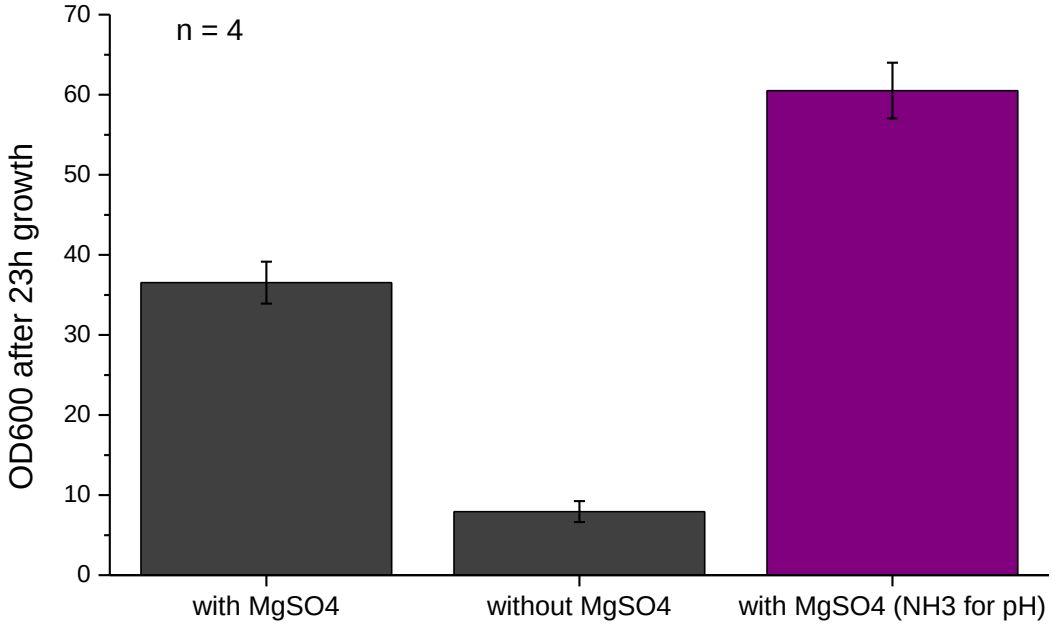

Figure 3.3: Improved cell growth with magnesium in feeding-solution (glucose 50 % (w/v), magnesium sulphate heptahydrate 1 % (w/v)) and ammonia for pH regulation (nitrogen source).

Figure 3.4 shows the production titer (mg/L) of N5R and the by-product N4'R during a fed-batch process over 48 hours. The formation of the rhamnosides starts with the expression of GTC by induction with IPTG (production phase). During the growth phase the feed starts with glucose limitation, which implies a rising dissolved oxygen (DO %), the so called "hunger peak". The feed starts at 1 mL/h/L and increases with an exponential feeding-rate ($\mu = 0.1\ h^{-1}$) up to 3 mL/h/L. The production phase is induced 24 h after inoculation. During the production phase the feed rate remains constant at 3 mL/h/L. Within a 48 hours fed-batch fermentation optical cell densities around 60 and product concentrations of 500 mg/L could be reached. Within a three-fold determination the main product N5R achieved concentrations of 430.65 ± 81.26 mg/L, N4'R of 98.42 ± 27.48 mg/L (Fig. 3.4).

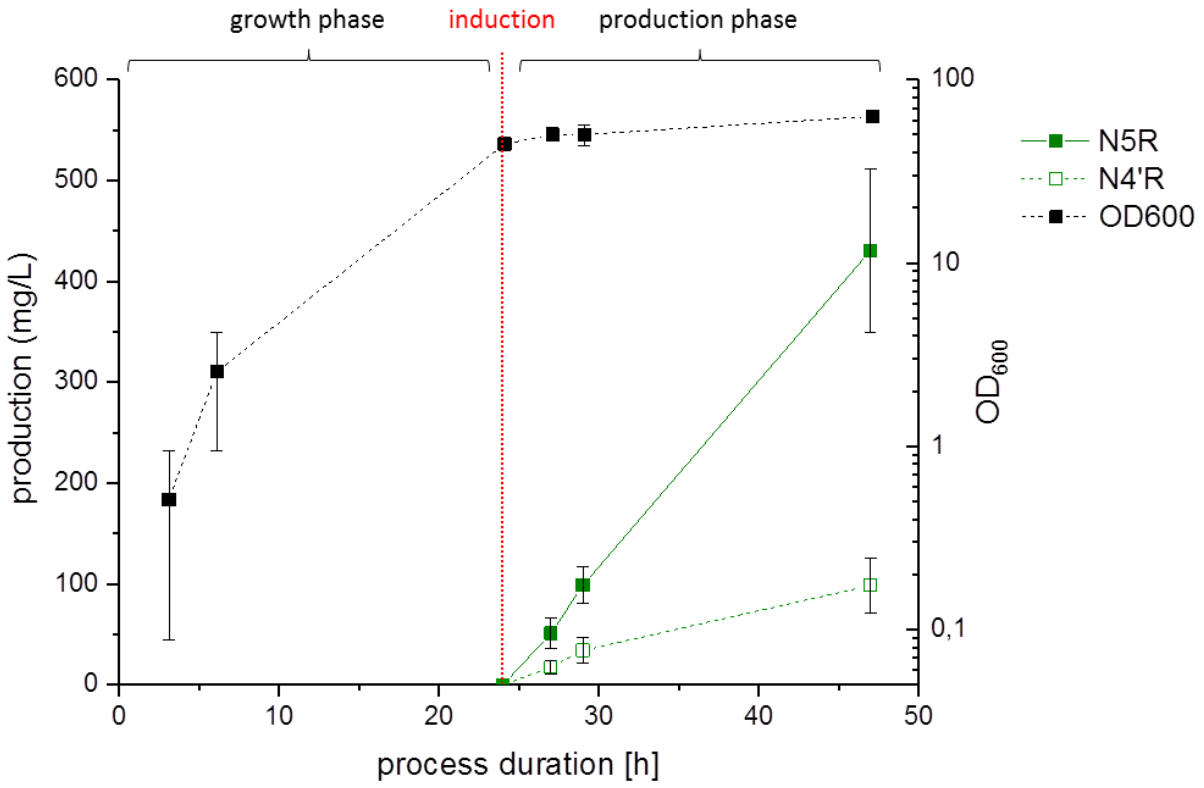

Figure 3.4: This plot shows the optical density OD at 600 nm (OD600) and the product concentration of N5R and the secondary product N4'R over the process duration (n = 3). The process is divided into two phases, the growth phase and the production phase.

3.3.3 Extraction of flavonoid-rhamnosides from cell pellet

Flavonoid-rhamnosides are exported from the cells and are available in the culture supernatant. To determine the ratio of extracellular and intracellular product after biotransformation of naringenin, the pellet was separated from the supernatant by centrifugation. The supernatant was analyzed by HPLC. The pellet was washed with ethyl acetate for extraction of the flavonoid-rhamnoside. Ethyl acetate was evaporated and the dried sample was resoluted in water for analytical HPLC. The results showed that the actual production yield is higher than the dissolved product in the culture supernatant (Fig. 3.5). Most of the produced flavonoid-rhamnosides are secreted into the culture medium, but a certain percentage remains in the cells or on the surface of the cells. Especially the more hydrophobic N4'R has higher product amounts in or at the cells than it in the culture supernatant. From the total yield of the biotransformation only 70 % of the products are in the supernatant and 30 % are found in the cell pellet (Fig. 3.5).

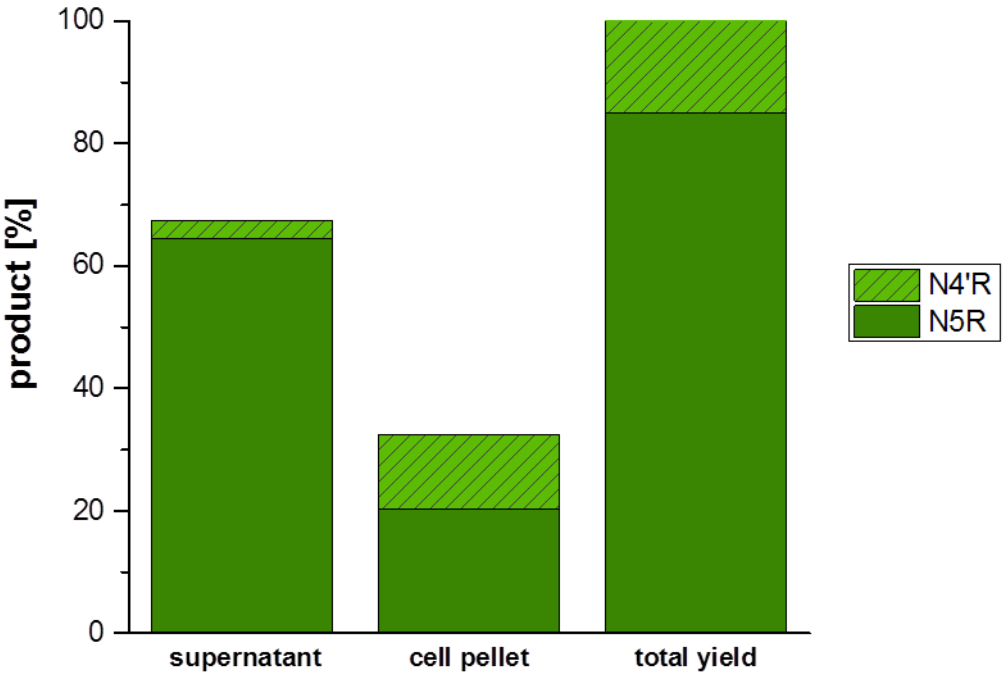

Figure 3.5: Product percentage of naringenin-5-O-rhamnoside and naringenin-4‘-O-rhamnoside in the culture supernatant and in the cell pellet. (Standard deviation is missing because only done once).

For the established down-stream processing only the supernatant is further purified (see chapter 3.5). So 30 % of the production yield gets wasted with the removal of the cells. This is a point for process optimization. One option is the extraction of the product out of the cell suspension, without prior cell removal. Another alternative is cell disruption for example by homogenization, where the cell content will be released. In both cases the down-stream processing becomes more difficult and cost-intensive. Extraction as well as homogenization have to be done with more than only one process step to reach a nearly 100 % yield. This is time-consuming and expensive. For extraction high amounts of solvents are necessary, which means high costs even with solvent recovery.

Instead of optimizations in the down-stream procedure, an improvement of the membrane transport is a more elegant approach. Therefore, the transport of glycosylated flavonoids over the outer membrane protein TolC has to be increased. Results of an improved product secretion by overexpression of TolC are presented in chapter 3.6.

3.2 Development of a repeated-batch process

In a batch or fed-batch process after a certain time the used medium becomes enriched with secondary metabolites and substances from lysed cells, which can be toxic for the intact cells and degrade the product. To increase the process duration and total yield while avoiding degradation of the naringenin-rhamnosides, an aim of this study was to develop a repeated-batch process. In a repeated-batch process part of the culture medium is harvested, whereas the cells remain in the bioreactor and the bioreactor is refilled with fresh medium. So the potentially toxic substances are removed from the culture and new substrates for cell growth and rhamnosylation reaction are provided. This extends the process time and increases the production yield, which depends on solubility and biocompatibility of the flavonoids. The maximum yield of each batch is limited by the product solubility and the conversion rate of the flavonoid defines the batch duration.

To realize the medium exchange of used against fresh medium a suitable methods is needed to remove the liquid without any cells. One possibility is to harvest the culture broth by a centrifuge or separator and clear the medium, which is then discarded. The cell mass has to be resuspended with the fresh medium and pumped back into the reactor. But cell viability suffers under these worst conditions. Another method is to filtrate the culture using a membrane to retain the cells. But since we are working with high cell densities, the filtration method and properties of the membrane must be chosen appropriately to avoid blocking of the filter membrane. Tangential flow filtration (TFF) turned out to be a suitable method when lead the retained cell suspension directly back into the reactor where growth conditions are optimal. Due to a tangential flow across the filter, there is no formation of a filter cake and a higher liquid removal rate could be achieved.

A repeated batch set-up with TFF module has been established for our process (Fig. 3.6). The culture broth is harvested over a 0.2 µm filter membrane. The products are removed with the permeate flow. The cells remain in the bioreactor with sufficient viability for repeated fermentation runs up to five batches. Fresh medium is pumped under reverse flow direction through the membrane into the bioreactor after up to 75 % of the reactor volume is harvested as clear filtrate. The flavonoid precursor is fed stepwise in every batch.

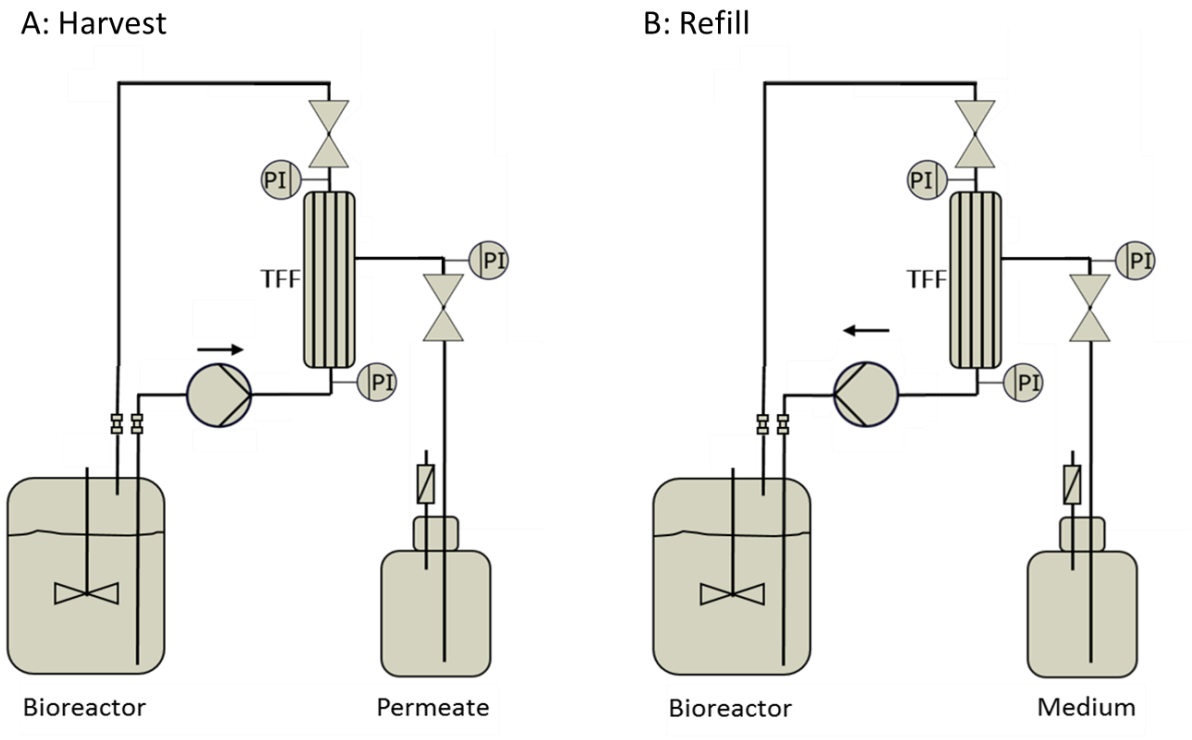

Figure 3.6: TFF system for harvest of the flavonoid-glycosides and medium exchange in a repeated-batch process. For the media exchange the culture broth is pumped over a tangential flow filtration module with 0,2 µm membrane. The retentate containing the cells is recirculated. The sterile permeate containing the product is harvested (A). After 50 to 75 % of the reactor volume is harvested, fresh medium flushes the membrane and adhering cells in opposite flow direction back into the bioreactor (B).

The data of two different repeated fed-batch runs for biotransformation of naringenin is plotted in Figure 3.7 and 3.8. During the first fed-batch the cells grow under an exponential feeding rate in the growth phase and with a constant feeding in the production phase, like it was discussed in chapter 3.1. The feed remain constant at this rate over the next batches of the process. After each fed-batch the culture medium was changed. Therefor the feed was stopped. The viable cells were retained by the filter membrane and recirculated into the bioreactor. The removed volume was replaced by fresh culture medium and new naringenin was added as substrate for biotransformation. With up to five batches a total yield of 1.1 g naringenin-5-O-rhamnoside (N5R) could be reached (Fig. 3.7). The N5R concentration (mg/L) of each batch is the sum of remaining product from the prior batch and new product build from freshly added precursor. The total yield of each batch depends on the harvested permeate volume, which is pooled and results in the total yield at the end of the repeated-batch process. In both runs after four batches around 950 mg N5R were produced (955 mg (Run 1, Fig. 3.7); 959 mg (Run 2, Fig. 3.8)). Run 2 were finished after 4 batches.

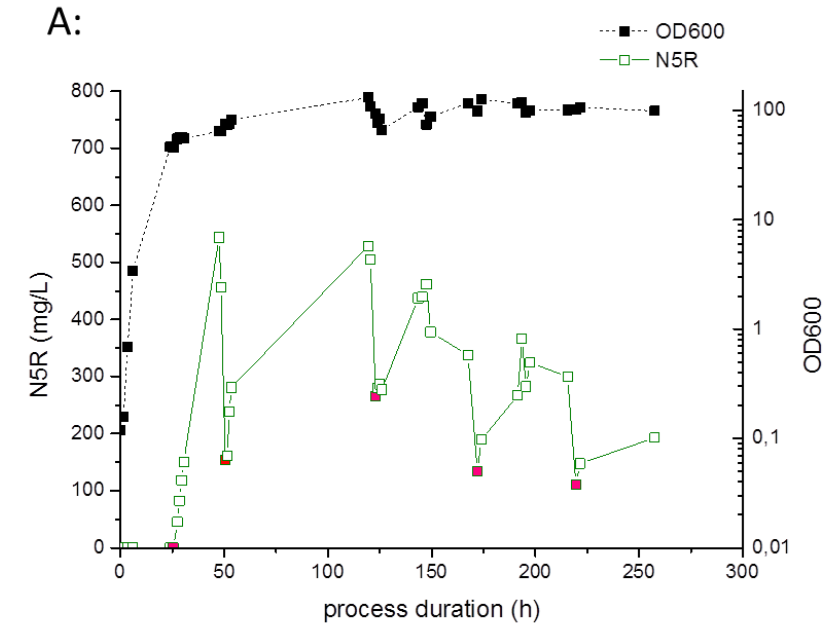

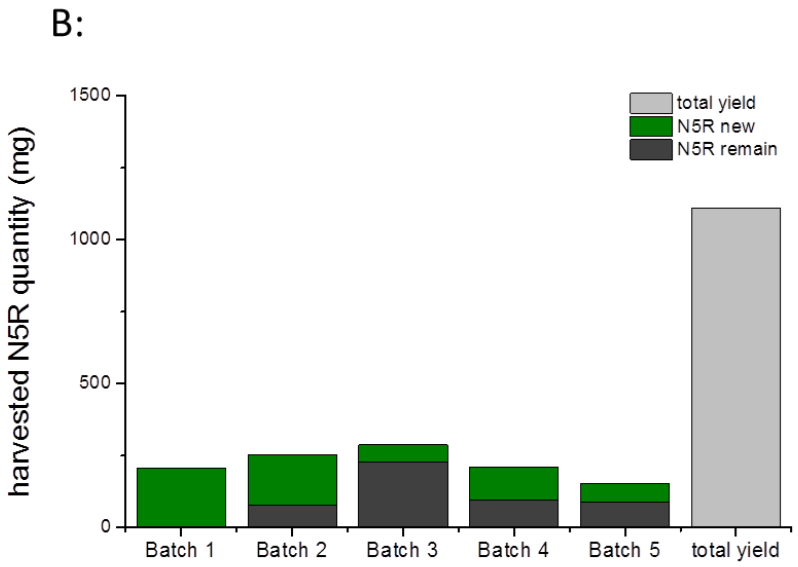

Batch N°	Batch duration [h]	Time total [h]	Permeate volume [mL]	Product [mg]	Total yield [mg]
1	23	23	450	205,62	205,62
2	72	95	500	252,32	457,94
3	47	142	850	287,08	745,02
4	48	190	700	209,95	954,97
5	42	232	800	154,18	1109,15

Figure 3.7: Repeated Fed-batch Run 1. A: N5R concentration (mg/L) and the optical density OD_{600} are plotted over the time. The red dots are the start-concentration of each batch. B: Product quantities of repeated-batch fermentation with five batches (initial culture volume: 500 ml). After the medium exchange N5R remains in the bioreactor (dark grey) and new N5R (green) is produced during the batch. The harvested product quantities of each permeate result in a total mass yield at the end of fermentation (light grey).

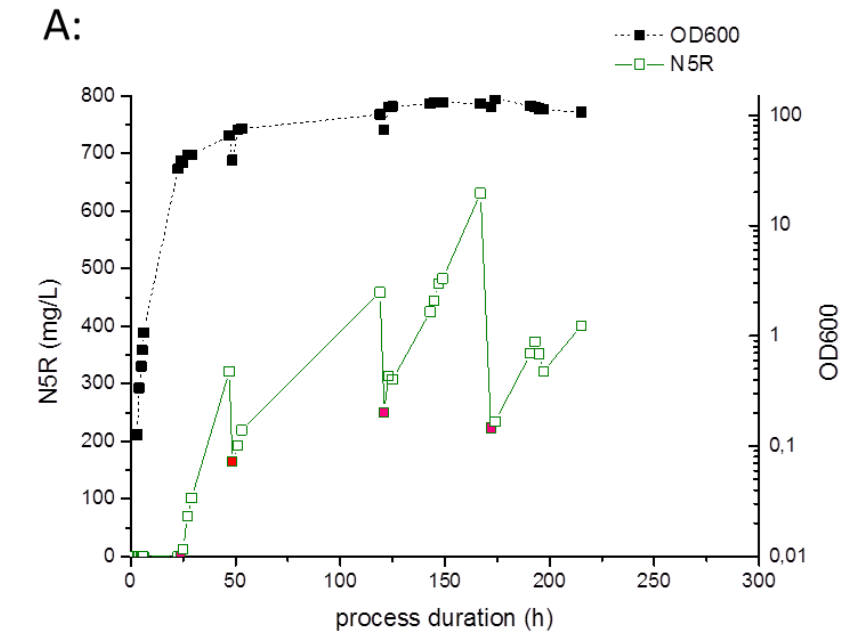

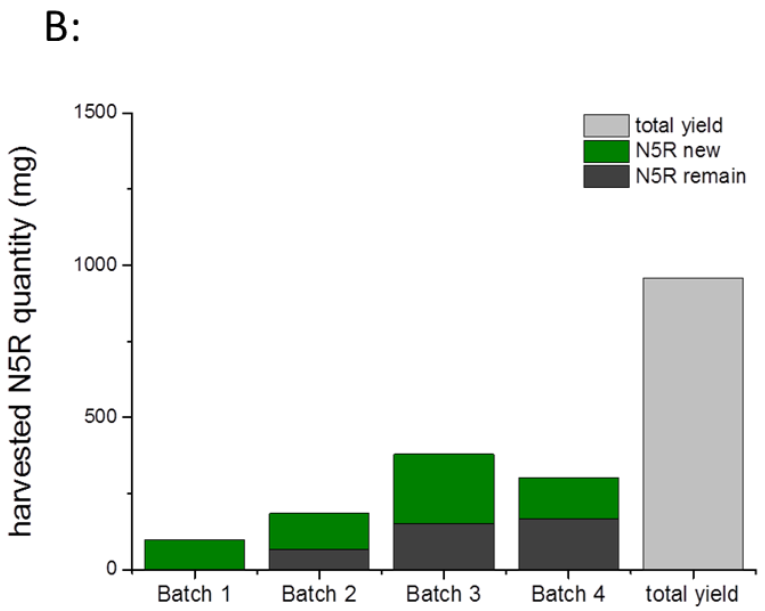

Batch N°	Batch duration [h]	Time total [h]	Permeate volume [mL]	Product [mg]	Total yield [mg]
1	23	23	300	96,49	96,49
2	72	95	400	183,48	279,97
3	48	143	600	378,62	658,59
4	48	191	750	299,95	958,54

Figure 3.8: Repeated Fed-batch Run 2. A: N5R concentration (mg/L) and the optical density OD_{600} are plotted over the time. The red dots are the start-concentration of each batch. B: Product quantities of repeated-batch fermentation with four batches (initial culture volume: 500 ml). After the medium exchange N5R remains in the bioreactor (dark grey) and new N5R (green) is produced during the batch. The harvested product quantities of each permeate result in a total mass yield at the end of fermentation (light grey).

With the repeated fed-batch procedure the process duration could be extended significantly up to 8 to 10 days instead of 48 to 72 hours (normal fed-batch duration) and a total yield of approximate 1 g could be achieved. Clearly, the main advantage is that the preparation and starting-up times as well as the post-processing time for sterilization and cleaning can be saved. Within 10 days four to five repeated fed-batches could be run. In the same time only two "normal" fed-batch processes with reduced process times and only a total yield of maximal 0.5 g (in the same reactor with a maximal end-volume of 1 L after 24 h in a fed-batch 500 mg/L were reached, see chapter 3.3.2) are possible to run.

One disadvantage is the high media consumption. Beside the culture medium also huge amounts of water and sodium hydroxide solution (0.1 – 1 M) are needed for cleaning. After each medium exchange, the TFF system has to be washed in three steps: pre-rinsing with water (to wash out remaining cellular material), cleaning with sodium hydroxide (dissolving of organics) and rinsing with water (neutralization). Sodium hydroxide is a common cleaning reagent in industrial manufacturing, as it is effective in removal of proteins and nucleic acids as well as in decontamination of viruses, bacteria, yeasts, fungi, and endotoxins.

Another disadvantage is the low reproducibility of the two consecutive runs (Fig. 3.7 and 3.8). The cells have a great impact on the tangential flow filtration due to their interaction with the membrane. Tangential flow filtration of high cell density fermentations sooner or later causes a blocking of the membrane, since the retentate becomes more and more concentrated. The duration of the filtration step and volume of the exchanged medium depends on the cell density and the quality of the cell culture. The pores of the membrane are getting blocked easier by cultures with low cell viability due to lysed cell material. This leads to variations in volume and product amount of the harvested permeate and has an impact on the further fermentation process. Such differences are not acceptable for an industrial production. Only a constant quality of the cell culture over the consecutive runs can ensure a reproducible medium exchange via TFF.

3.3 Biotransformation of Hesperetin with GtfC

For the production of the healthcare candidate hesperetin-5-O-rhamnoside (H5R) the optimized strain Rosetta gami 2 (DE3) pET-19b::*gtfC*, pRSFDuet-1::*ndk*::*tmk*, pCDFDuet-1::*rmlA*::*rmlC* was used (see chapter 2.1). This strain overexpressed the enzymes thymidylate kinase (TMK), and nucleotide diphosphate kinase (NDK) for dTTP synthesis, as well as the enzymes G-1-P thymidylyltransferase (RmlA), and dTDP-4-dehydrorhamnose 3,5-epimerase (RmlC) of the dTDP-rhamnose synthesis pathway for an increased dTDP-rhamnose level in the cells (see chapter 1.5).

For the production of H5R a fermentation process on minimal medium has been aspired. A major advantage of minimal medium is its chemically defined composition with known amounts and types of contents. In complex medium like terrific broth (TB) the main component is yeast extract, which is an undefined mixture of cell contents from yeast cells like amino acids, protein degradation products and vitamins. Even with a fixed supplier the quality of the yeast extract can vary depending on the lot number. This has an undesirable impact on the fermentation process and leads to variations and incomparableness of product quality and yield. Because of that, for production processes the use of yeast extract should be avoided. The main points of the pros and cons of complex (undefined) and minimal (defined) medium are listed in table 3.2.

Table 3.2: Pros and contras for minimal medium and complex medium.

Minimal medium		**Complex medium**	
pro	**contra**	**pro**	**contra**
chemical composition is known (defined)	limited growth factors	provides complex range of nutrients	yeast extract (undefined)
high reproducibility	higher costs	low costs	high variations possible (lot number of yeast extract)
stable process with constant production yields	preparation is more complicated due to the many single components	simple preparation (yeast extract, tryptone, glycerol, phosphate buffer)	inconsistent production yields
independence from suppliers	necessity of exact knowledge of required nutrients for certain process	contains all essential nutrients for a common *E. coli* fermentation process	high supplier dependency

The minimal medium used for the biotransformation of hesperetin was the M29 medium with supplemention of yeast extract (composition see chapter 2.3). The reason for this was that the production of flavonoid-rhamnosides without yeast extract resulted in very low product concentration. So the addition of different concentrations of yeast extract was tested and the production of flavonoid-rhamnosides was twice as much with addition of yeast extract (Fig. 3.9). Highest production was achieved with 2.5 g/L yeast extract. Addition of 1 g/L and 5 g/L yeast extract resulted in 83 % and 78 % rhamnosylation, respectively. Without yeast extract in the medium rhamnosylation was only 46 % (Fig. 3.9).

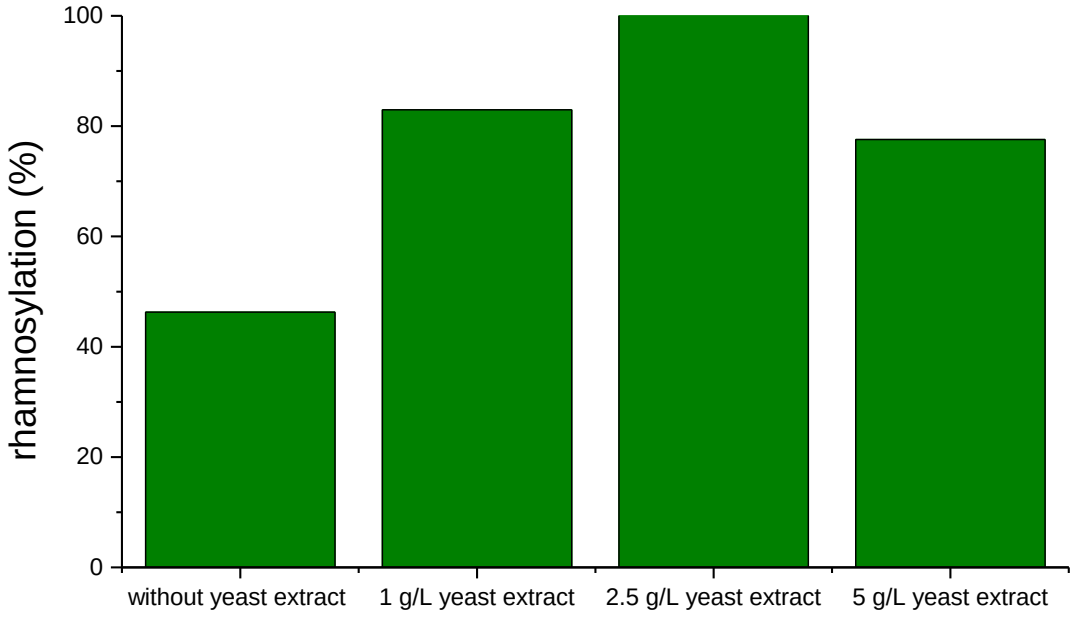

Figure 3.9: Production of flavonoid-rhamnosides (%) with GtfC in M29 medium without and with supplementation of yeast extract. (Standard deviation is missing because only done once).

Nevertheless with the M29 medium the production yields of the main product H5R were lower than expected. Because of concentrations of 500 mg/L in N5R production (see chapter 3.1), the product concentration of H5R was expected to be in the same range. But the maximal achieved concentration of H5R was only 70.54 mg/L. Instead H3'R achieved higher concentrations than H5R of 277.25 mg/L (Fig. 3.10 B). Several optimizations to increase the production yield failed (data from master thesis of Robert Knoll see appendix, A7).

On the assumption that minimal medium is not suitable for the glycosylation of flavonoids in *E. coli* due to a lack of necessary nutrients, the medium was changed back from minimal to

complex TB medium. Due to the different nutrients in the medium there is a complete different product ratio in the biotransformation of hesperetin with TB medium. The concentration of H3'R could be doubled to 599.36 mg/L and the second by-product hesperetin-di-rhamnoside achieved high concentrations of 825.53 mg/L at the end of the process after 48 hours (Fig. 3.10 A). But still the concentration of the target product H5R remains low at 141.71 mg/L (Fig. 3.10 A).

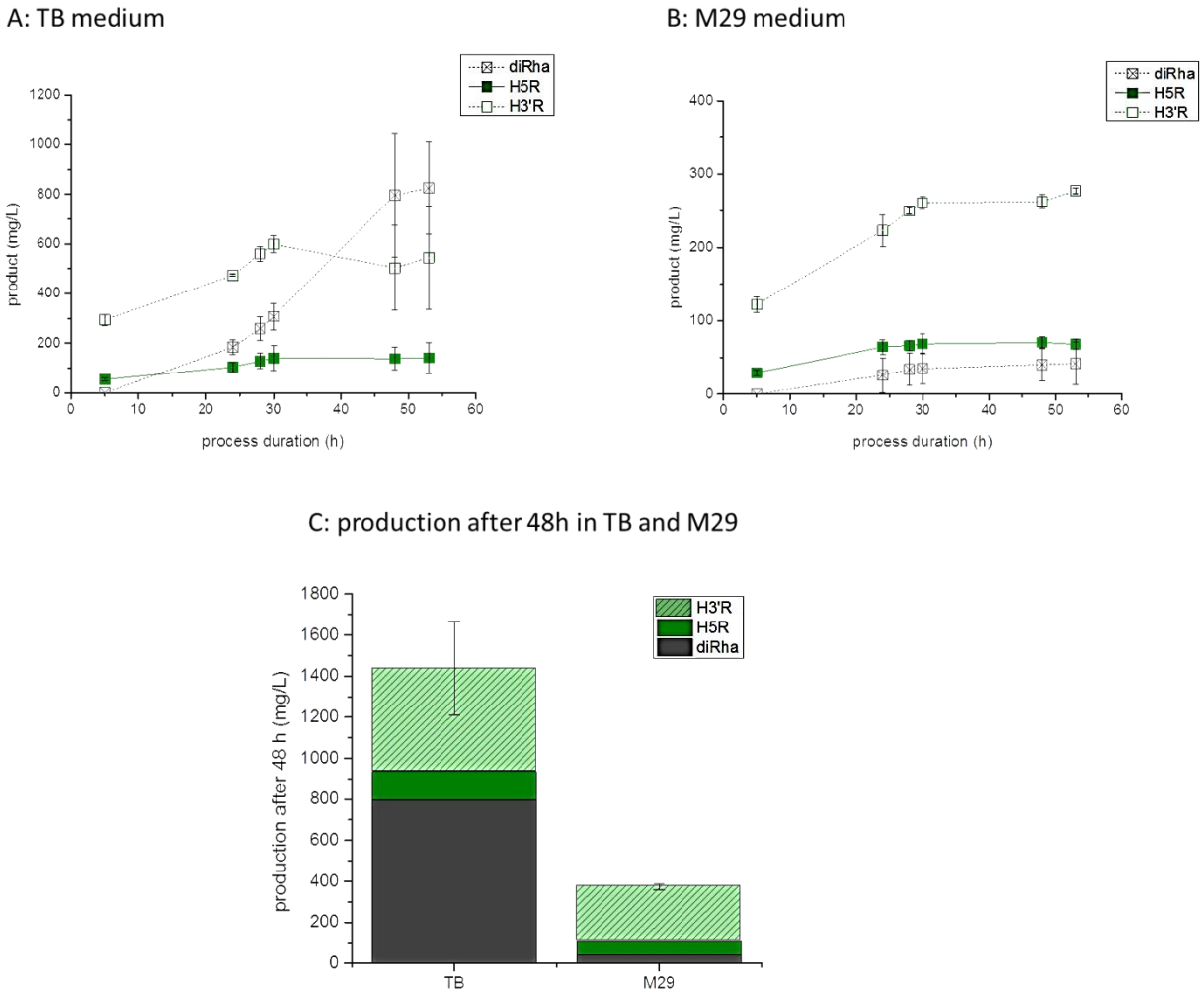

Figure 3.10: Product concentrations of hesperetin biotransformation. A: Concentration of hesperetin-products in fed-batch fermentation with terrific broth (TB) medium (n=3). B: Concentration of hesperetin-products in fed-batch fermentation with M29 medium (n=3). C: Product concentration after 48h biotransformation in TB and M29 medium (n=3).

In comparison to the biotransformation on minimal medium with maximal 400 mg/L production titer, with TB medium the sum of all hesperetin-glycosides produced by GtfC could achieve a production titer of 1400 mg/L after 48 hours (Fig. 3.10 C).

These results show that the complex components of yeast extract are necessary for high production yields of hesperetin-rhamnosides with Rosetta gami 2 (DE3). This could be due to missing growth factors, as well as a low solubility of the aglycon and the products in minimal medium. Due to the low solubility the availability and uptake of the aglycon by the cells is reduced. The insoluble products accumulate in the cells. Some substances of the complex TB medium seem to increase the solubility. It could be shown, that the solubility of H5R in TB medium is much higher than in minimal medium (data from Robert Knoll, Fig. 3.11). 10 mg of hesperetin, 15 mg H3'R, and 100 mg H5R, respectively, were suspended in 5 mL medium and mixed by shaking at 28 °C for 48 h. In TB medium H5R concentration of 4 g/L was measured. In M29 medium only 300 mg/L H5R were in solution (Fig. 3.11). H3'R concentrations of 530 mg/L in TB medium and 280 mg/L in M29 medium were measured (Fig. 3.11). Concentrations of the aglycon hesperetin in TB medium and M29 medium were in the same range, only up to 35 mg/L hesperetin were solved at a temperature of 28 °C (Fig. 3.11). So the uptake of the aglycon might not be the reason; instead the low solubility of the rhamnosides limited their maximal concentration in M29 medium. It is not clear, which might be the relevant components for an increased solubility in TB medium.

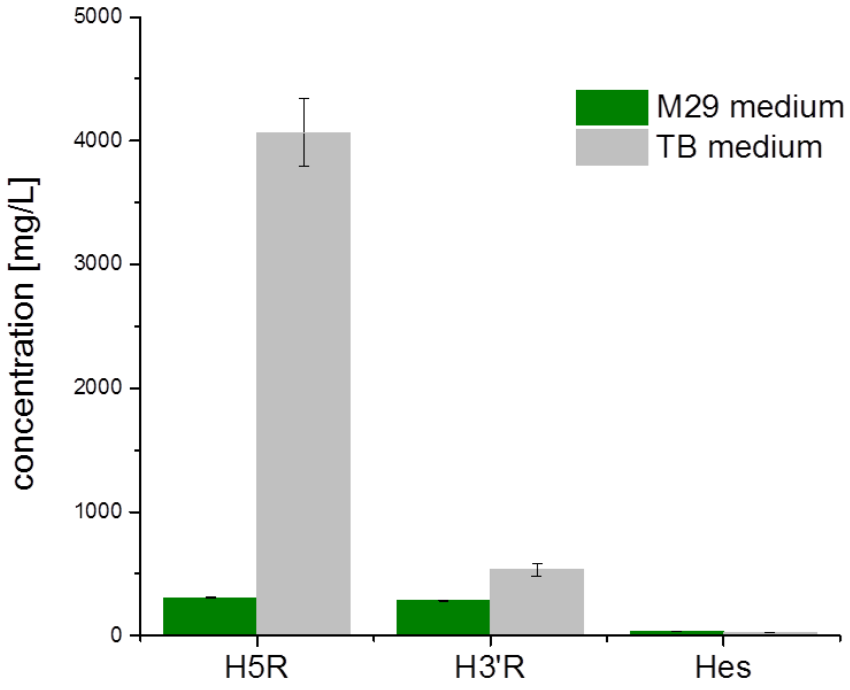

Figure 3.11: Solubility of hesperetin, hesperetin-5-O-rhamnoside, and hesperetin-3'-O-rhamnoside in TB medium and M29 medium were compared (n=3). 10 mg of hesperetin, 15 mg H3'R, and 100 mg H5R, respectively, were suspended in 5 mL medium and mixed by shaking at 28 °C for 48 h. Data from Robert Knoll (2017).

If a defined medium should be used, the composition of M29 medium had to be optimized by adding the missing substances. Due to the fact that the missing components were unknown and there wasn't enough time for an elaborate medium optimization, TB medium was chosen to be the medium for the production of H5R.

Because of the product ratios of hesperetin biotransformation with GtfC, where H5R wasn't the main product but instead the one with the lowest production yield, the glycosyltransferase GtfC was identified as not suitable for the rhamnosylation of hesperetin at the 5-O position. The preferred rhamnosylation products of GtfC were also discussed before in chapter 3.1. That is why alternative glycosyltransferases were screened and a new glycosyltransferase GtfD has been identified for the production of H5R (see chapter 3.4).

3.4 Flavanone-rhamnoside production with GtfD

GtfC proved to be unsuitable for the production of H5R. Therefore, glycosyltransferases were screened in order to identify regioselective GTs for the 5-OH position of hesperetin. The glycosyltransferase GtfD from *Dyadobacter fermentans* was identified as a suitable GT for the 5-O-rhamnosylation. The *E. coli* strain Rosetta gami 2 (DE3) pET19b::*gtfD*, pRSFDuet-1::*ndk*::*tmk*, pCDFDuet-1::*rmlA*::*rmlC* was used (see chapter 2.1).

The product ratios of the biotransformation of hesperetin with the enzymes GtfC and GtfD are compared in Figure 3.12. The cells were cultivated in TB medium in a fed-batch process over 48 hours. Whereas with GtfC the concentration of the H5R was only around 140 mg/L and the lowest of the produced glycosides (Fig. 3.12 A and C), with GtfD H5R became the main product with a 30-fold higher concentration of 2892.68 mg/L (Fig. 3.12 B and C). H3'R was barely built and the hesperetin-di-rhamnoside concentration has been halved compared to the biotransformation with GtfC (Fig. 3.12 C). With GtfC the production of H5R stagnates and H3'R concentration decreases after 30 h, but with GtfD the production of H5R continues until end of fermentation after 48 h (Fig. 3.12 A and B). These results show that GtfD is very suitable for the biotransformation of hesperetin. With GtfD the target product H5R occurs as the main product and furthermore GtfD has a much higher activity than GtfC. Product concentration of H5R ranges now in gram scale (2.9 g/L) instead of milligram scale.

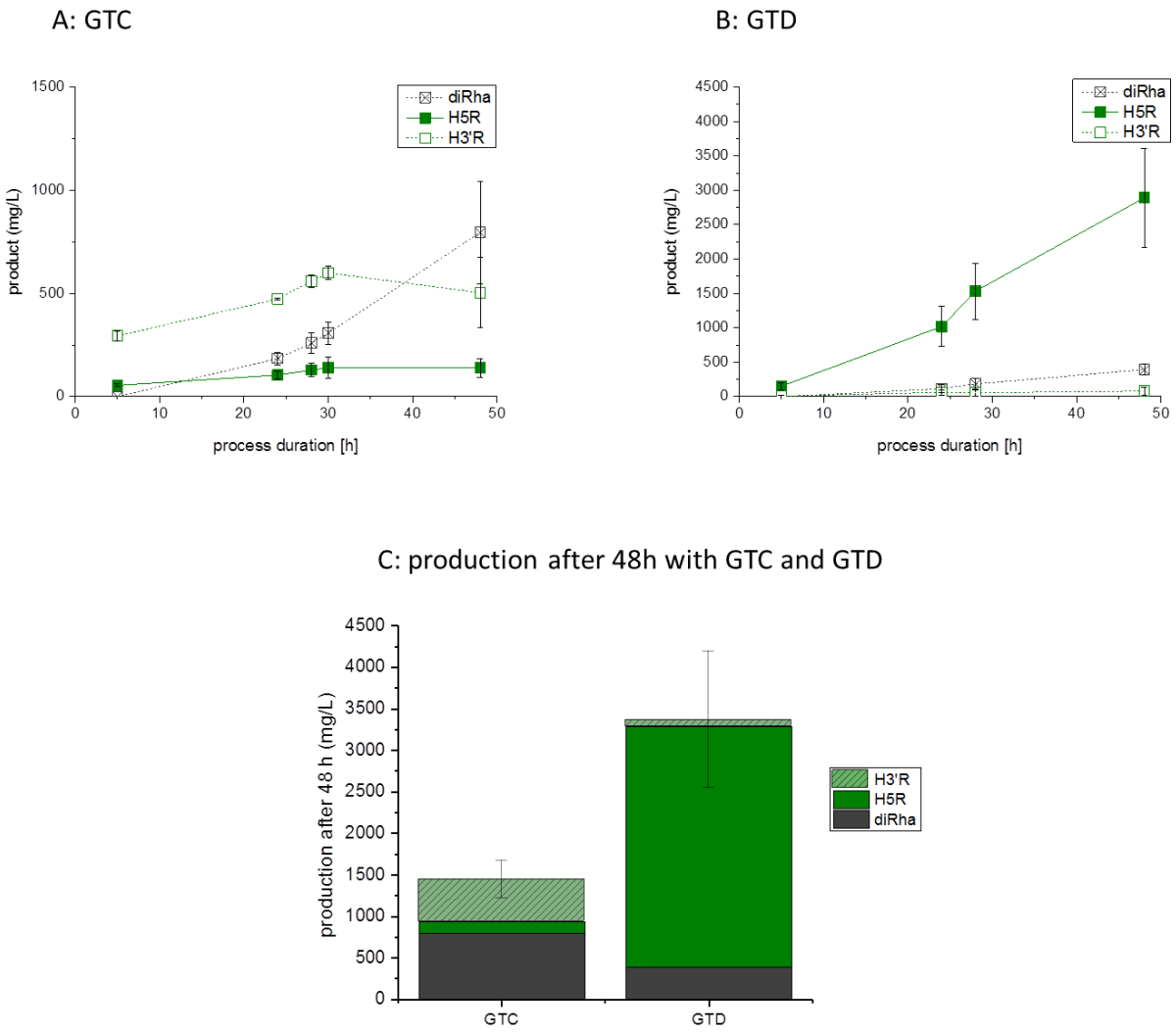

Figure 3.12: Hesperetin-rhamnoside production with the glycosyltransferases GtfC (A) and GtfD (B). The production after 48h biotransformation with GtfC and GtfD is compared (C) (n=3).

Additionally, GtfD was also compared to GtfC in whole cell biotransformations of naringenin. After 24 h fed-batch fermentation in TB medium N5R concentration of 472.74 mg/L with GtfC was reached. With GtfD the concentration of N5R has been doubled and reached 1096.74 mg/L after 24 h (Fig. 3.13 C). With GtfC product formation of N5R of approximate 1000 mg/L after 54 h could be reached (only done once) and then N5R production stagnates (Fig. 3.13 A). Instead, with GtfD after a process duration of 70 h N5R concentration of 2631.34 mg/L could be reached. The product is formed until the end of the process, enabling longer process durations (Fig. 3.13 B).

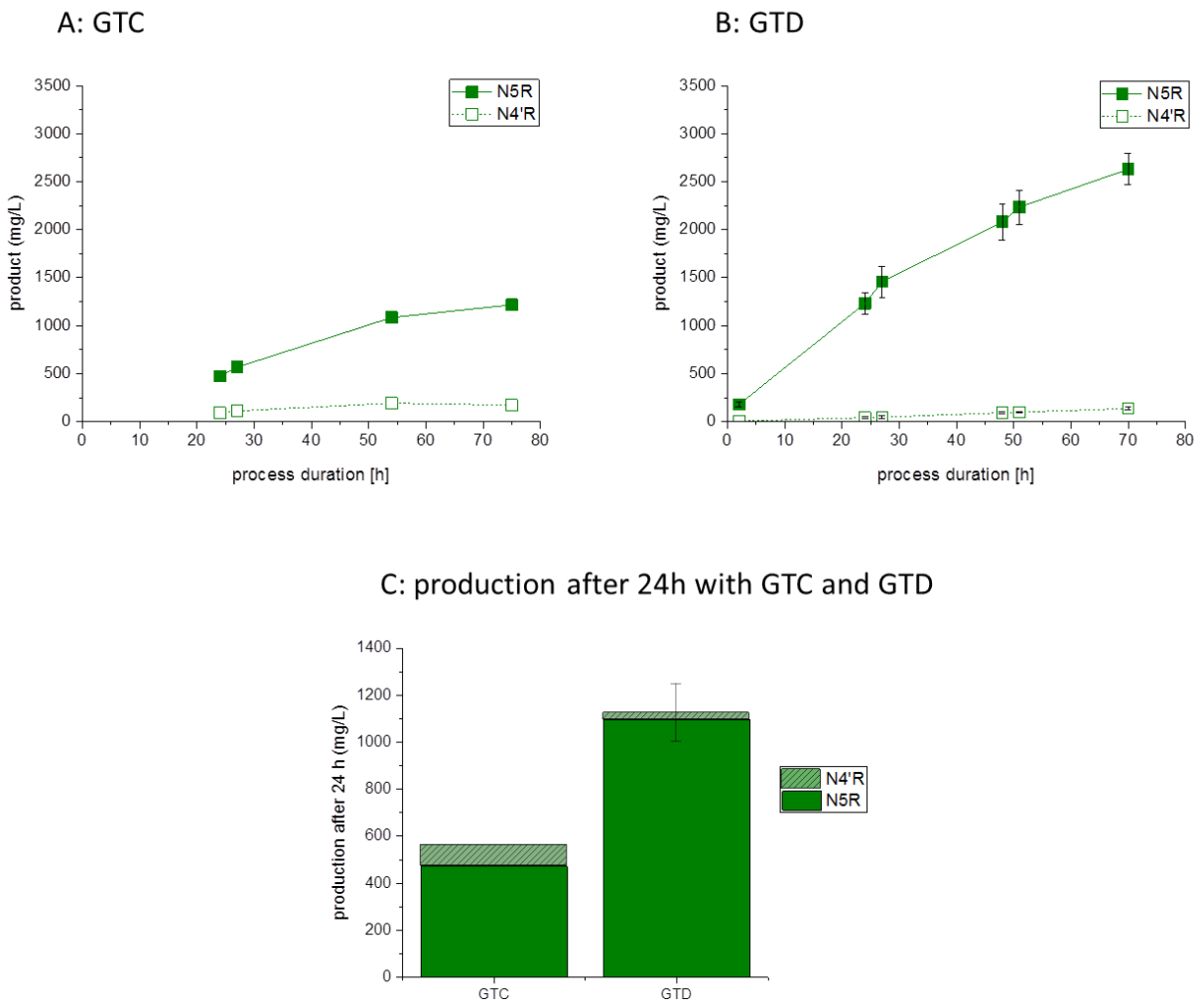

Figure 3.13: Naringenin-rhamnoside production with the glycosyltransferases GtfC (A) (Standard deviation is missing because only done once) and GtfD (B) (n=3). The production after 24h biotransformation with GtfC and GtfD is compared (C).

3.4.1 Biotransformation of hesperetin with GtfD in 10 liter-scale

The glycosylation of hesperetin with glycosyltransferase GtfD was scaled-up to a 10 L-scale fed-batch process and the candidate H5R could be successfully produced in gram-scale. In Figure 3.14 the process parameters of such fermentation run are plotted over the process time.

The cells grow over more than 80 hours with high cell viability to an OD_{600} around 45 (Fig. 3.14). During exponential growth phase the dissolved oxygen (DO) decreases to the set-point of 30%, where it is hold by stirrer regulation (400 to 800 rpm). When the carbon source is limited, the dissolved oxygen increases as a "hunger peak" (Fig. 3.14 after 18h). Then the fed-batch with glucose ($y=10\ e^{0.1*t}$, until constant feed rate of 30 mL/h) starts and DO oscillates

around 30% for the remaining process time. During exponential cell growth the carbon dioxide concentration in the exhaust rises and remains then constant during the production phase (Fig. 3.14).

With start of the fed-batch phase 5 g/L of the precursor hesperetin and 100 µM IPTG for induction were supplemented to the fermentation broth. H5R could be produced in a stable process over process duration of 87 hours. The concentration of H5R increased until the end of the fermentation (Fig. 3.14). At the end of fermentation the increased cell density with an OD_{600} of over 40 resulted in a higher demand of oxygen. This could be seen in a rising CO_2 in the exhaust and an increase in the stirrer speed N (rpm) to maintain a constant DO% (Fig. 3.14). The dissolved oxygen is one of the most critical values in *E. coli* fermentation and has to be regulated by the stirrer to a constant level to avoid oxygen limitation and oscillating cultivation conditions. At such conditions acetat accumulation can occur and negatively affect the production of the recombinant GtfD and the yield of H5R (Schmidt 2005).

It could be shown that the developed fed-batch process for biotransformation of hesperetin with GtfD in TB-medium could be transferred to a 10-fold scale and H5R could be produced to concentrations of nearly 3.5 g/L (Fig. 3.14).

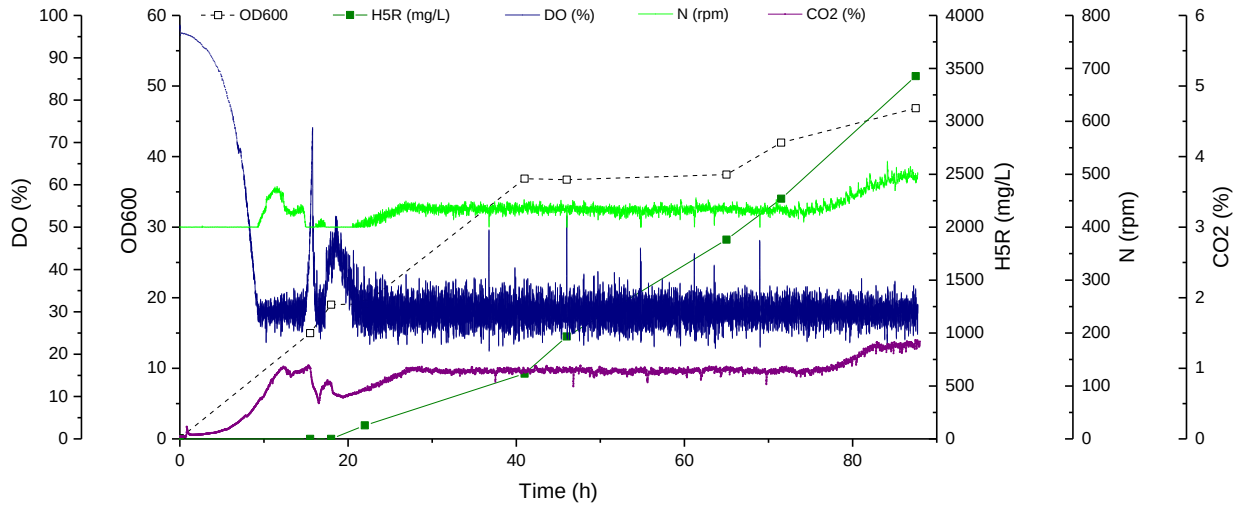

Figure 3.14: Process diagram of H5R production with glycosyltransferase GtfD in a 10 L-scale stirring tank bioreactor. Product concentration, optical density OD (UV 600nm), dissolved oxygen (DO %), stirrer speed N (rpm) and CO2 (%) in exhaust of one single run are plotted.

3.5 Purification of naringenin-5-O-rhamnoside and hesperetin-5-O-rhamnoside

For each of the two bioactive candidates H5R and N5R there is a characteristic fingerprint of the analytical UHPLC-MS-MS at the end of the biotransformation. For UHPLC analytics a reversed phase C18 column is used (for more information see chapter 2.5.3). The UHPLC chromatogram of the hesperetin-5-O-rhamnoside production with GtfD consists of 7 peaks (Fig. 3.15). First peak is the injection peak. Then the hesperetin glycosides are eluted from the column in order of the hydrophilic to the more hydrophobic one. Peak 2 is the hesperetin-di-rhamnoside, followed by the main product hesperetin-5-O-rhamnoside at a retention time of 3:19 min. The hesperetin-3'-O-rhamnoside has a retention time of 3:61 min. The hydrophobic precursor hesperetin with a retention time of 4:00 min is almost depleted (Fig. 3.15).

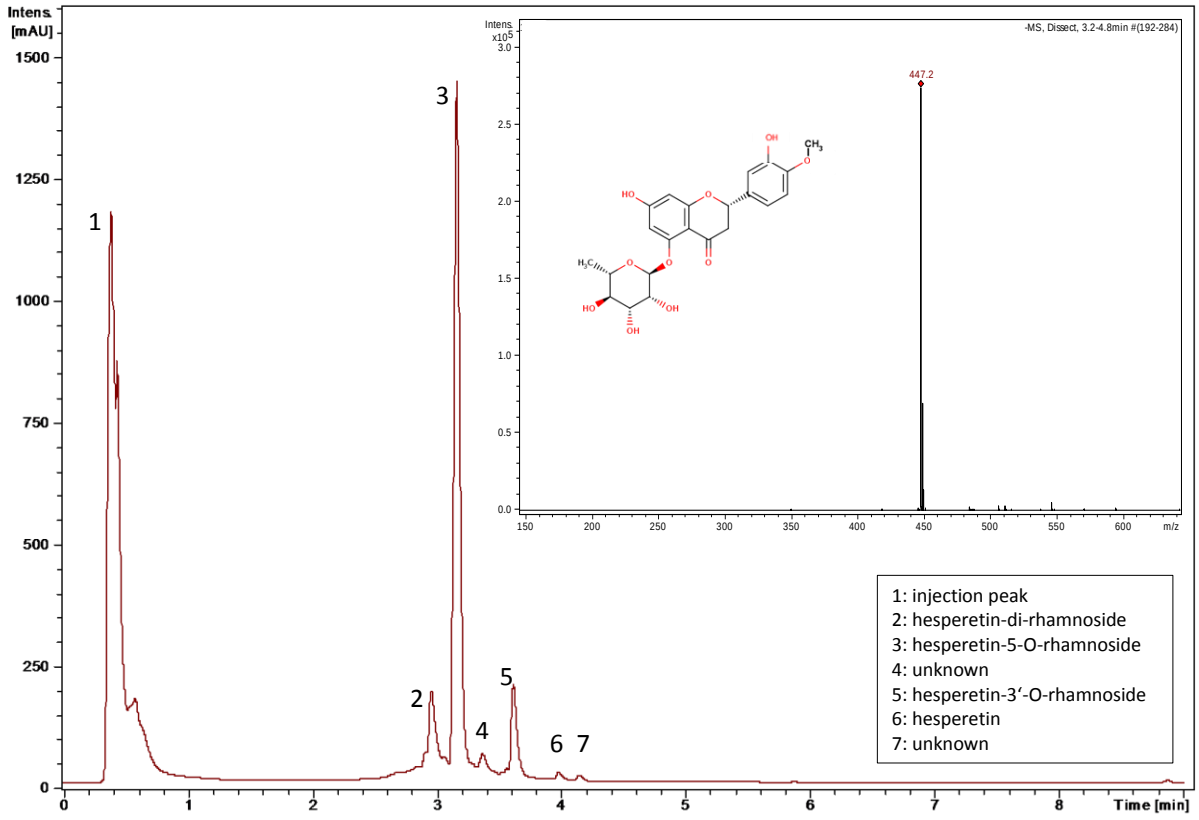

Figure 3.15: UHPLC-MS-MS results from hesperetin-5-O-rhamnoside production with GtfD at the end of fermentation. The main product H5R (peak 3) has a molar mass of 448 g/mol.

The UHPLC chromatogram of the naringenin-5-O-rhamnoside production with GtfD consists of only 5 peaks, including the injection peak (peak 1). The naringenin-5-O-rhamnoside

(peak 2) occurs as a characteristic double-peak at a retention time of 3:10 min and naringenin-4'-O-rhamnoside (peak 3) at a retention time of 3:60 min (Fig. 3.16).

Like most of the flavanones naringenin and hesperetin have a chiral carbon atom in position 2, resulting in (R)- and (S)-enantiomers, which can have different biological activities (Yanez et al. 2007). So the naringenin-5-O-rhamnosides can be a glycoside of a single stereoisomer (2S-naringenin or 2R-naringenin) or a stereoisomer mixture. The double-peak leads to the assumption that the N5R occurs as a mixture of two isomers (Fig. 3.16, peak 2). When compounds are stereochemically unstable, in a racemization process an equilibrium is reached between the two stereoisomers. This can be induced by external factors such as temperature, pH and others. Flavanones with a free hydroxy group in the C4'-position, like naringenin, racemize easier than flavanones with a methoxy group, like hesperetin (Yanez et al. 2007).

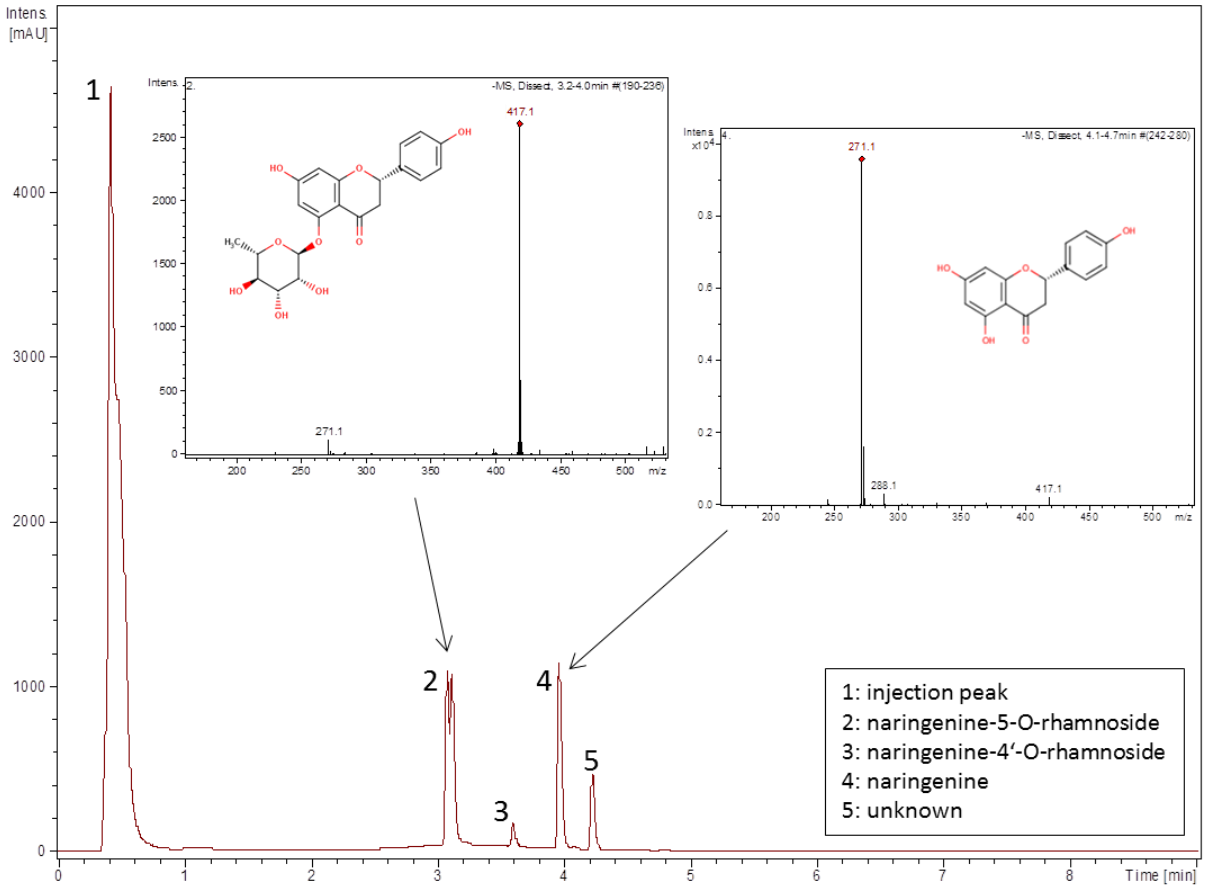

Figure 3.16: UHPLC-MS-MS results from naringenin-5-O-rhamnoside production with GtfD at the end of fermentation. The main product N5R (peak 2) has a molar mass of 418 g/mol and the precursor, which is not fully converted, has a molar mass of 272 g/mol.

The precursor naringenin (peak 4) is not completely converted (Fig. 3.16). The last peak after the precursor (Fig. 3.15 peak 7, Fig. 3.16 peak 5) was expected to be a modification of the precursor molecule. But this wasn't further investigated yet.

In the down-stream process the produced glycosides were separated from other components. Due to the fact that the glycosides are secreted into the culture broth, there is no need of cell disruption. The cells were removed by tangential flow filtration (TFF) through a hydrophilic polyethersulfone membrane (0.2 µm). The permeate flow containing the product was further purified by preparative chromatography using C18 and pentafluoro-phenyl (PFP) columns (Fig. 3.17).

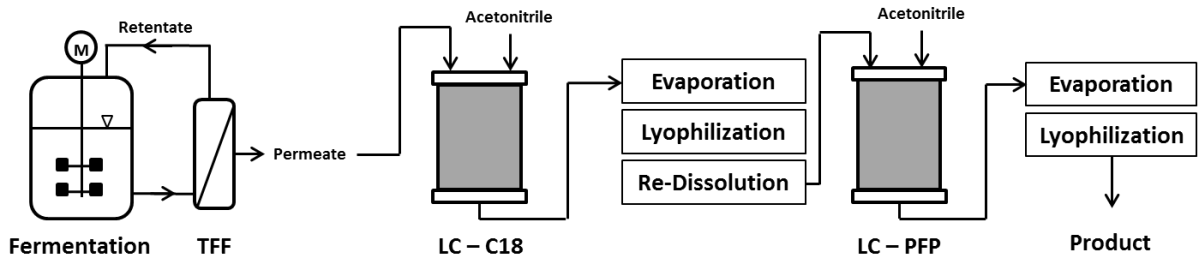

Figure 3.17: Process scheme of the DSP. The process includes the following steps: harvest via TFF membrane (0.2 µm) for cell-free permeate, and purification and enrichment of product over two reversed phase chromatography steps (C18 and Pentafluorphenyl (PFP)).

The following chromatogram shows the collected fractions of a C18 chromatography of 1 liter sterile filtrated culture broth of a hesperetin biotransformation loaded onto an Agilent SB-C18 column (21.2 mm internal diameter x 250 mm length, 7 µm particle size). The fraction RP2 (25 % acetonitrile) contains the hesperetin-5-O-rhamnoside. The hesperetin-3'-O-rhamnoside is mainly found in the RP5 fraction (40 % acetonitrile). Fraction RP6 contains the precursor hesperetin (Fig. 3.18).

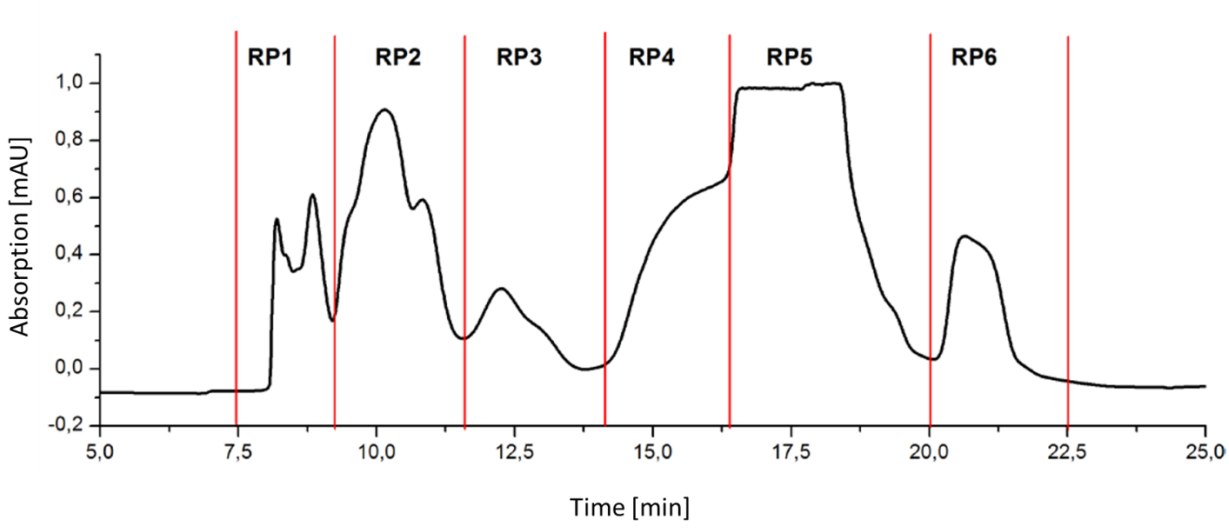

Figure 3.18: Chromatogram of 1 liter hesperetin-biotransformation purification using a C18 column (21.2 mm internal diameter x 250 mm length, 7 µm particle size). Sample were loaded with a flow rate of 20 mL/min and eluted with step gradient of acetonitrile (A) and water with 0.05 % formic acid (B): 1. 0 – 5 min 10:90 (A:B), 2. 5.1 – 15 min 25:75, 3. 15.1 – 25 min 40:60, 4. 25.1 – 30 min 100:0, 5. 30.1 – 40 min 10:90. RP2 (H5R) and RP5 (H3'R) are product fractions. Chromatogram from Anton Letzer (2016).

The product fractions after the first chromatography step were evaporated to remove the solvent acetonitrile and analyzed by UHPLC-MS-MS. Product fractions with sufficient purity were freeze-dried for product storage or, if necessary, for storage of the fraction until the next chromatography step (LC-PFP). When a second chromatography step was necessary, it was done by Henning Rosenfeld (data not available). The lyophilized product is a yellowish to light yellow brown powder.

During this work the down-stream process had been optimized. The first chromatography step was changed to solid phase extraction (SPE) with flash cartridges containing the sorbent instead of HPLC columns. HPLC columns are much more expensive because they have to withstand high pressures and are packed more densely than flash cartridges. HPLC columns have a particle size of 2 – 10 µm, whereas SPE cartridges have larger particle sizes between 20 and 100 µm (or even larger e.g. Amberlite (an acrylic resin), 560-710 µm). Advantages of SPE are a lower solvent consumption and a faster separation (time saving).

For the SPE different materials similar to the reverse phase materials of the HPLC were tested. The experiments were conducted within the master thesis of Charles Wiedenhöfer. The materials are listed in Table 3.3.

Table 3.3: SPE materials tested for the adsorption and desorption of the flavonoide-glycosides hesperetin-5-O-rhamnoside and naringenin-5-O-rhamnoside.

	supplier	adsorbent	particle size [µm]	pore diameter [Å]	surface [m²/g]
AloxN	Macherey-Nagel	aluminium oxide	60 - 150	60	150
Amberlite XAD-7	Sigma-Aldrich	acrylic resin	560 - 710	300 - 400	380
C18 Hydra	Macherey-Nagel	octadecyl-modified silica	45	60	500
C6H5	Macherey-Nagel	phenyl-modified silica	45	60	500
C6H11	Macherey-Nagel	cyclohexyl-modified silica	45	60	500
Davisil 633	Sigma-Aldrich	silica gel	35 - 75	60	480
HR-X	Macherey-Nagel	polystyrene-divinylbenzene resin	45	55	1000
SiOH	Macherey-Nagel	silica (unmodified)	45	60	500
XTR	Macherey-Nagel	kieselguhr	45	60	500

The C18 Hydra, C6H5 and C6H11 turned out to be the most suitable materials (Fig. 3.19). The adsorption of N5R at the materials AloxN, Amberlite, Davisil 633, SiOH and XTR is very low. N3'R instead adsorbs very well at AloxN, but doesn't desorb. Also N3'R adsorbs better than N5R at Amberlite and XTR. However the adsorption of N3'R at Amberlite, Davisil 633, SiOH and XTR is low. N5R and N3'R showed similar results with C18 Hydra, C6H5 and C6H11. At this materials adsorption and also desorption was the best. HR-X showed also good adsorption of N5R and N3'R, but a low desorption.

Based on these results the preparative RP-HPLC was replaced by RP-SPE with C18 Hydra material. For more information about the SPE method see chapter 2.6.3.

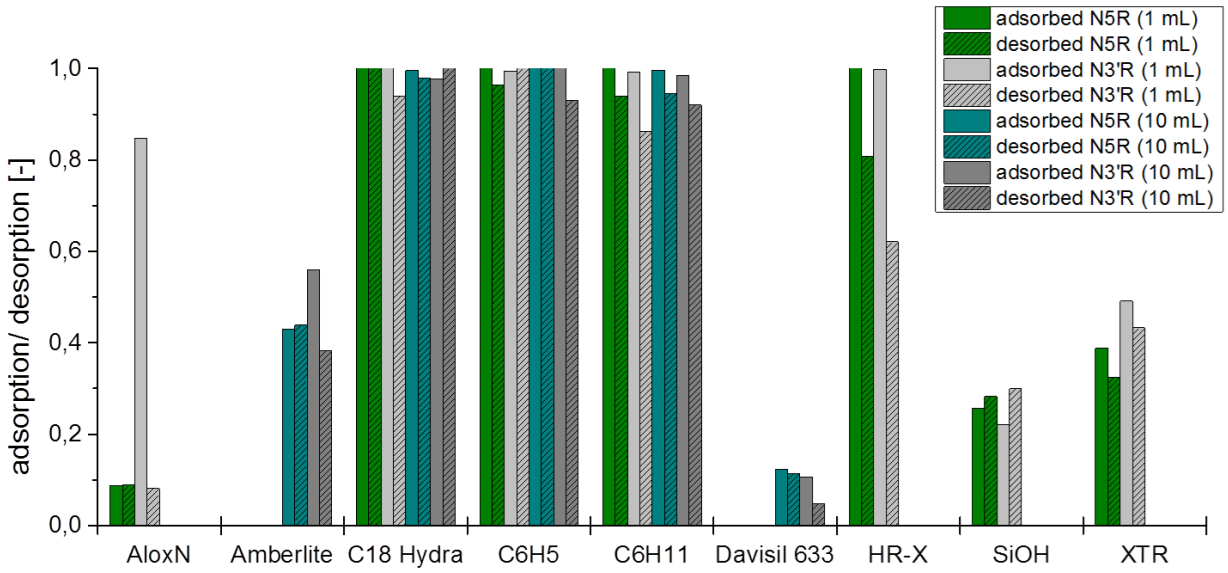

Figure 3.19: Adsorption and desorption of N5R and N3'R (normalized). 1 mL or 10 mL of the sample containing the two naringenin-rhamnosides (c_{N5R} = 0,3072 mg/ mL, $c_{N3'R}$ = 0,113 mg/ mL) was load on to 1000 mg SPE material at room temperature. Data from Charles Wiedenhöfer (2016). (Standard deviation is missing because only done once).

As another optimization of the down-stream process the solvent had to be changed. Since acetonitrile is listed as class 2 solvent in the guidance from the FDA (Food and Drug Administration), for the preparative chromatography acetonitrile had to be replaced by another solvent listed in class 3. From the FDA solvents are grouped by class from 1 to 3 (Guidance for Industry, Q3C Impurities: Residual Solvents). Class 1 solvents should be avoided in the manufacture of pharmaceutical products because of their unacceptable toxicity and environmental hazard. Solvents in class 2 should be limited. Class 3 solvents are known as less toxic with no risk to human health at levels normally accepted in pharmaceuticals.

For the choice of an alternative solvent it had to be considered, that the solvent must be mixable with water for gradient elution and should have the same or better elution capacity than acetonitrile. Acetone turned out to be a suitable solvent, which is categorized as class 3 from the FDA, is miscible with water and has a stronger polarity and elution effect than acetonitrile. But acetone is not suitable for the established UV detection of flavonoids and their glycosides at 254 nm because the adsorption of acetone overlaps with the adsorption of the flavonoids. Within the wavelength range from 254 to 350 nm of flavonoids, the detection had to be done at 350 nm. At this wavelength acetone has no adsorption anymore. In preparative chromatography or SPE, where it is common to overload the column with the sample, the elution peaks of the product and by-products can be detected, but the adsorption

of flavonoids at 350 nm is too low for an analytical detection, especially of lower product concentrations. That's why for analytical HPLC acetonitrile has been further used as eluent. For preparative SPE acetonitrile could be replaced by acetone.

Since higher product concentrations were reached during fermentation, the product fraction of SPE contained a high concentration of the product, which is kept dissolved by the solvent. In the next process step, where the solvent is removed, the product precipitates. This precipitate can be collected by filtration and is then lyophilized to remove residual water (Fig. 3.20). During evaporation only 50 % of the product in the SPE fraction can be precipitated. The remaining product had to be further purified over HPLC, but doesn't reach the same quality than the precipitate (Fig. 3.22).

Figure 3.20 shows the process scheme of the new down-stream with SPE and product-precipitation.

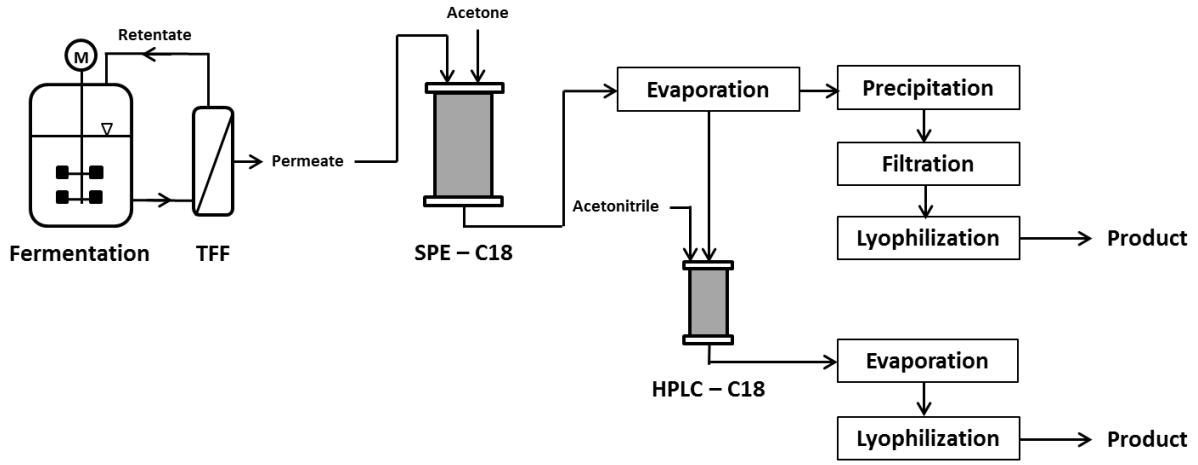

Figure 3.20: Process scheme of the new DSP with product purification and enrichment over a solid-phase extraction cartridge (C18). Due to high concentrations in the product fraction, the rhamnoside precipitates during evaporation of the solvent. The remaining, dissolved product has to be further purified over HPLC or has to be discarded.

A filter cake of the precipitated product H5R is shown on the picture below (Fig. 3.21).

Figure 3.21: Filter cake of H5R after precipitation and filtration.

After lyophilization the precipitated glycosides are obtained as a slightly colored white powder, as for example the rhamnoside of hesperetin H5R (Fig. 3.22). The remaining product, which is not precipitated, has a brown color (Fig. 3.22), that can't be removed by RP-HPLC. It is not worth the effort to purify the remaining product over HPLC, when the brown color cannot be removed. That's why the yield of the precipitate should be improved, so that the loss is small enough to discard the rest.

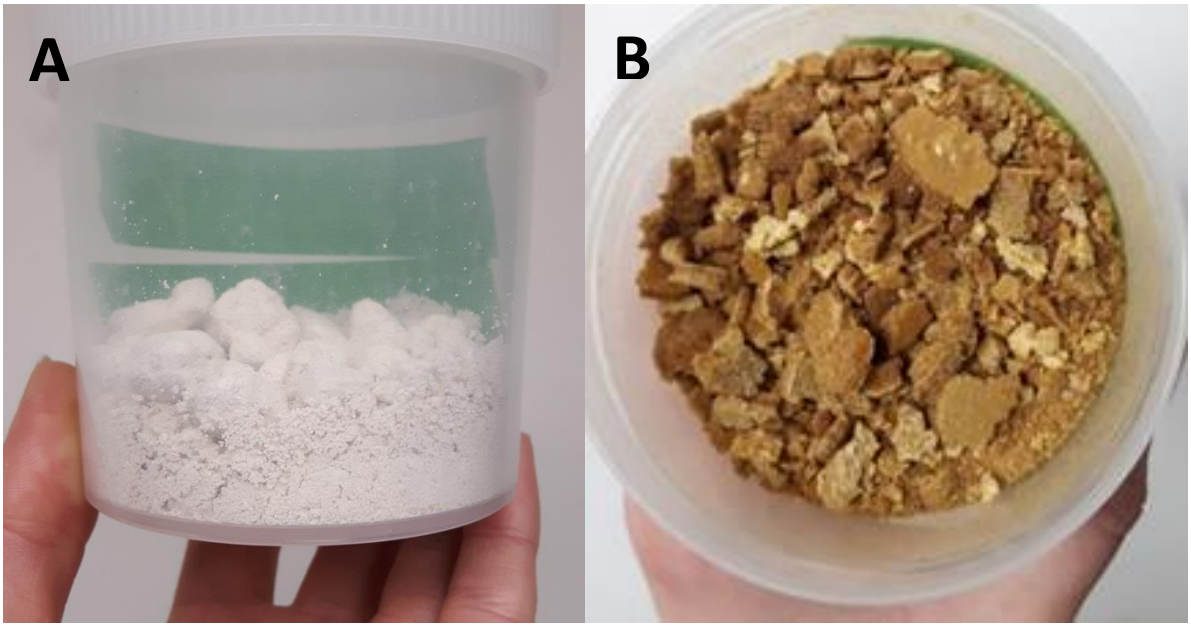

Figure 3.22: Precipitated H5R lyophilisate is a light, white powder (A). The lyophilisate of the remaining product purified over HPLC has a brown color (B).

The white powdered lyophilisates of H5R and N5R were examined under a phase-contrast microscope. The microscopies show the crystalline structure of the polyphenolic glycosides hesperetin-5-O-rhamnoside (H5R) (Fig. 3.23 A) and naringenin-5-O-rhamnoside (N5R) (Fig. 3.23 B).

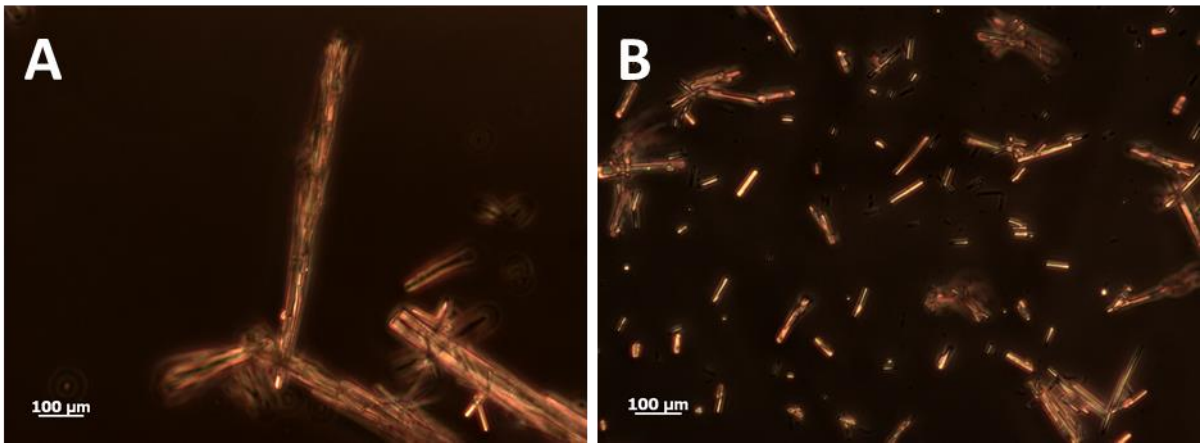

Figure 3.23: Crystalline structure of purified H5R (A) and N5R (B) under a phase-contrast microscope, 40-fold magnification.

3.6 TolC overexpression for an improved glycoside production

As shown in chapter 3.3.2 only a certain percentage of the glycosylated product is secreted into the culture supernatant. To improve the transport out of the cell and enhance the production yield the overexpression of the outer membrane protein TolC, which is part of several membrane efflux systems, has been implemented. The *tolC*-gene was cloned with a plasmid into the *E. coli* strain MG1655 *Δpgi ΔgalU Δrec::Mhex* (constructed by Constantin Ruprecht) as well as the gene for the glycosyltransferase GtfD. The production of N5R was compared with the same strain without overexpression of the *tolC*-gene (but *tolC* was not knocked out). For detailed information about the strains see chapter 2.1.

N5R production with and without *tolC* overexpression was conducted as 6-fold determination in shake flasks in 20 mL TB medium with dextrin (5%). First data was received in summer (Fig. 3.24). Same experiment was repeated three month later in winter and showed different results (Fig. 3.25).

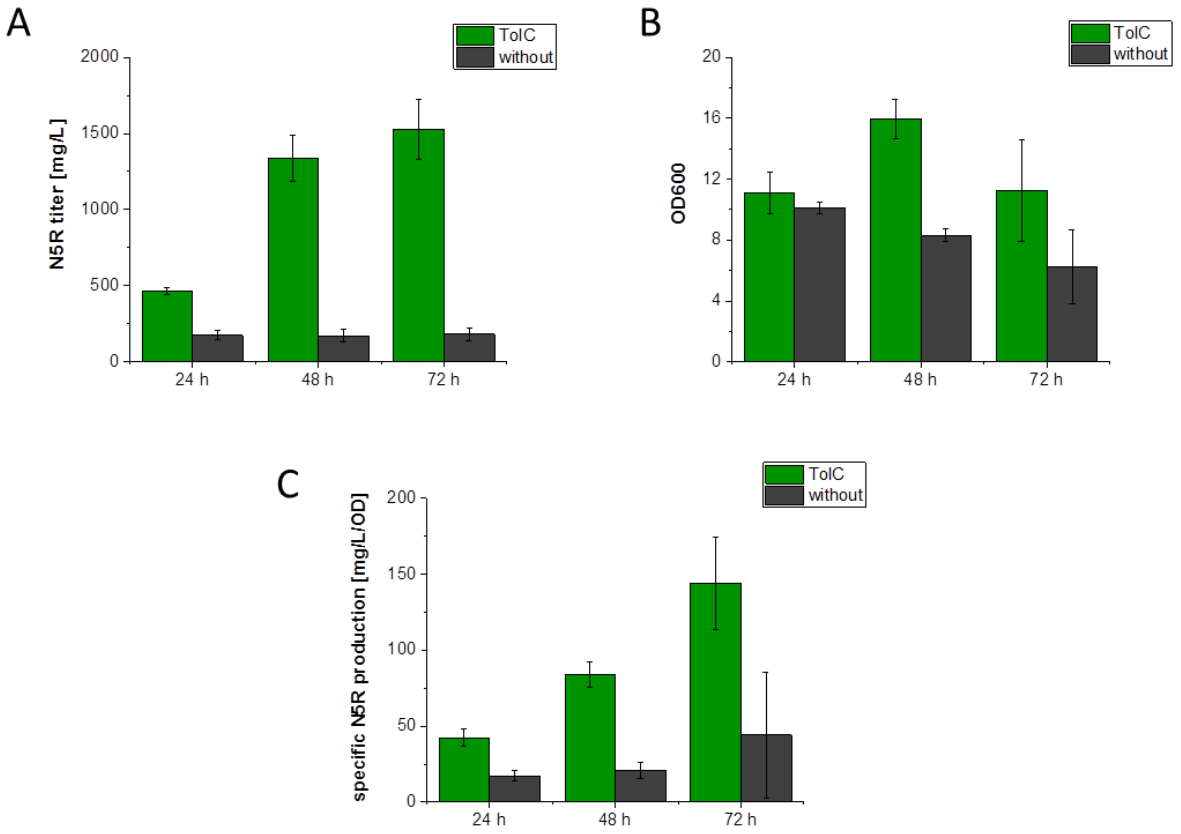

Figure 3.24: Data from N5R production with (green) and without (grey) TolC overexpression in shake flasks (n=6). Naringenin supply 5 g/L A: N5R concentration (mg/L). B: Cell density OD (600 nm). C: Specific N5R production (mg/L/OD). Runs were performed during summer months.

In the first experiment the TolC-strain achieved N5R concentrations of 1500 mg/L, whereas the strain without TolC overexpression only reached concentrations of 200 mg/L (Fig. 3.24 A). The results from the other experiment show nearly the same concentration of up to 200 mg/L N5R for the strain without TolC overexpression (Fig. 3.25 A). But with TolC overexpression only up to 600 mg/L were produced (Fig. 3.25 A), which is nearly a third of the concentration reached in the experiment in summer. The TolC-strain has grown to an OD_{600} of 11 to 16 (Fig. 3.24 B) and only to an OD_{600} of 7 to 8 in the second experiment (Fig. 3.25 B). The OD_{600} values of the strain without TolC overexpression showed no big differences and were in both experiments around an OD_{600} of 8 to 10 (Fig. 3.24 B and Fig. 3.25 B). The lower cell growth of the TolC-strain could be an indicator for a bad cell viability of the cryo-culture and may explain the lower N5R production in the second experiment, which was performed three month later. Repeated thawing and freezing of the cryo-culture can negatively impact the quality. Still, in the second experiment the overexpression of TolC seems to significantly improve the production titer.

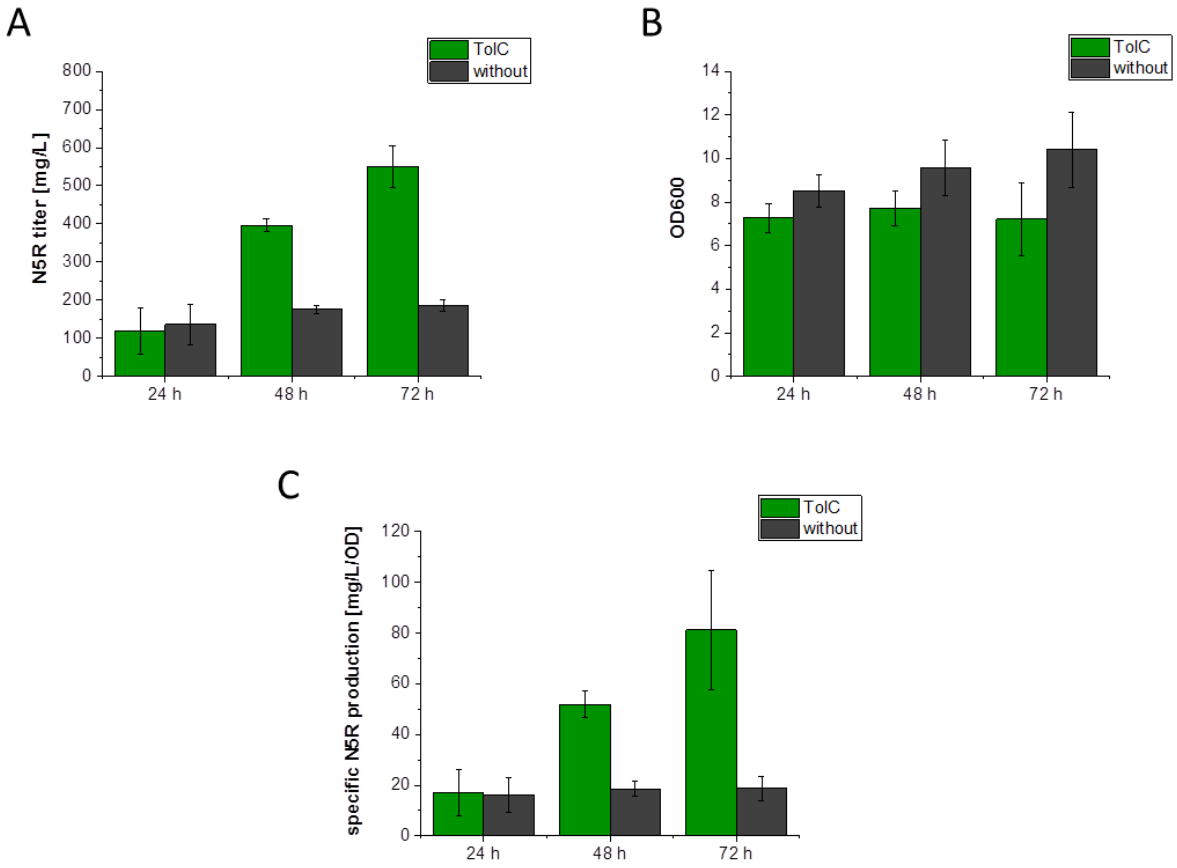

Figure 3.25: Data from N5R production with (green) and without (grey) TolC overexpression in shake flasks (n=6). Naringenin supply 5 g/L. A: N5R concentration (mg/L). B: Cell density OD (600 nm). C: Specific N5R production (mg/L/OD). Runs were performed during winter months.

The specific N5R production in the first experiment rises from around 40 mg/L/OD after 24 h to 140 mg/L/OD after 72 h for the TolC-strain. After 48 h the specific production of N5R is around 80 mg/L/OD (Fig. 3.24 C). The strain without TolC overexpression shows a constant lower specific production of 20 mg/L/OD at 24 and 48 h, except of the 72 h value of 40 mg/L/OD with a high standard deviation (Fig. 3.24 C).

The second experiment shows nearly the same results for the strain without TolC overexpression. The specific N5R production is constant around 20 mg/L/OD at all three times of measurement (Fig. 3.25 C). The specific production of the TolC-strain is 20 mg/L/OD after 24 h, 50 mg/L/OD after 48 h and around 80 mg/L/OD after 72 h of fermentation (Fig. 3.25 C).

In Figure 3.26 the N5R production at different naringenin concentrations between 1 g/L and 10 g/L with and without TolC overexpression was examined. Different precursor concentrations did not show any effect on the N5R production. Only 1 g/L was not enough of

the precursor for the biotransformation with the TolC-strain, so that the concentration of 1500 mg/L could not be reached (Fig. 3.26).

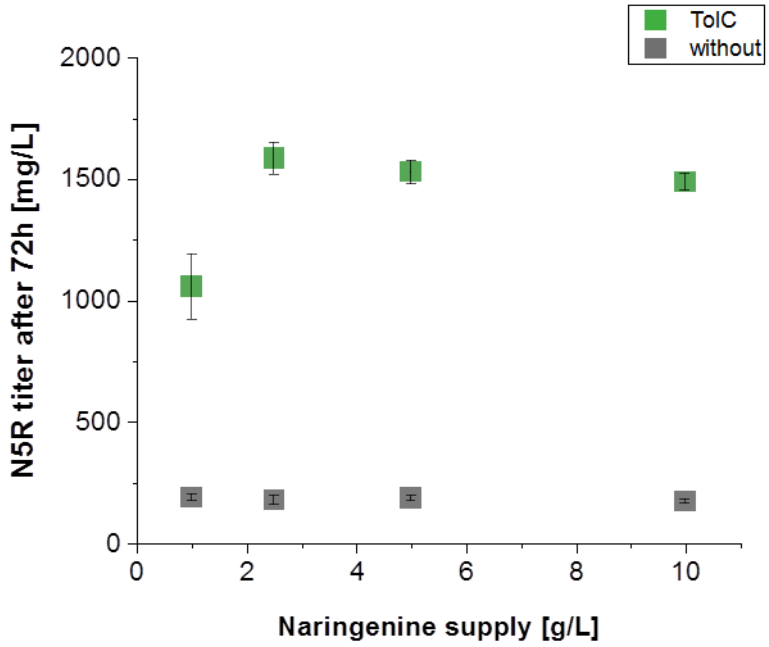

Figure 3.26: N5R production at different naringenin concentrations with and without TolC overexpression in shake flasks (n=3). Runs were performed during summer months.

The experiments above showed that the product concentration of flavonoid-glycosides can be increased up to 8-fold by an improved transport of the glycosides out of the cell due to overexpression of TolC.

For future steps in this project the *tolC*-gene should be cloned into a production strain and biotransformation should be done in a larger scale in bioreactor to compare the production titer. TolC as an outer membrane protein is only one part of the multi drug efflux pumps, which are organized as tripartite systems (see chapter 1.6). So the two other proteins, the efflux protein, located in the cytoplasmatic membrane, and the membrane-fusion protein, located in the periplasmic space, should be overexpressed as well. There are many different multi drug efflux pumps, like for example AcrAB-TolC, AcrAD-TolC, AcrEF-TolC, EmrAB-TolC, EmrKY-TolC, MdtABC-TolC, MdtEF-TolC, MacAB-TolC or EntS-TolC, which could be screened for an improved transport of flavonoid-glycosides.

4 Conclusion

The use of flavonoids in cosmetic or healthcare applications is limited by their low solubility and bioavailability. Glycosylation has positive impact on these properties and can further increase the stability and detoxification of flavonoids. The glycosylation of flavonoids can take place *in vivo* in a whole cell biotransformation with recombinant glycosyltransferases of family GT 1, where novel glycosides can be produced. But in most approaches the production yields of flavonoid-glycosides were significantly below 1 g/L (Tab. 1.1). To my best knowledge, only two research groups were able to reach higher concentrations. De Bruyn *et al.* (2015b) and Pei *et al.* (2016) developed a growth coupled glycosylation system in metabolic engineered *E. coli* with sucrose as carbon source and could produce 1.2 g/L of quercetin-3-O-rhamnoside (De Bruyn et al. 2015b) and 3.6 g/L kaempferol-3-O-glucoside (Pei et al. 2016).

In this work a production process for the rhamnosylation of naringenin and hesperetin were developed to produce novel 5-O-rhamnosides. In a fed-batch fermentation on glucose with an *E. coli* strain expressing the glycosyltransferase GtfD from *Dyadobacter fermentans* the target products naringenin-5-O-rhamnoside (N5R) and hesperetin-5-O-rhamnoside (H5R) could be produced with concentrations of 2.6 g/L and 2.9 g/L, respectively. Scale-up of the rhamnosylation process of hesperetin with GtfD to a 10 L-scale fed-batch fermentation resulted in 3.5 g/L H5R over a process duration of 72 hours. Instead, glycosylation of hesperetin with the metagenome-derived GtfC resulted in a complete different production profile with production titers below 1 g/L. The concentration of the target product H5R was very low at around 0.1 g/L and the by-product hesperetin-3'-O-rhamnoside was built with 0.6 g/L. As main product a hesperetin-di-rhamnoside was produced with 0.8 g/L. These results showed that GtfC is not a suitable enzyme for the rhamnosylation of hesperetin at the 5-O-position. GtfC prefers the 3'-O-position over the 5-O-position, if it is available. This has also been shown for the flavone diosmetin. Nevertheless, different novel rhamnosides of chrysin and biochanin A (5-O-, 5,7-di-O-), diosmetin and hesperetin (3'-O-, 5-O-), and naringenin (5-O-, 4'-O-) could be identified as products of GtfC. These NMR-identified rhamnosides are to my best knowledge not described so far, showing the great potential of GtfC to produce novel flavonoid-rhamnosides as bioactive candidates with health-promoting effects.

During process development a repeated fed-batch procedure was established to increase the production yield by extended process duration. The culture medium is changed over TFF after

each fed-batch while the cells remain in the bioreactor. The next fed-batch starts with fresh medium and new precursor. With four or five fed-batches the process duration could last 8 or 10 days instead of 48 to 72 hours in a normal fed-batch and the time-consuming preparation, sterilization and pre-cultivation as well as the post-processing for decontamination and cleaning can be saved. During the medium exchange the cell culture becomes concentrated and the used medium containing the products is harvested. The duration of the medium exchange and volume of the removed and replaced medium depends on the cell viability. The membrane gets blocked easier by cultures with low cell viability due to lysed cell material. This leads to variations in volume and product amount of the harvested permeate and has impact on the next fed-batch. This means that with the repeated fed-batch procedure there is no reproducibility, which is impracticable for a production process. Therefore, the production of flavonoid glycosides has been done in normal fed-batch fermentations.

With regard to a large scale production process, minimal medium has been strived to be used for the fermentation instead of complex medium because of its advantages like high reproducibility, stable processes and independence from suppliers. But it could be shown that it is not possible to exclude yeast extract from the medium, without a loss of 50 % of production yield. Even with addition of yeast extract the production yields with minimal medium were lower than expected and could not reach the gram scale as with complex medium. So the complex terrific broth medium had been used for biotransformations in this work.

For higher production yields the export of the rhamnosides should be improved by the overexpression of the outer membrane protein TolC. Biotransformation of naringenin with an *E. coli* strain overexpressing the *tolC*-gene was compared to biotransformation with the same strain without overexpression of TolC. Results from small scale experiments showed that the production of naringenin-5-O-rhamnoside (N5R) can be increased up to 8-fold by an improved membrane transport due to overexpression of TolC. These promising results are showing the possibility to significantly increase the production titers of the 5-O-rhamnosides H5R and N5R by optimization of the membrane transport via multi drug efflux pumps.

Literature

Ahn, B. C., Kim, B. G., Jeon, Y. M., Lee, E. J., Lim, Y., Ahn, J.-H., J. Microbiol. Biotechnol. 19 (2009) 387–390.

Barreca, D., Gattuso, G., Bellocco, E., Calderaro, A., Trombetta, D., Smeriglio, A., Laganà, G., Daglia, M., Meneghini, S., Nabavi, S. M., Biofactors. 43 (2017) 495–506.

Blattner, F. R., Plunkett, G. 3rd., Bloch, C. A., Perna N. T., Burland V., Riley M., Collado-Vides J., Glasner J. D., Rode C. K., Mayhew G. F., Gregor J., Davis N. W., Kirkpatrick H. A., Goeden M. A., Rose D. J., Mau B., Shao Y., Science 277 (1997) 1453–1462.

Bowles, D., Isayenkova, J., Lim, E.-K., Poppenberger, B., Curr. Opin. Plant. Biol. 8 (2005) 254–263.

Chmiel, H., 3. Edition (2011) *Bioprozesstechnik*, Springer.

Christensen, D. G., Orr, J. S., Rao, C. V., Wolfe, A, J., Appl. Environ. Microbiol. 83 (2017) e03034–16.

De Bruyn, F., Maertens, J., Beauprez, J., Soetaert, W., De Mey, M., Biotechnol. Adv. 33 (2015a) 288–302.

De Bruyn, F., Van Brempt, M., Maertens, J., Van Bellegem, W., Duchi, D., De Mey, M., Microb. Cell. Fact. 14 (2015b) 138–150.

De Groot, N. S., Ventura, S., FEBS Letters 580 (2006) 6471–6476.

De Mey, M., De Maeseneire, S., Soetaert, W., Vandamme, E., J. Ind. Microbiol. Biotechnol. 34 (2007) 689.

Dittrich, C. R., Vadali, R. V., Bennett, G. N., San, K.-Y., Biotechnol. Prog. 21 (2005) 627–631.

Federici, L., Walas, F., Luisi, B., Curr. Sci. 87 (2004) 190–196.

Görke, B., Stülke, J., Nat. Rev. Microbiol. 6 (2008) 613–624.

Han, S. H., Kim, B. G., Yoon, J. A., Chong, Y., Ahn J.-H., Appl. Environ. Microbiol. 80 (2014) 2754–2762.

He, X.-Z., Li, W.-S., Blount, J. W., Dixon, R. A., Appl. Microbiol. Biotechnol. 80 (2008) 253–260.

Horváth, C., Trends Analyt. Chem. 1 (1981) 6–12.

Kim, B.-G., Kim, H. J., Ahn, J.-H., J. Agric. Food Chem. 60 (2012) 11143–11148.

Kim, S. Y., Lee, H. R., Park, K., Kim, B.-G., Ahn, J.-H., Appl. Microbiol. Biotechnol. 99 (2015) 2233–2242.

Kiuru, M., Academic dissertation (2002) *Molecular basis of hereditary leiomyomatosis and renal cell cancer (HLRCC)*, Helsinki University.

Krishnakumar, N., Sulfikkarali, N., RajendraPrasad, N., Karthikeyan, S., Biomed. Prev. Nutr. 1 (2011) 223–231.

Lee, C.-H., Jeong, T.-S., Choi,Y.-K., Hyun, B.-H., Oh, G.-T., Kim, E.-H., Kim, J.-R., Han, J., Bok, S.-H., Biochem. Biophys. Res. Commun. 284 (2001) 681–688.

Lewis, W. K., Whitman, W. G., Ind. Eng. Chem. 16 (1924) 1215–1220.

Liao, J.-X., Fan, N.-L., Liu, H., Tu, Y.-H., Sun, J.-S., Org. Biomol. Chem. 14 (2016) 1221–1225.

Lim, E.-K., Ashford, D. A., Hou, B., Jackson, R. G., Bowles, D. J., Biotechnol. Bioeng. 87 (2004) 623–631.

Lim, E.-K., Ashford, D. A., Bowles, D. J., ChemBioChem 7 (2006) 1181–1185.

Liu-Smith, F. and Meyskens, F., Mol. Nutr. Food Res. 60 (2016) 1264–1274.

Lusk, J. E., Williams, R. J. P., Kennedy, E. P., J. Biol. Chem. 243 (1968) 2618–2624.

Malla, S., Pandey, R. P., Kim, B.-G., Sohng, J. K., Biotechnol. Bioeng. 110 (2013) 2525–2535.

Manach, C., Scalbert, A., Morand, C., Remesy, C., Jimenez, L., Am. J. Clin. Nutr. 79 (2004) 727–747.

Marce´, R. M., Borrull, F., J. Chromatogr. A 885 (2000) 273–290.

Melander, W. R., Horváth, C., Chromatographia 18 (1984) 353–361.

Miler, M., Živanović, J., Ajdžanović, V., Oreščanin-Dušić, Z., Milenković, D., Konić-Ristić, A., Blagojević, D., Milošević, V., Šošić-Jurjević, B., Exp. Gerontol. 84 (2016) 49–60.

Monod, J., Annu. Rev. Microbiol. 3 (1949) 371–394.

Pandey, R. P., Malla, S., Simkhada, D., Kim, B.-G., Sohng, J. K., Appl. Microbiol. Biotechnol. 97 (2013) 1889–1901.

Parajuli, P., Pandey, R. P., Trang, N. T. H., Chaudhary, A. K., Sohng, J. K., Microb. Cell. Fact. 14 (2015) 76–88.

Pei, J., Dong, P., Wu, T., Zhao, L., Fang, X., Cao, F., Tang, F., Yue, Y., J. Agric. Food Chem. 64 (2016) 7966–7972.

Piddock, L. J. V., Nat. Rev. Microbiol. 4 (2006) 629–636.

Poole, C. F., Chromatographia 82 (2019) 49–64.

Poole, C. F., Lenca, N., Liquid Chromatography (Second Edition) Fundamentals and Instrumentation (2017) 91–123.

Prinz, W. A., Aslund, F., Holmgren, A., Beckwith, J., J. Biol. Chem. 272 (1997) 15661–15667.

Rabausch, U., Juergensen, J., Ilmberger, N., Böhnke, S., Fischer, S., Schubach, B., Schulte, M., Streit; W. R., J. Appl. Environ. Microbiol. 79 (2013) 4551–4563.

Rey, L., May, J. C., 3. Edition (2010) *Freeze-Drying/Lyophilization of Pharmaceutical and Biological Products*, Drugs and the Pharmaceutical Sciences 206.

Rey, L., Drugs and the Pharmaceutical Sciences 206 (2010) 1–29.

Roepke, J., Bozzo, G. G., ChemBioChem 14 (2013) 2418–2422.

Ruprecht, C., Bönisch, F., Ilmberger, N., Heyer, T. V., Haupt, E. T. K., Streit, W. R., Rabausch, U., Metab. Eng. (2019), unpublished (Submission no: MBE_2019_64).

Sanger, F., Nicklen, S., Coulson, A. R., Proc. Nati. Acad. Sci. USA 74 (1977) 5463–5467.

Schmidt, F. R., Appl. Microbiol. Biotechnol. 68 (2005) 425–435.

Simkhada, D., Kim, E. M., Lee, H. C., Sohng, J. K., Mol. Cells 28 (2009) 397–401.

Simkhada, D., Lee, H. C., Sohng, J. K., Biotechnol. Bioeng. 107 (2010) 154–162.

Slámová, K., Kapešová, J., Valentová, K., Int. J. Mol. Sci. 19 (2018) 2126–2144.

Sørensen, H. P., Mortensen, K. K., Microb. Cell. Fact. 4 (2005) 1.

Stanisic, D., Costa, A. F., Fávaro, W. J., Tasic, L., Seabra, A. B., Durán, N., J. Nanomed. Nanotechnol. 9 (2018) 515–520.

Stülke, J., Hillen, W., Curr. Opin. Microbiol. 2 (1999) 195–201.

Sun, J., Laval, S., Yu, B., Synthesis 46 (2014) 1030–1045.

Teramoto, M., Zhang, Z., Shizuma, M., Kawasaki, T., Kawarabayasi, Y., Nakamura, N., Advances in Applied Biotechnology, Prof. Marian Petre (Ed.) (2012) 225–234.

Thuan, N. H., Pandey, R. P., Thuy, T. T., Park, J. W., Sohng, J. K., Appl. Biochem. Biotechnol. 171 (2013a), 1956–1967.

Thuan, N. H., Park, J. W., Sohng, J. K., Process Biochem. 48 (2013b), 1744–1748.

Thuan, N. H., Malla, S., Trung, N. T., Dhakal, D., Pokhrel, A. R., Chu, L. L., Sohng, J. K., World J. Microbiol. Biotechnol. 33 (2017) 36-46.

Tripoli, E., Guardia, M. L., Giammanco, S., Majo, D. D., Giammanco, M., Food Chem. 104 (2007) 466–479.

Usach, I., Taléns-Visconti, R., Magraner-Pardo, L., Peris, J. E., Food Chem. Toxicol. 80 (2015) 80–84.

Ververidis, F., Trantas, E., Douglas, C., Vollmer, G., Kretzschmar, G., Panopoulos, N., Biotechnol. J. 2 (2007) 1235–1249.

White-Phillip, J., Thibodeaux, C. J., Liu, H., Methods Enzymol. 459 (2009) 521–544.

Wolfe, A. J., Microbiol. Mol. Biol. Rev. 69 (2005) 12–50.

Yanez, J. A., Andrews, P. K., Davies, N. M., J. Chromatogr. B 848 (2007) 159–181.

Yoon, J.-A., Kim, B.-G., Lee, W. J., Lim, Y., Chong, Y., Ahn, J.-H., Appl. Environ. Microbiol. 78 (2012) 4256–4262.

Zgurskaya, H. I., Krishnamoorthy, G., Ntreh, A., Lu, S., Front. Microbiol. 2: 189 (2011).

Zhang, C., Chen, X., Stephanopoulos, G., Too, H.-P., Biotechnol. Bioeng. 113 (2016) 1755–1763.

Zillich, O.V., Schweiggert-Weisz, U., Eisner, P., Kerscher, M., Int. J. Cosmet. Sci. 37 (2015) 455–464.

Supervised student projects during this work:

2016 Nele Bredehöft „Entwicklung und Validierung einer HPLC-Methode zur Prozess- und Qualitätsanalytik für einen biotechnologischen Prozess zur Herstellung von glycosylierten Flavonoiden“ (Bachelor thesis, University of Applied Science, Hamburg)

2016 Charles Wiedenhöfer „Downstream Processing und Automatisierung der biokatalytischen Produktion glykosylierter Polyphenole“ (Master thesis, Hamburg University of Technology)

2016 Boby Tendi Rik Mandenda „Aufreinigung und Identifizierung von *E. coli* Stoffwechselprodukten für die Charakterisierung des Bioprozesses zur Glykosylierung von Polyphenolen“ (Bachelor thesis, University of Applied Science, Hamburg)

2016 Anton Letzer „Aufreinigung und Scale-Up von glykosylierten Flavonoiden für Stabilitätsuntersuchungen in Hautcremes“ (Bachelor thesis, University of Applied Science, Hamburg)

2017 Robert Knoll “Simulation and comparison of hesperetin glycosylation by whole-cell biocatalysis in different complex and defined media” (Master thesis, University of Applied Science, Hamburg)

Appendix

A1 – Results from *in vitro* tests of hesperetin-5-O-rhamnoside and naringenin-5-O-rhamnoside on skin tissue models (Bioalternatives)

A1.1 Inflammatory effects in normal human epidermal keratinocytes (NHEK)

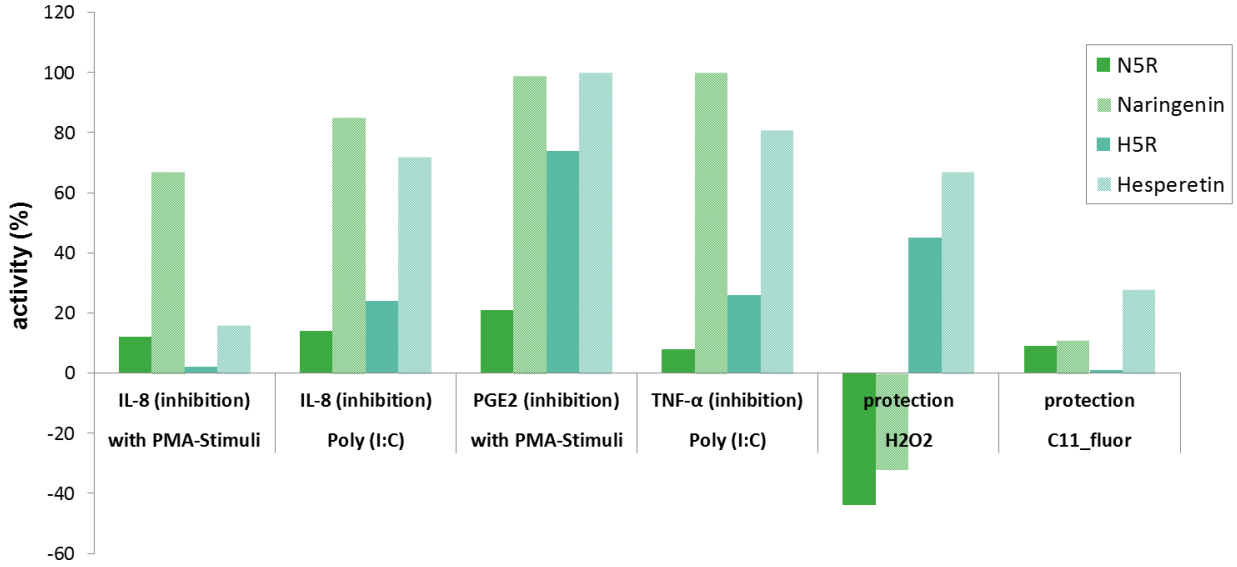

A1.2 Cell regeneration in normal human dermal fibroblasts (NHDF)

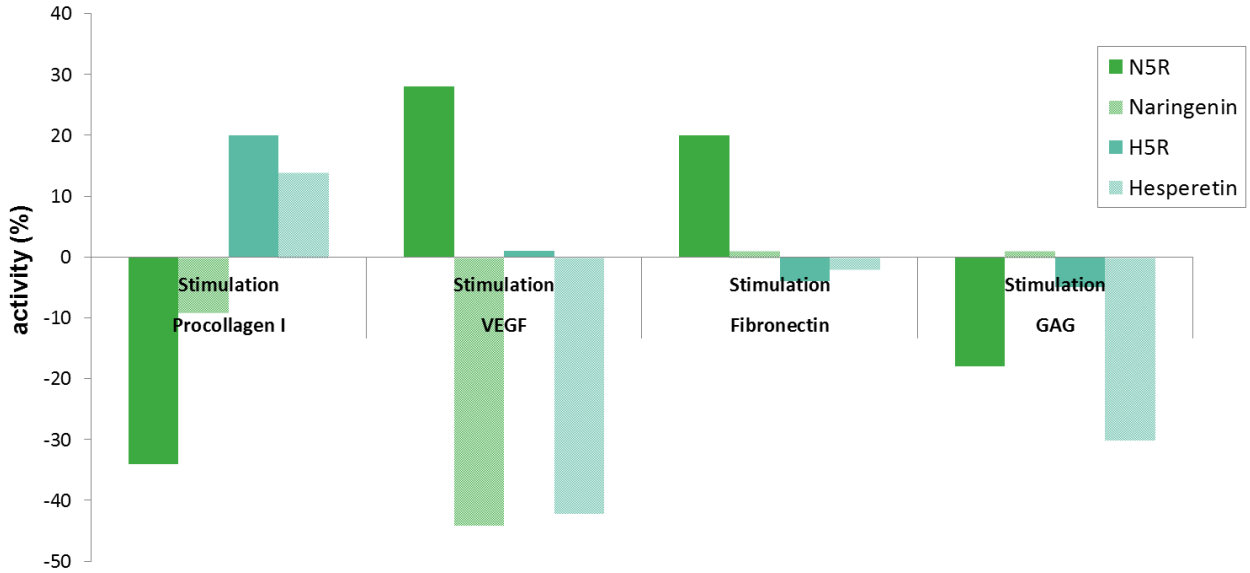

A2 – Protein sequences of glycosyltransferases GtfC and GtfD

A2.1 GtfC (codon optimized)

A2.2 GtfD (codon optimized)

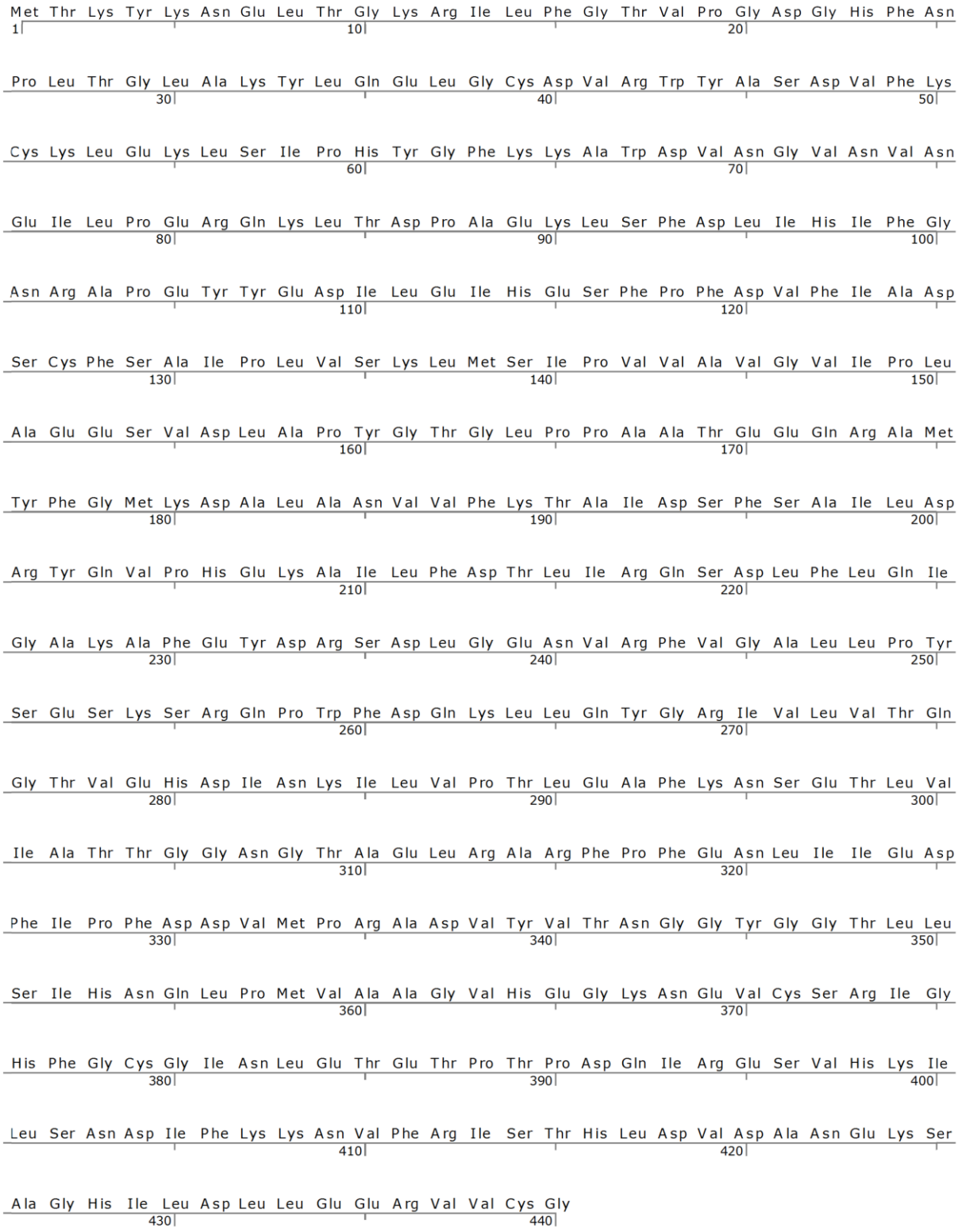

A3 – Plasmid maps

A3.1 pET19b::gtfC

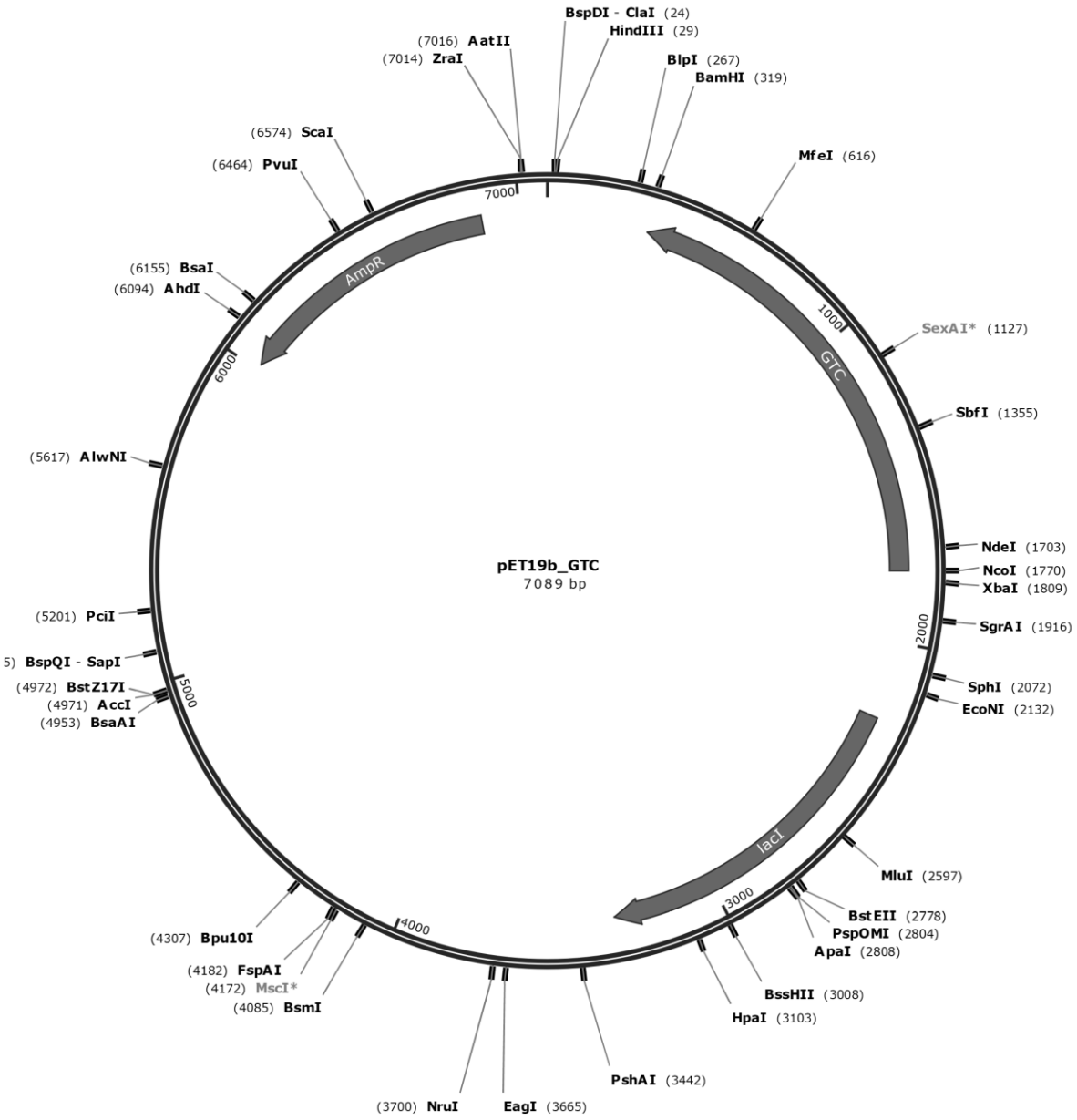

A3.2 pET19b::gtfD

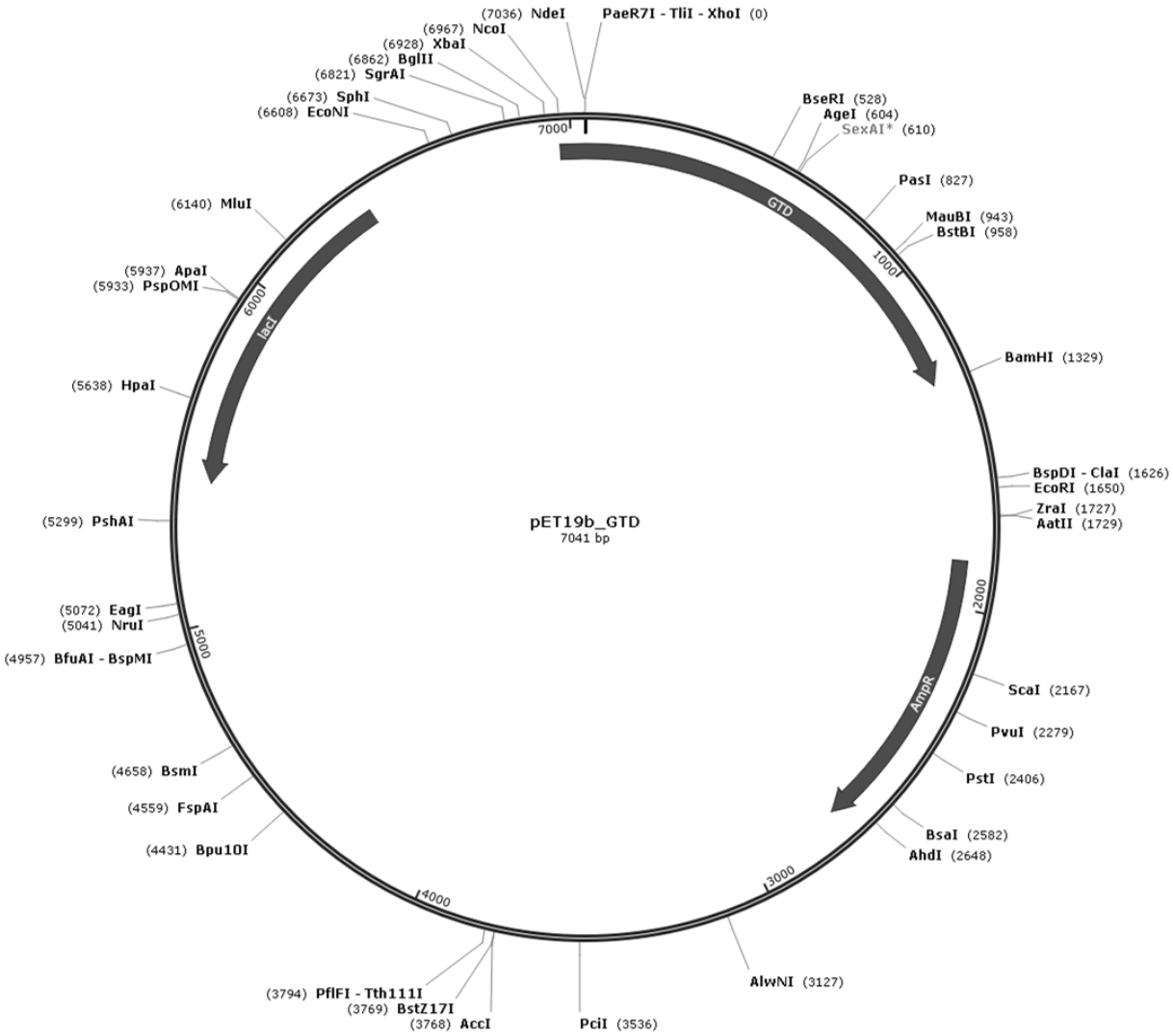

A3.3 pRSFDuet-1::ndk::tmk

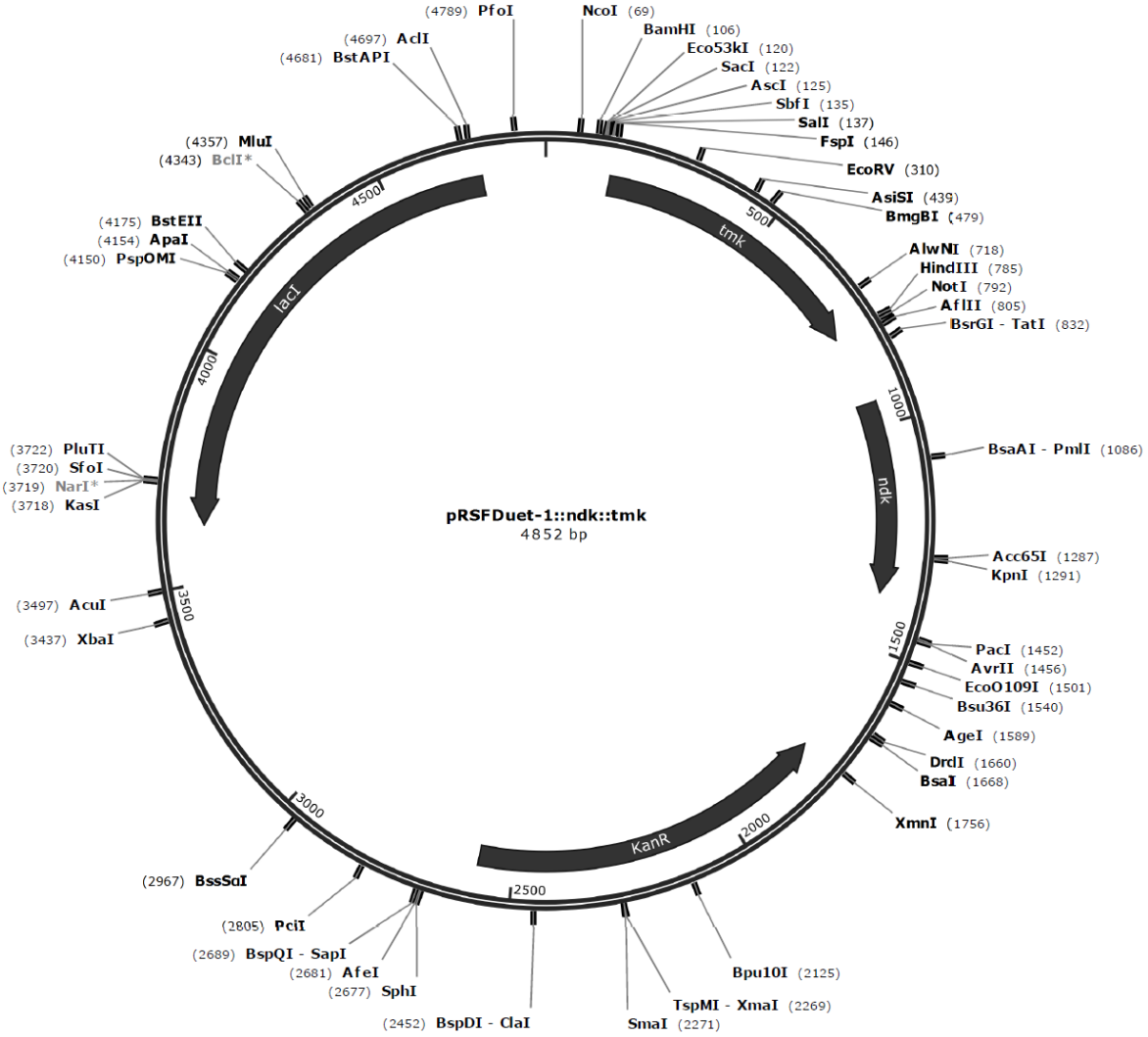

A3.4 pCDFDuet-1::rmlA::rmlC

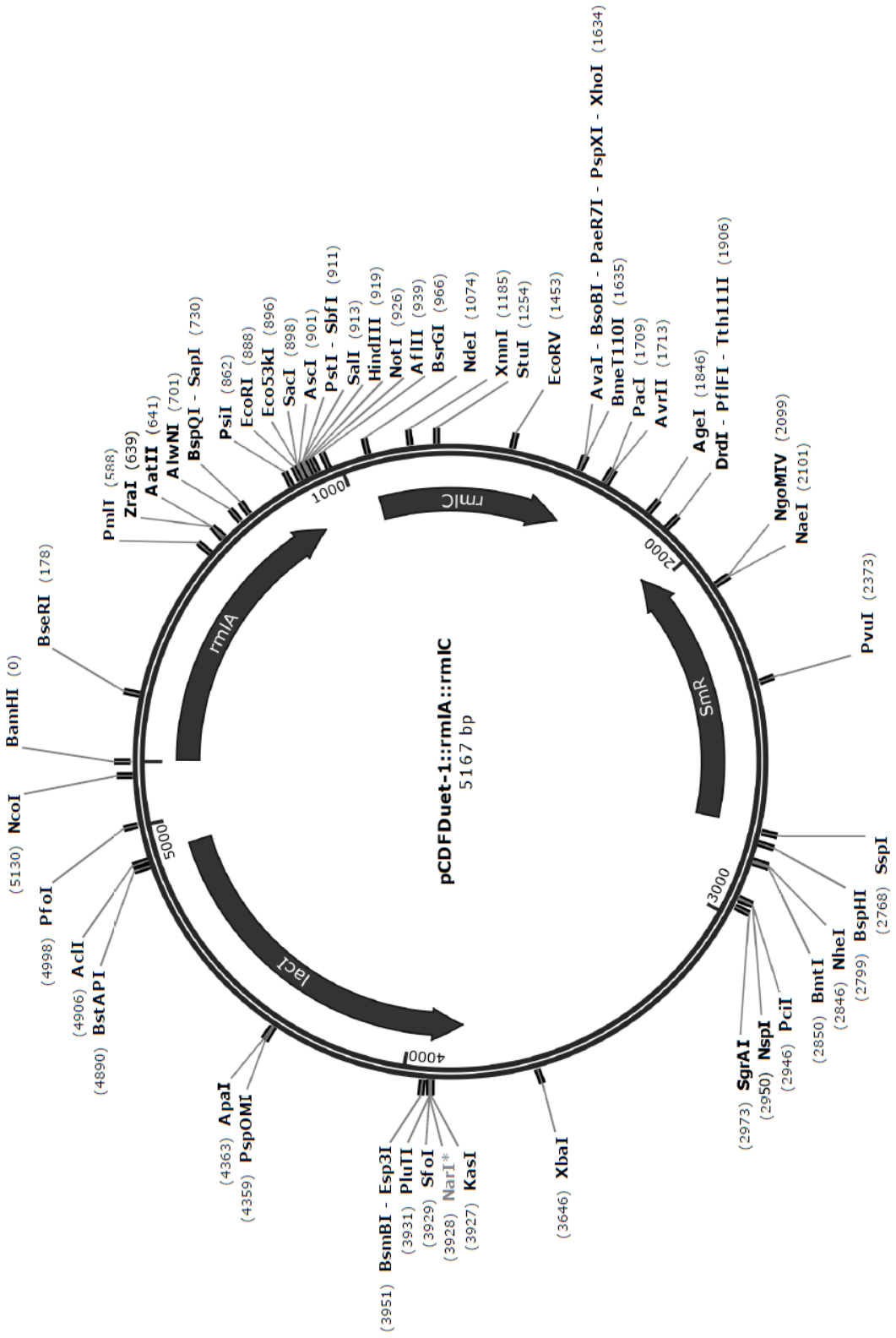

A3.5 pTrcHisA::gtfD

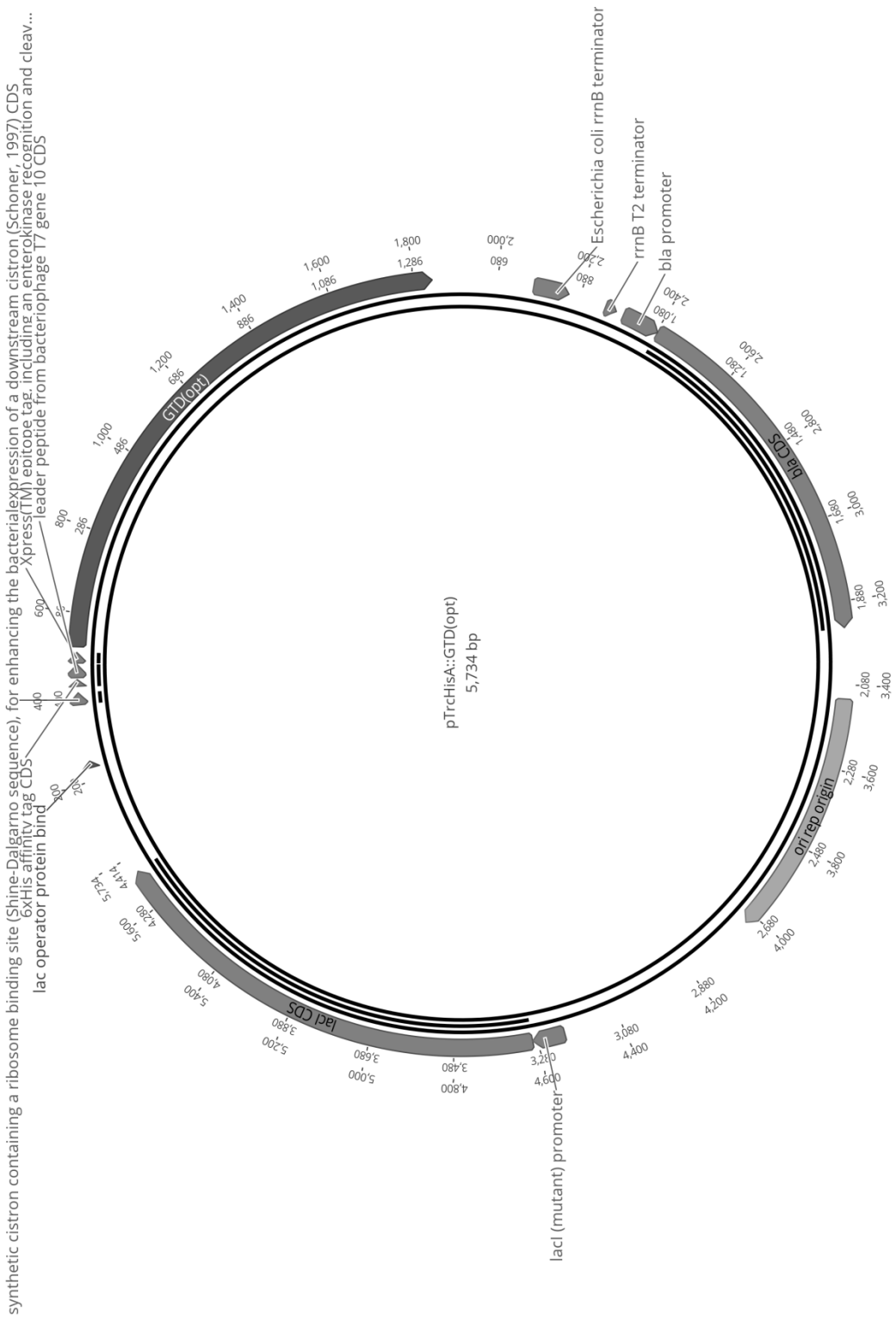

A3.6 pRSF-malZp::tolC

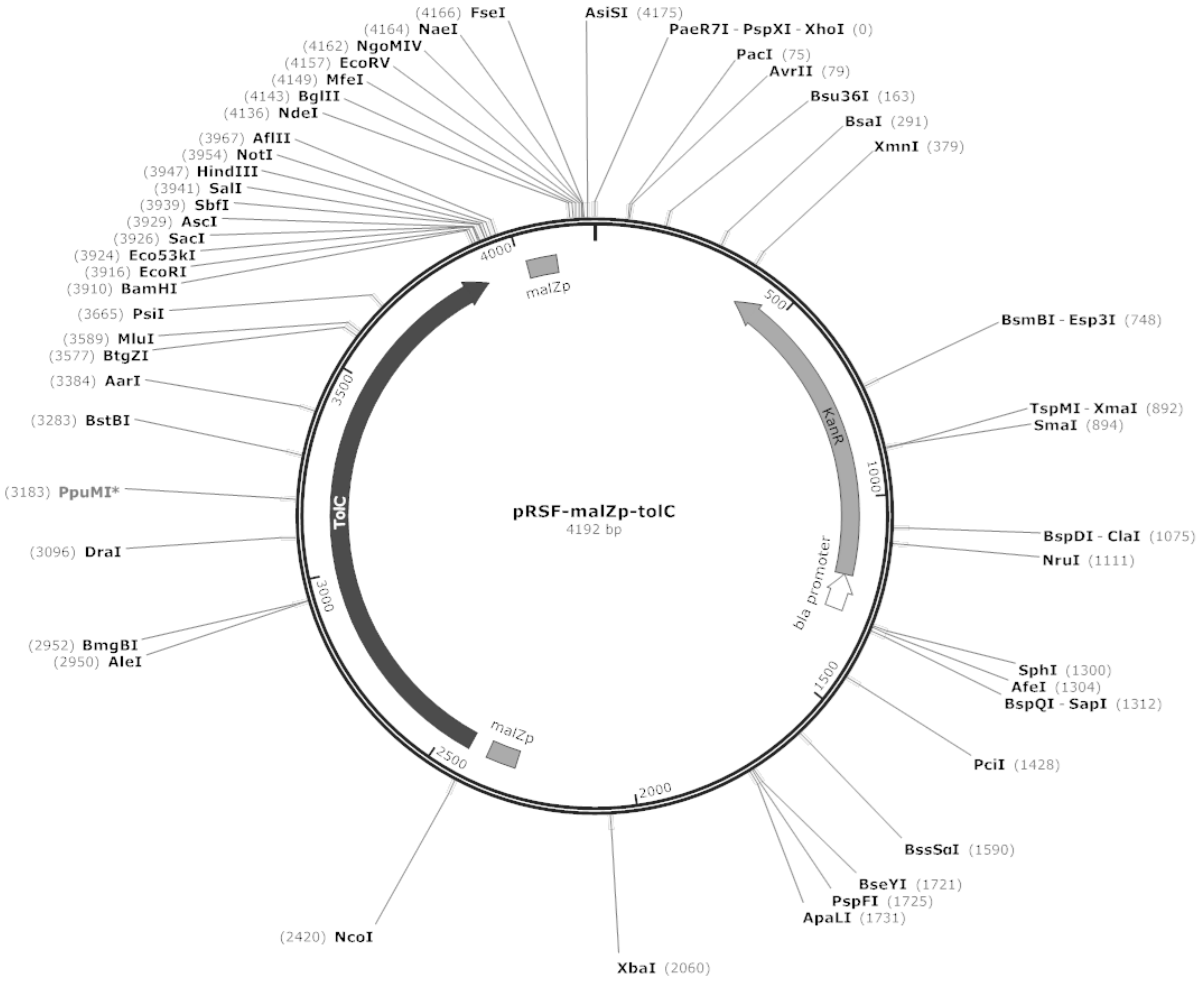

A4 – Chemicals and equipment

A4.1 Technical data of the used bioreactors

	DASGIP® **Parallel Bioreactor System (Eppendorf)**	**BioFlo® 320** **Bioreactor System (Eppendorf)**
Working volumes	320 – 1500 mL	3.5 – 10.5 L
Vessel	Four vessels, borosilicate glass	Borosilicate glass, stainless steel dished-bottom
Software	DASware control V5.0	DASware control V5.0
Agitation	Rushton Impeller, direct drive, 100 – 1600 rpm	Rushton Impeller, direct drive, 25 – 1200 rpm
Temperature	heating and cooling integrated in DASGIP Bioblock (water)	over stainless steel dish-bottom (water)
Gassing	Sparger	Sparger
Exhaust	Water-cooled	Water-cooled
pH control	Acid and/or base titration, sensor from Mettler Toledo (control range 2 – 12)	Acid and/or base titration, sensor from Mettler Toledo (control range 2 – 12)
DO control	Cascade to agitation speed, sensor from Mettler Toledo (control range 0 – 200%)	Cascade to agitation speed, sensor from Mettler Toledo (control range 0 – 200%)
Level/ foam	capacitive sensor with ceramic sealing	capacitive sensor with polyethylen sealing
Pumps	Four peristaltic pumps for each bioreactor (acid, base, antifoam, feed), 0.3 – 9.5 mL/h	Four peristaltic pumps (acid, base, antifoam, feed), Watson-Marlow Pumps 1, 2, and 3: 5 – 25 rpm Pump 4: 20 –100 rpm

A4.2 Equipment

Device/ instrument	**Manufacturer**
Autoclave VX-120	Systec
Autoclave 5075 ELV	Tuttnauer
Autoclave LVSA 50/70	Zirbus Technology
Balance ABJ220-4NM	Kern
Balance PCB1000-2	Kern
Balance ME54	Mettler Toledo
Centrifuge MiniSpin Plus	Eppendorf
Centrifuge 5804 R	Eppendorf
Centrifuge Sorvall RC 6 Plus	Thermo Scientific
Centramate™ 500 S TFF system	Pall
Supor PES membrane cassettes (0.2 µm)	Pall
HPLC device Elite LaChrom	VWR-Hitachi
Column Zorbax SB-C18, 4.6 x 250 mm, 5 µm	Agilent Technology
Flash-LC Pump-Manager C-615	Büchi
CHROMABOND Flash RS 330/ 800 C18 ec	Macherey-Nagel
Varian PrepStar SD-1	Agilent technology
RP Säule C18Htec 50 x 250 mm, 7 µm	Macherey-Nagel
1260 Infinity II Preparative LC System	Agilent Technology
Column SB-C18 21.2 x 250 mm, 7 µm	Agilent Technology
UHPLC UltiMate 3000	Thermo Scientific
UHPLC column Nucleoshell RP18 EC100, 2 x 100 mm, 2.7 µm	Macherey-Nagel
Mass spectrometer micrOTOF-Q	Bruker Daltonics
Laminar flow workbench Herasafe H12	Heraeus Instruments
Electrophoresis PowerPac Basic	Bio-Rad Laboratories
Molecular Imager Gel Doc XR System	Bio-Rad Laboratories
Freeze dryer Alpha 2-4 LSCplus	Christ
Spectrophotometer BioPhotometer	Eppendorf
Vacuum evaporator Syncore Polyvap R-6	Büchi
BioRad T100 PCR Thermal Cycler	Bio-Rad Laboratories
Gene Pulser Xcell Electroporation System	Bio-Rad Laboratories
TRACE C2 Control Glucose Sensor	TRACE Analytics

A4.3 Chemicals

Substance	**Supplier**
Agarose	Roth
Acetonitrile HPLC Grade	J. T. Baker
Acetonitrile UHPLC Grade ChemSolute	Th. Geyer
Acetone HPLC Grade ChemSolute	Th. Geyer
Trifluoroacetic acid	Roth
Glycerol	Roth
Formic acid	Roth
Glucose	Roth
NaOH	Thermo Scientific
Antifoam SE-15	Sigma
H_3PO_4	Roth
$MgSO_4$	Merck
NaCl	Roth
$CaCl_2$	Roth
NH_4Cl	Merck
Ampicillin	Roth
Streptomycin	Roth
Kanamycin	Roth
Spectinomycin	Sigma
Tris	Roth
EDTA	Sigma
Acetic acid	Roth
Ethidium bromide	Roth
H_2KPO_4	Merck
K_2HPO_4	Merck
Yeast extract	Roth
Tryptone	Roth
Casein hydrolysate	Roth
IPTG	Sigma
GeneRuler 1 kb DNA Ladder	Thermo Scientific
dNTP mix (10 mM each)	Thermo Scientific

A4.4 Enzymes

Enzymes	**Supplier**
NcoI	Thermo Scientific
BamHI	Thermo Scientific
DCS polymerase	DNA cloning service
Pfu polymerase	DNA cloning service
T4 ligase	Thermo Scientific

A4.5 Kits

Kit	**Manufacturer**
Presto Mini Plasmid Kit	Geneaid
GenepHlow Gel/PCR Kit	Geneaid

A5 – NMR data of flavonoid-rhamnosides produced by GtfC

A5.1 Biochanin-5-O-α-L-rhamnoside

^{1}H-NMR (400 MHz DMSO-d6): δ = 8.21 (s, 1H), 7.42 (d, J = 8.7 Hz, 2H), 6.96 (d, J = 8.7 Hz 2H), 6.55 (d, J = 1.9 Hz, 1H), 6.48 (d, J = 1.9 Hz, 1H), 5.33 (d, J = 1.7 Hz, 1H), 5.1 – 4.1 (br, nH), 3.91 (br, 1H), 3.86 (d, J = 9.7, 1H), 3.77 (s, 3H), 3.48 (br, superimposed by impurity, 1H), 3.44 (impurity), 3.3 (superimposed by HDO), 1.10 (d, J = 6.2 Hz, 3H)

A5.2 Biochanin-5,7-O-α-L-rhamnoside

^{1}H-NMR (400 MHz DMSO-d6): δ = 8.21 (s, 1H), 7.43 (d, J = 8.5 Hz, 2H), 6.97 (d, J = 8.6 Hz, 2H), 6.86 (d, J = 1.8 Hz, 1H), 6.74 (d, J = 1.8 Hz, 1H), 5.53 (d, J = 1.6 Hz, 1H), 5.41 (d, J = 1.6 Hz, 1H), 5.15 (s, 1H), 5.00 (s, 1H), 4.93 (s, 1H), 4.83 (s, 1H), 4.70 (s, 1H), 3.93 (br, 1H), 3.87 (br, 1H), 3.85 (br, 1H), 3.77 (s, 3H), 3.64 (dd, J = 9.3,3.0 Hz, 1H), 3.54 (dq, J = 9.4, 6.4 Hz, 1H), 3.44 (dq, J = 9.4, 6.4 Hz, 1H), 3.34 (br, 1H), 1.13 (d, J = 6.1 Hz, 3H), 1.09 (d, J = 6.1 Hz, 3H)

A5.3 Chrysin-5-O-α-L-rhamnoside

^{1}H-NMR (400 MHz DMSO-d6): δ = 8.01 (m, 2H), 7.56 (m, 3H), 6.66 (s, 1H), 6.64 (d, J = 2.1 Hz, 1H), 6.55 (d, J = 2.1 Hz, 1H), 5.33 (d, J = 1.5 Hz, 1H), 5.01 (s, 1H), 4.85 (d, J =4.7 Hz, 1H), 4.69 (s, 1H), 3.96 (br, 1H), 3.87 (md, J = 8.2 Hz, 1H), 3.54 (dq, J = 9.4, 6.2 Hz, 1H), 3.3 (superimposed by HDO), 1.11 (d, J = 6.1 Hz, 3H)

A5.4 Chrysin-5,7-O-α-L-rhamnoside

^{1}H-NMR (400 MHz DMSO-d6): δ = 8.05 (m, 2H), 7.57 (m, 3H), 7.08 (s, 1H), 6.76 (d, J = 2.3 Hz, 1H), 6.75 (s, 1H), 5.56 (d, J = 1.6 Hz, 1H), 5.42 (d, J = 1.6 Hz, 1H), 5.17 (s, 1H), 5.02 (s, 1H), 4.94 (s, 1H), 4.86 (s, 1H), 4.71 (s, 1H), 3.97 (br, 1H), 3.88 (dd, J = 9.5,3.1 Hz, 1H), 3.87 (br, 1H), 3.66 (dd, J = 9.3,3.4 Hz, 1H), 3.56 (dq, J = 9.4, 6.2 Hz, 1H), 3.47 (dq, J = 9.4, 6.2 Hz, 1H), 3.32 (superimposed by HDO, 2H), 1.14 (d, J = 6.2 Hz, 3H), 1.11 (d, J = 6.2 Hz, 3H)

A5.5 Diosmetin-3'-O-α-L-rhamnoside

^{1}H-NMR (400 MHz DMSO-d6): δ = 7.76 (m, 2H), 7.18 (d, J = 9.3 Hz, 1H), 6.88 (s, 1H), 6.47 (d, J = 1.8 Hz, 1H), 6.19 (d, J = 1.8 Hz, 1H), 5.46 (d, J = 1.6 Hz, 1H), 5.04 (s, 1H), 4.89 (s, 1H), 4.76 (s, 1H), 3.88 (br, 1H), 3.87 (s, 3H), 3.68 (dm, J = 8.9 Hz, 1H), 3.63 (dq, J =9.4, 6.4 Hz, 1H), 3.30 (superimposed by HDO, 1H), 1.12 (d, J = 6.2, 3H)

A5.6 Diosmetin-5-O-α-L-rhamnoside

^{1}H-NMR (600 MHz DMSO-d6): δ = 7.45 (dd, J = 8.5,2.3 Hz, 1H), 7.36(d, J = 2.3 Hz, 1H), 7.06 (d, J = 8.6 Hz, 1H), 6.61 (d, J = 2.3 Hz, 1H), 6.54 (d, J = 2.3 Hz, 1H), 6.45 (s, 1H), 5.32 (d, J = 1.7 Hz, 1H), 3.96 (dd, J = 3.5, 2.0 Hz, 1H), 3.86 (m, 1H), 3.85 (s, 3H), 3.54 (dq, J =9.4, 6.3 Hz, 1H), 3.30 (superimposed by HDO, 1H), 1.11 (d, J = 6.2, 3H)

A5.7 Hesperetin-3'-O α-L-rhamnoside

^{1}H-NMR (400 MHz, DMSO-d6): δ =1.10 (3H, d, J = 6.24 Hz, CH3), 2.72 und 2.79 (2H, ABM-System, 9.89, 3.18 Hz, H3(a) / H3(b)), 3.33 – 3.15 (1H, m, Hb), 3.69 – 3.55 (2H, m, Ha + Hc), 3.79 (3H, s, OCH3), 3.86 (1H, dd, 3.25, 1.73 Hz, Hd), 5.26 (1H, d, 1.64 Hz, He), 5.50 (1H, dd, 12.26, 3.18 Hz, H2), 5.89 und 5.91, 2H, AB-System, 2.2 Hz, H6 / H8), 7.05 (1H, d, 8.48 Hz, H5'), 7.14 (1H, dd, 8.48, 2.04 Hz, H6'), 7.18 (1H, d, 2.04 Hz, H2')

A5.8 Hesperetin-5-O-α-L-rhamnoside

^{1}H-NMR (400 MHz, DMSO-d6): δ = 1.10 (3H, d, J = 6.26 Hz, CH3), 2.45 (m, H-3(a), superimposed by DMSO), 2.97 (1H, dd, J = 12.5, 16.5 Hz, H3(b)), 3.27 (1H, t, 9.49 Hz, H(b)), 3.48 (m, H(a), superimposed by HDO), 3.76 (3H, s, OCH3), 3.9 -3.8 (2H, m, H(c),Hd), 5.31 (1H, d, 1.76 Hz, He), 5.33 (1H, dd, 12.5, 2.83 Hz, H2), 6.03 (1H,d, 2.19 Hz, H6/H8), 6.20 (1H, d, 2.19 Hz, H6/H8), 6.86 (1H, dd, 8.2, 2.0 Hz, H6'), 6.90 (1H, d, 2.0 Hz, H2'), 6.93 (1H, d, 8.2 Hz, H5')

A5.9 Naringenin-4'-O-α-L-rhamnoside

^{1}H-NMR (600 MHz, Methanol-d4): δ 7.44 (d, J = 8.7 Hz, 2H), 7.12 (d, J = 8.7 Hz, 2H), 6.30 (d, J = 2.1 Hz, 1H), 6.17 (d, J = 2.1 Hz, 1H), 6.05 (d, J = 0.9 Hz, 1H), 5.91 (d, J = 2.2 Hz, 1H), 5.88 (d, J = 2.2 Hz, 1H), 5.46 (d, J = 1.8 Hz, 1H), 5.41 (dd, J = 12.8, 3.1 Hz, 1H), 4.00 (dd, J = 3.5, 1.8 Hz, 1H), 3.84 (dd, J = 9.5, 3.5 Hz, 1H), 3.63 (dq, J = 9.6, 6.2 Hz, 1H), 3.46 (t, J = 9.5 Hz, 1H), 3.11 (dd, J = 17.1, 12.8 Hz, 1H), 2.74 (ddd, J = 17.1, 3.1, 1.2 Hz, 1H), 2.36 (d, J = 0.8 Hz, 3H), 1.23 (d, J = 6.2 Hz, 3H).

A5.10 Naringenin-5-O-α-L-rhamnoside

^{1}H-NMR (600 MHz, DMSO d6): δ = 7.30 (d, J = 6.9 Hz, 2H), 7.29 (d, J = 6.9 Hz, 2H), 6.79 (d, J = 8.6 Hz, 2H), 6.78 (d, J = 8.6 Hz, 2H), 6.22 (d, J = 2.3 Hz, 1H), 6.20 (d, J = 2.2 Hz, 1H), 6.02 (d, J = 2.2 Hz, 1H), 6.01 (d, J = 2.2 Hz, 1H), 5.38 (dd, J = 12.7, 3.1 Hz, 1H), 5.35 (dd, J = 13.0, 2.5 Hz, 1H), 5.31 (d, J = 1.8 Hz, 1H), 5.27 (d, J = 1.9 Hz, 1H), 3.90 3.88 (m, 1H), 3.88 3.85 (m, 1H), 3.85 3.80 (m, 2H), 3.50 (dq, J = 9.2, 6.2 Hz, 1H), 3.48 (dq, J = 9.1, 6.2 Hz, 1H), 3.29 (t, J = 9.8 Hz, 2H), 3.07 2.98 (m, 2H), 2.55 2.48 (m, 2H), 1.12 (d, J = 6.2 Hz, 3H), 1.10 (d, J = 6.2 Hz, 3H).

A6 – HPLC chromatograms of GtfC products after 24h biotransformation

Chromatograms from Ruprecht *et al.* 2019 (Supplementary)

A6.1 Biochanin A with GtfC

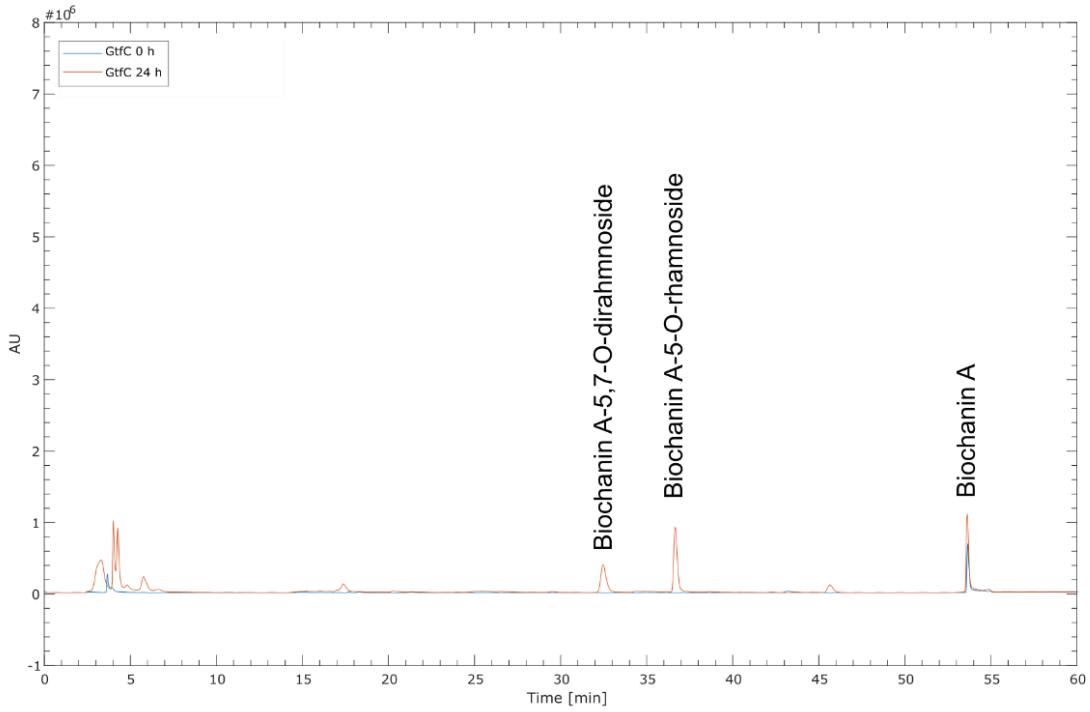

A6.2 Chrysin with GtfC

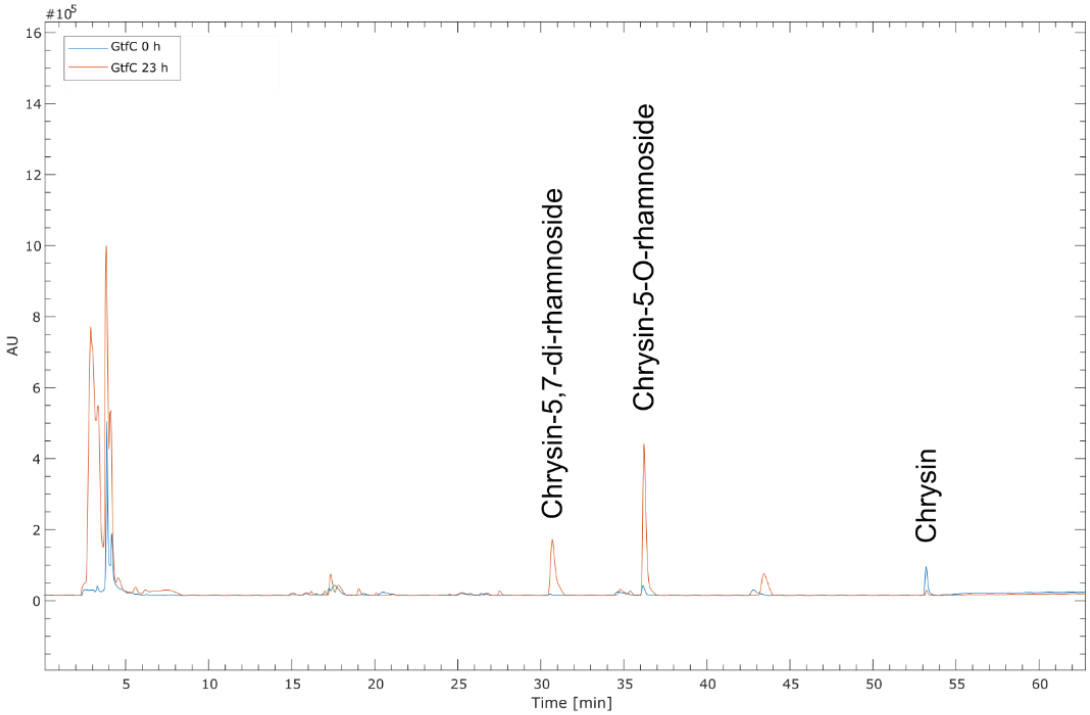

A6.3 Diosmetin with GtfC

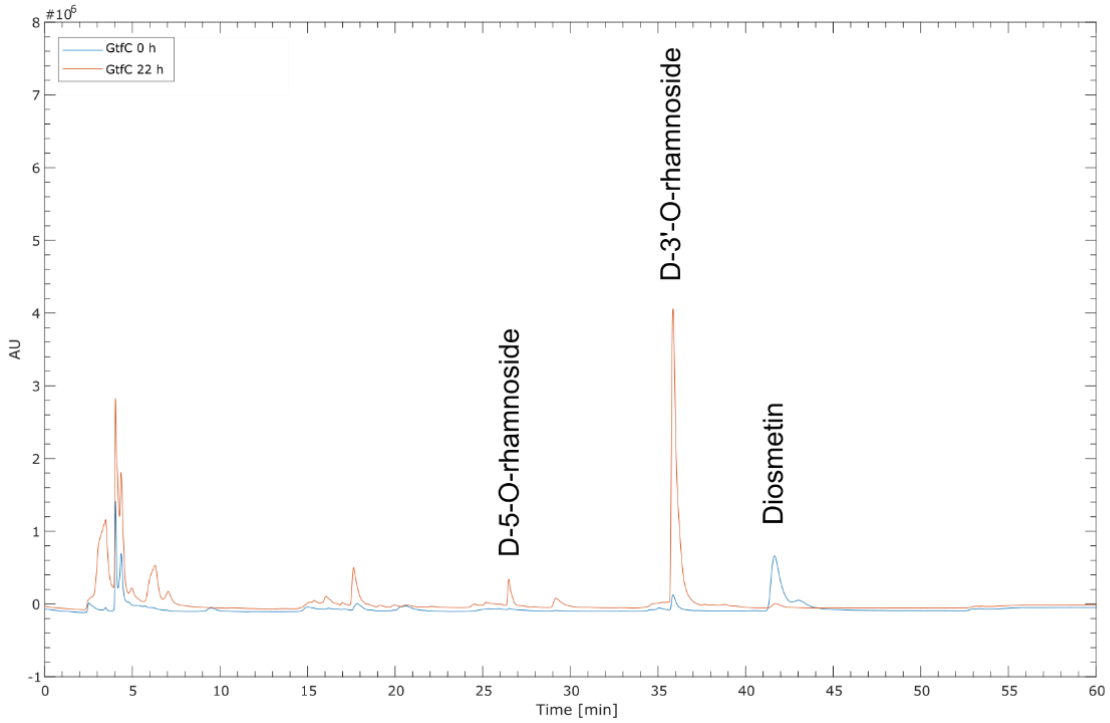

A6.4 Naringenin with GtfC

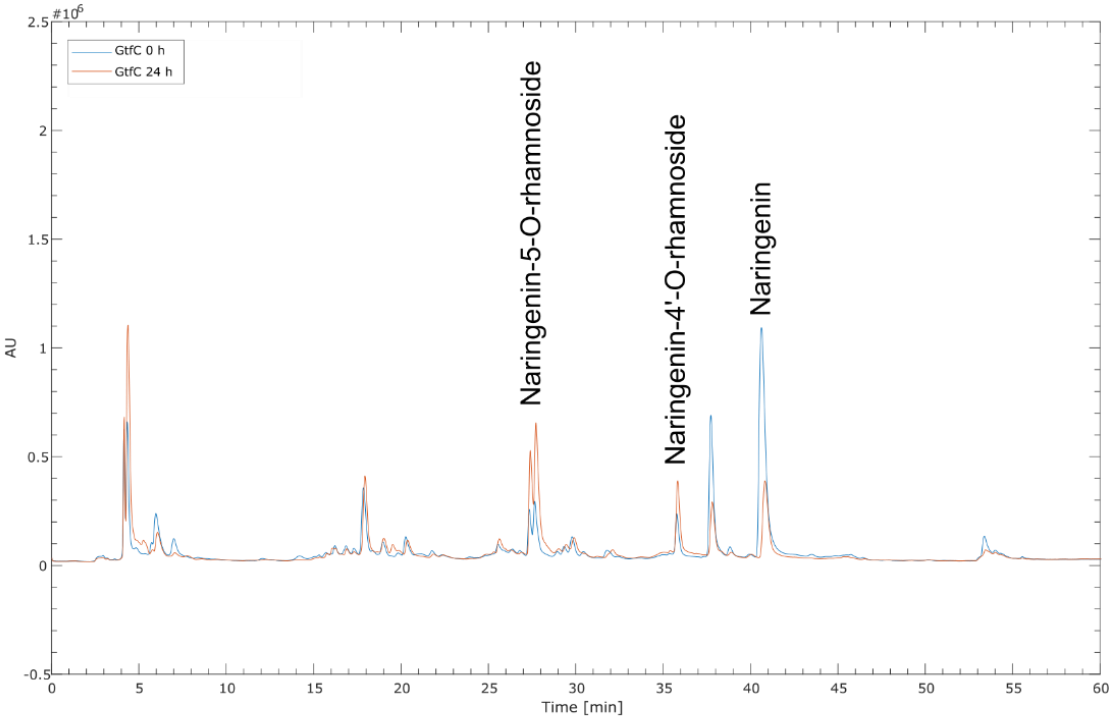

A7 – Optimization experiments for hesperetin-5-O-rhamnoside production in M29 medium (data from Robert Knoll, master thesis)

A7.1 Influence of different feeding strategies (biotransformation with GtfC)

Exp. increase $q_{X/Xw} = 0.1\ h^{-1}$ from $1\ mL\ h^{-1}$ to $3\ mL\ h^{-1}$, then exp decrease by $-0.025\ h^{-1}$

Phase	m_{XL}, g	$\bar{q}_{X/X}$, h^{-1}	$\bar{q}_{S/X}$, $g\ g^{-1}\ h^{-1}$	$\bar{y}_{X/S}$, $g\ g^{-1}$	$\bar{q}_{H5R/X}$, $mg\ g^{-1}\ h^{-1}$	$\bar{q}_{H3'R/X}$, $mg\ g^{-1}\ h^{-1}$	$\bar{q}_{H5R/V}$, $mg\ L^{-1}\ h^{-1}$	$\bar{q}_{H3'R/V}$, $mg\ L^{-1}\ h^{-1}$	m_{H5R}, mg	$m_{H3'R}$, mg
Batch	1.020	0.3497	0.1156	3.024	-	-	-	-	-	-
Fed Batch	3.202	0.08240	0.3091	0.2665	-	-	-	-	-	-
Production	9.907	0.02973	0.1001	0.2969	0.2206	0.4997	2.366	6.971	46.01	117.7

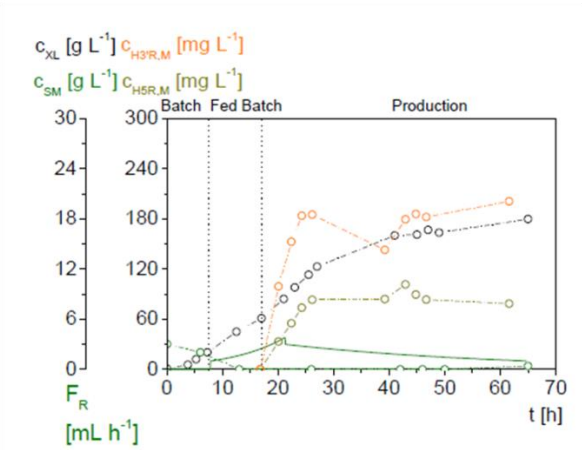

Exp. increase $q_{X/Xw} = 0.1\ h^{-1}$ from $1\ mL\ h^{-1}$ to $3\ mL\ h^{-1}$, then 2^{nd} order polynomial with $F_R(t) = 3\ mL\ h^{-1}$ - 0.0001 $\cdot\Delta t$ - 0.0005 $\cdot\Delta t^2$

Phase	m_{XL}, g	$\bar{q}_{X/X}$, h^{-1}	$\bar{q}_{S/X}$, $g\ g^{-1}\ h^{-1}$	$\bar{y}_{X/S}$, $g\ g^{-1}$	$\bar{q}_{H5R/X}$, $mg\ g^{-1}\ h^{-1}$	$\bar{q}_{H3'R/X}$, $mg\ g^{-1}\ h^{-1}$	$\bar{q}_{H5R/V}$, $mg\ L^{-1}\ h^{-1}$	$\bar{q}_{H3'R/V}$, $mg\ L^{-1}\ h^{-1}$	m_{H5R}, mg	$m_{H3'R}$, mg
Batch	1.185	0.3866	0.1350	2.8645	-	-	-	-	-	-
Fed Batch	3.254	0.04899	0.3295	0.1487	-	-	-	-	-	-
Production	7.742	0.02353	0.1047	0.2248	0.2677	0.6329	2.538	6.129	48.40	126.80

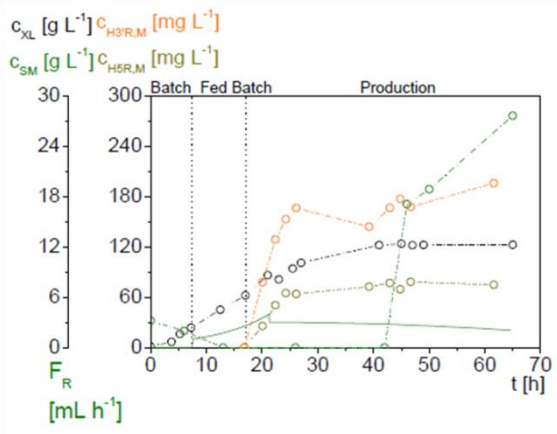

Exp. decrease with 0.016 h^{-1} from 3 mL h^{-1} to 1 mL h^{-1}

Phase	m_{XL}, g	$\bar{q}_{X/X}$, h^{-1}	$\bar{q}_{S/X}$, g g^{-1} h^{-1}	$\bar{y}_{X/S}$, g g^{-1}	$\bar{q}_{H5R/X}$, mg g^{-1} h^{-1}	$\bar{q}_{H3'R/X}$, mg g^{-1} h^{-1}	$\bar{q}_{H5R/V}$, mg L^{-1} h^{-1}	$\bar{q}_{H3'R/V}$, mg L^{-1} h^{-1}	m_{H5R}, mg	$m_{H3'R}$, mg
Batch	1.199	0.3500	0.1157	3.2025	-	-	-	-	-	-
Fed Batch	4.240	0.08511	0.3521	0.2418	-	-	-	-	-	-
Production	8.551	0.01638	0.1019	0.1607	0.1913	0.5354	2.042	6.169	28.15	119.2

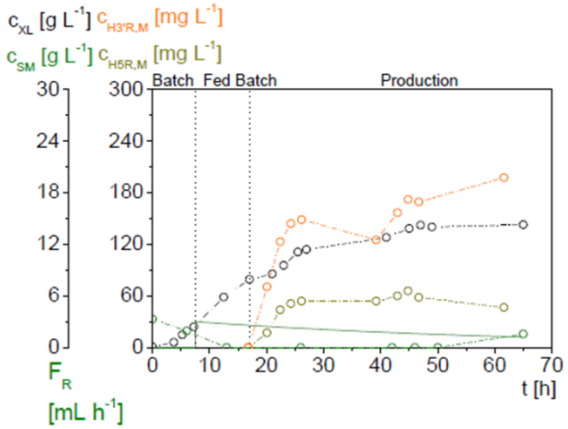

A7.2 Influence of different complex components in M29 (biotransformation with GtfD)

Growth on M29 + yeast extract

Phase	$\bar{q}_{X/X}$, h^{-1}	$\bar{q}_{H5R/X}$, mg g^{-1} h^{-1}	$\bar{q}_{Hes/V}$, mg g^{-1} h^{-1}	$\bar{q}_{H5R/V}$, mg L^{-1} h^{-1}	$\bar{q}_{Hes/M}$, mg L^{-1} h^{-1}	m_{H5R}, mg
Batch	0.1052	-	-	-	-	-
Fed Batch and Production	0.005031	0.07511	0.009209[1]	1.982	0.06878[1]	1.482
Yeast extract add.	0.009580	0.9641	-0.4264	6.361	-0.2813	17.03

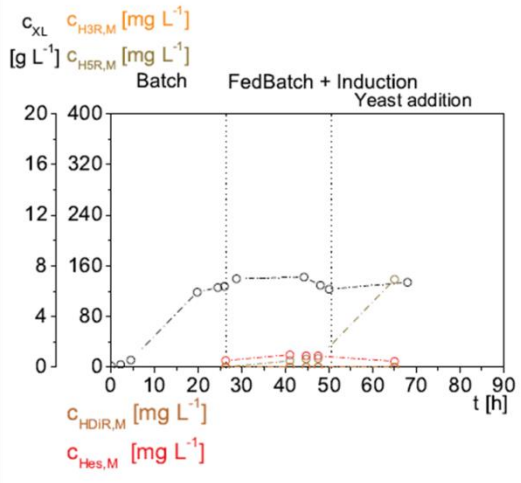

Growth on M29 + casein lysate

Phase	$\bar{q}_{X/X}$, h^{-1}	$\bar{q}_{H5R/X}$, mg g^{-1} h^{-1}	$\bar{q}_{Hes/V}$, mg g^{-1} h^{-1}	$\bar{q}_{H5R/V}$, mg L^{-1} h^{-1}	$\bar{q}_{Hes/M}$, mg L^{-1} h^{-1}	m_{H5R}, mg
Batch	0.1148	-	-	-	-	-
FedBatch and Production	0.01731	0.1072	0.08587[1]	1.431	0.5816[1]	4.487
Casein lysate add.	0.005730	0.6095	-0.2762	3.983	-1.825	25.39

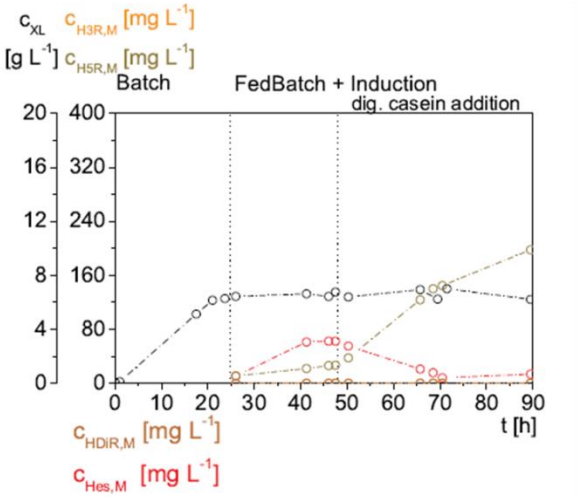

Growth on M29 + vitamin mix

Phase	$\bar{q}_{X/X}$, h^{-1}	$\bar{q}_{H5R/X}$, mg g^{-1} h^{-1}	$\bar{q}_{Hes/V}$, mg g^{-1} h^{-1}	$\bar{q}_{H5R/V}$, mg L^{-1} h^{-1}	$\bar{q}_{Hes/M}$, mg L^{-1} h^{-1}	m_{H5R}, mg
Batch	0.1043	-	-	-	-	-
Fed Batch and Production	0.01510	0.1226	-0.09168[1]	0.7332	-0.6546[1]	2.961
Enzyme mix add.	-0.008637	0.3307	-0.02838	1.6873	-0.1136	10.95